Report - CFD (conventional CFD)

PROJECT P3VENTI – HANDELINGSPERSPECTIEF GEBRUIK EN SYSTEEMCONFIGURATIE (D4.1)
(project phase 2025)

EINDHOVEN UNIVERSITY OF TECHNOLOGY

Date	Our reference	Version
September 12 2025	BE2025-2055379	1.0

Built Environment
Building Physics and Services

T +31 (0)40 247 2400
m.g.l.c.loomans@tue.nl

www.tue.nl

Authors
Marcel Loomans
Twan van Hooff
Peng Qin
Eugene Mamulova

Contents

1. Introduction[1]

The research program *Pandemic Preparedness and Ventilation* (*P3venti*) was initiated to develop knowledge on the role of airborne spread (aerogenic route) of viruses and other pathogens, to increase the effectiveness of using ventilation as a mitigation measure and to develop methods and tools to support government and social partners in often complex and sensitive decision making. The knowledge developed has application in society in mind.

For research into the spread of virus particles and other pathogens in a room, computational fluid dynamics (CFD) is an important tool. It can provide high-resolution whole-flow field data on the relevant parameters in space, allows us to evaluate the exposure to pathogens in controlled situations, and to investigate the effect of interventions in the design phase.

However, modeling will always require some degree of simplification of the complex world. This also accounts for CFD. The context of modeling airborne spread of pathogens introduces extra requirements besides the mere modeling of the airflow (velocity and temperature). Therefore, in the first phase (2022) of Program Line (PL) II, the focus was put on modeling and simulation using CFD. Some important aspects related to modeling the spread of virus particles were investigated. They relate to the modeling of (viral) particles, the human emission of (viral) particles, breathing, and the disturbance of airflow because of motion. The work in 2022 prepared for the simulation of cases for rooms in long term care facilities (LTCF) intended to be executed in the remainder of the program. Later, cases for selected types of sports facilities (NL: maatschappelijk urgente sportvoorzieningen; MUSV) were added to the research objectives.

In 2023, the work that started in 2022 was continued with the intention of answering research questions to understand the best way to calculate the exposure risk for a space and ventilation concept, identifying the important boundary conditions for such modeling. Apart from conventional CFD, also the option of fast-CFD was researched. Due to some delays in the availability of measurement data several of the original intentions at the time were not achieved, though instead new knowledge was developed or research continued from the work in 2022.

In 2024 the intention was to model representative cases for a LTFC lay-out, as identified by PLIV. Earlier results showed that the complexities encountered for such a case had to be preceded with a simpler case to better understand and analyze the general flow field characteristics. These measurements are also more easy to investigate for the fast CFD methods. These measurements have been used to also further investigate the effect of source momentum and direction (refer to breathing versus speaking) on the aerosol concentration distribution. This work was finalized in 2025 and has been published as a journal paper in the journal Building and Environment (https://doi.org/10.1016/j.buildenv.2025.113328). This also accounts for the analysis of the effectiveness of the ventilation when the source location is unknown. This was published in a conference paper published and presented at the Healthy Buildings Europe Conference in June 2025.

After the measurements for the more simplified case, the complex set-up as encountered in a living room of a LTCF and also in MUSV was revisited and several measurements were performed by TNO towards in the 2nd half of 2024 and in Q1 2025. For these more complex measurements a new, more complex, supply diffuser was installed in the test facility. After initial testing, it was needed to analyze this supply in more detail through additional measurements in order to assure that the supply was modeled correctly in CFD. These measurements had to be incorporated in the tight measurement scheme for the test facility, which included bioaerosol measurements as performed by University Utrecht.

In the end, the LTCF-case with the complex supply diffuser was analyzed (modeled) in full detail as intended for the other cases that have been measured. A draft journal article has been written to communicate this work. Through this work and the LTCF case the advantage of the use of CFD is shown, i.e.

[1] The introduction was partly copied from the report from 2023 an 2024 as the main goal of the work hasn't changed.

the ease with which changes can be made to the air change rate and to the configuration of the supply and exhaust. In total more than 1000 simulations were run for this case, addressing the effect of three different air change rates, three different supply and exhaust configurations and two different design parameters for the supply, for a dense grid of potential source locations in the room.

For the fast CFD techniques, the focus in 2025 was on modeling the simpler case (with heat sources) to identify the potential of the individual techniques, including simulation of contaminant distribution. Apart from that, the manuscript that described the protocol was submitted to the journal *Developments in the Built Environment* and, after acceptance, published in July (https://doi.org/10.1016/j.dibe.2025.100716). Details of this work can be found in the separate D4.2 report.

Repeating from the last year, we again notice that the original intentions envisaged for this part of the work within P3Venti were not fully achieved. We hoped to have analyzed more cases that were measured in the test facility. The delay with which that data has come available and the delay in having access to the test facility for performing measurements of the supply and its subsequent analysis affected the options to perform the full analysis of the cases as envisaged. However, we were able to analyze one case in the manner as intended. This analysis clearly shows its value in the work on developing better ventilation configurations with reduced exposure risk in mind.

The information as developed within PLII has also been used to develop the 'Handelingsperspectief Systeemconfiguratie', which contains as well general information on ventilation and on the design of ventilation systems as information on how to perform a credible CFD simulation, or assess whether such a simulation was done in a credible way.

Apart from P3Venti, information useful for P3Venti was also derived from the work performed within the parallel CLAIRE and MIST projects in which TU/e is closely involved (TNO as well). Apart from the research, in the context of P3Venti also presentations have been prepared to inform the public about the P3Venti research, and the aligned CLAIRE and MIST projects. Most prominent was the presentation at the Healthy Buildings Europe 2025 conference in Reyjavik, Iceland, and at COBEE 2025 in Eindhoven. In these presentations the work performed within P3Venti was shared.

The above introduction provides a brief summary of the work done within PLII (handelingsperspectief Gebruik en Systeemconfiguratie) in 2025. Part of this work has been reported in individual articles/papers that have been published or intended to be published either in scientific journals or scientific conferences. The remainder of this report summarizes this information for the work on conventional CFD. For the part referring to hast methods (fast CFD) a separate report has been prepared that summarizes the work on that topic.

As indicated, the original plan was not fully followed. Nevertheless, with the research performed we were able to add new knowledge to the field and support the writing of the 'handelingsperspectieven' which was the overall goal of the work within P3Venti. Where relevant, individual published or presented contributions have been grouped in the appendix of this report. For simplicity, they have not been edited to fit the layout of this report and are included in the Appendix. First a short summary is provided on the conventional CFD results.

2. Conventional CFD

2.1. Overview

Figure 1 provides an overview of the work performed within PLII. The left part of the figure refers to the several modeling issues that come into play when analysing exposure to aerosols with the use of CFD. The right part of the figure refers to the cases that were defined for LTCF and MUSV and measured in the test facility.

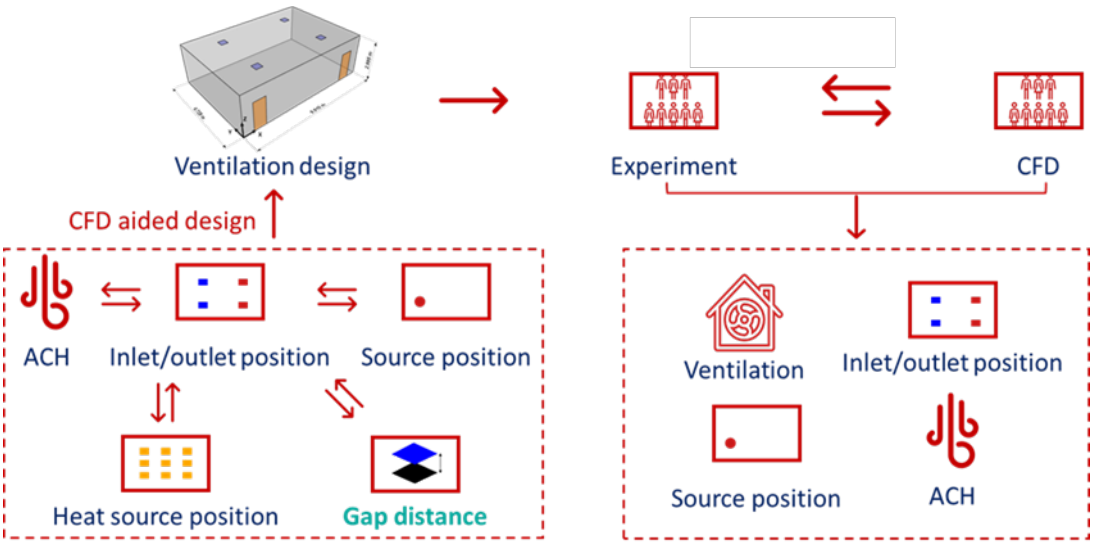

Figure 1. Overview of the research related to conventional CFD and the LTFC and MUSV cases to be investigated.

While the number of cases for LTCF and MUSV analysed with CFD was delayed and not fully completed due to measurement data that was not available or at a later time, many issues related to modeling were analysed and resolved. This new knowledge helped in better understanding issues related to modeling and design of room ventilation with aerosol (pathogen) exposure in mind. The table below provides a short summary of the main outcomes with respect to modeling exposure to aerosols (pathogens). Details have been reported earlier/elsewhere.

Topic	Short summary
Particle (aerosol) modeling	Three different ways of particle modeling have been investigated: Lagrangian, Eularian (scalar), Eularian (drift-flux). The analysis concluded that the drift-flux model is able to calculate concentration fields, while taking into account the settling velocity of particles. There is a need to include gravitational force for particles >2.5 µm (at least >5 µm)
Respiratory emission	Constant breathing and inhalation velocities were compared to a sinusoidal breathing condition. The conclusion is that it is possible to simply the sinusoidal breathing condition, though a sensitivity analysis was needed to define the best boundary conditions for that.
People movement	Different ways of modeling movement in a CFD model were investigated. Explicit modeling of movement in CFD is complex and not advised. An alternative approach through the implementation of a momentum source may induce the effect of movement (mixing). However, as long movement is confined to short-term disturbances, the assumption is that the overall effect on the exposure (dose) is limited. Therefore, it is not advised to model movement explicitly or implicitly (through a momentum source).
Particle residence time	The particle residence time is of importance as infectivity of a virus decays with time. If, for a virus released in the air, the time interval is known, the exposure risk can be better assessed. A procedure based on the radioactive tracer method was developed and tested. It is based on two passive tracers that are released simultaneously from the same pollutant source with the same

	release rate conditions. However, one of the tracers is inert, whereas the other one is considered 'radioactive' with a decay constant γ [s^{-1}].
Sensitivity of ACH on contaminant distribution	For a validated cleanroom case it was shown that complete mixing cannot be expected for a situation with an air change rate <6-10 h^{-1}. Such high values generally can only be expected in hospital environments. Normally, ventilation rates will be much lower and contaminant gradients in the room can be expected and should be considered.
In-room ventilation efficiency	As for pathogen exposure we are interested in analysing the performance of ventilation for an in-room source and in-room receiver which position we may not know in advance, a procedure was developed to assess such performance. It takes advantage of the use of CFD to relatively quickly simulate large numbers of cases. The procedure gives insights in the in-room ventilation effectiveness that was unavailable otherwise (earlier).
Source modeling	For modeling of the contaminant (aerosols) from a breathing persons, the effect of momentum and direction was investigated. Though for the assessment of in-room ventilation efficiency, no momentum is assumed (normal breathing), if activities such as speaking and singing are expected and source locations are known beforehand, then it may be wise to include a momentum and direction in the simulation model to represent the typical activity and analyse the ventilation design better.
Supply modeling	The modeling of the supply is a very important parameter when simulating a flow field with the help of CFD. Different types of supply openings have been investigated. From very simple to a supply that is used in practice. The analysis of that supply showed a high sensitivity to its design and application (see Figure below). I.e. small design changes can have large effects and use of the supply for different ACH can result in a different throw.

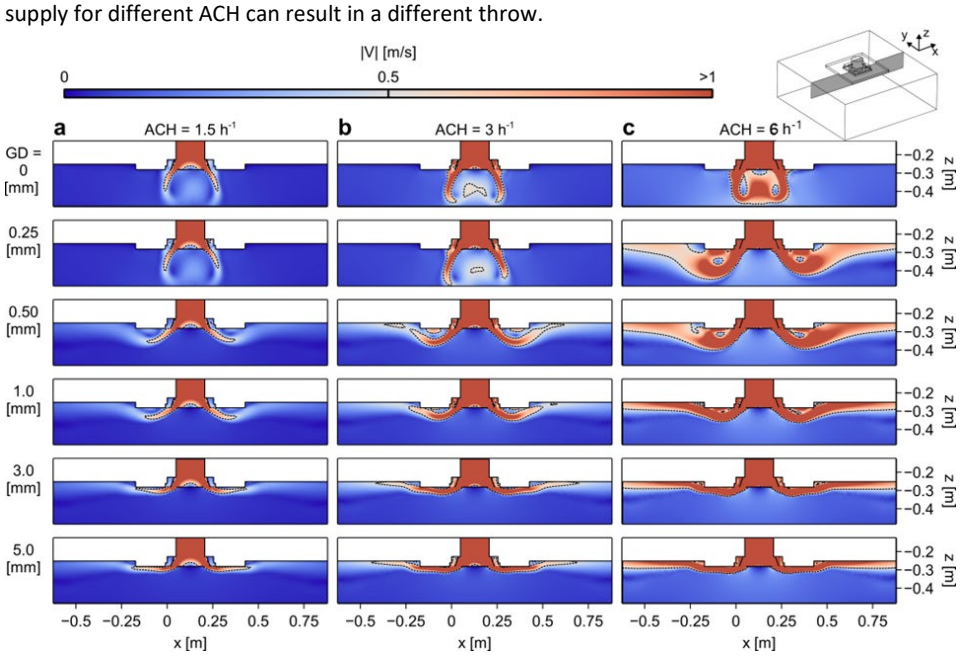

Figure Table. Analysis of the supply conditions as function of its design of the supply (GD = gap distance) and the ACH. Notably, small differences can have a large effect. The results were compared with measurements performed at the supply.

Ultimately, one LTCF case was investigated in full detail and representative for a procedure to investigate other cases for analysis of exposure to pathogens.

The assessment contained the following steps (covering ~1000 simulations):

- Validation with measurement data
- Define cases for comparison (different configurations supply and exhaust; different ACH; different design supply [gap distance])
- Perform assessment procedure for in-room ventilation assessment (i.e. many grid source locations)
- Analysis of the results

Figure 2 presents an example result for the velocity field at 1.2 m height (breathing height) for three different configurations of supply and exhaust and two different ACH. The difference in velocity magnitude identifies the increased air movement for the higher ACH. Figure 3 presents the contaminant distribution for the different locations of the source in the breathing plane. The graphs show, per ACH, 121 different locations of the source and how this affects the contaminant distribution in the breathing plane. Apart from the distribution, as the normalization is done towards theoretically perfectly mixed concentration for ACH = 1 h^{-1}, a higher ACH decreases the overall concentration. This result is also shown in Figure 4, but here the concentration fields are presented as the average concentration. Similarly to Figure 3, the position in the graph identifies the location of the source in the room.

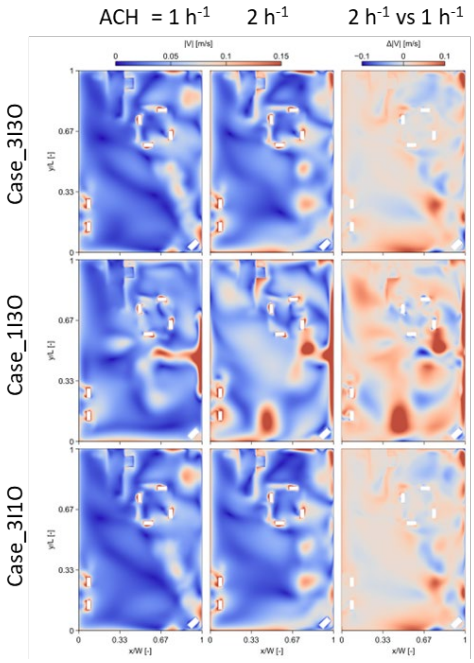

Figure 2. Velocity contour fields for the different cases (xI inlets and yO outlets; x,y = 1 or 3) for ACH = 1 or 2 h^{-1} and the difference in velocity magnitude between both ACH-cases.

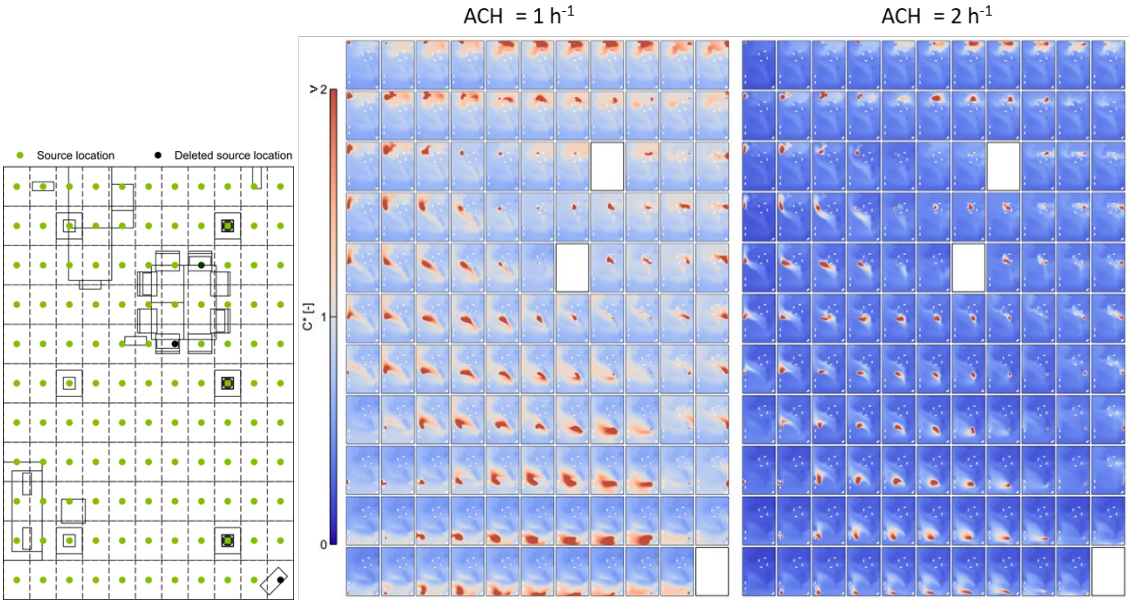

Figure 3. Normalized contaminant distribution at the breathing plane (1.2m height) as function of the source position [left figure] and two different ACH for the case with three inlets (located right) and three outlets (located left). Note the results are normalized to the exhaust concentration for ACH=1 h^{-1}. The results are presented for the case with three inlet and three outlets.

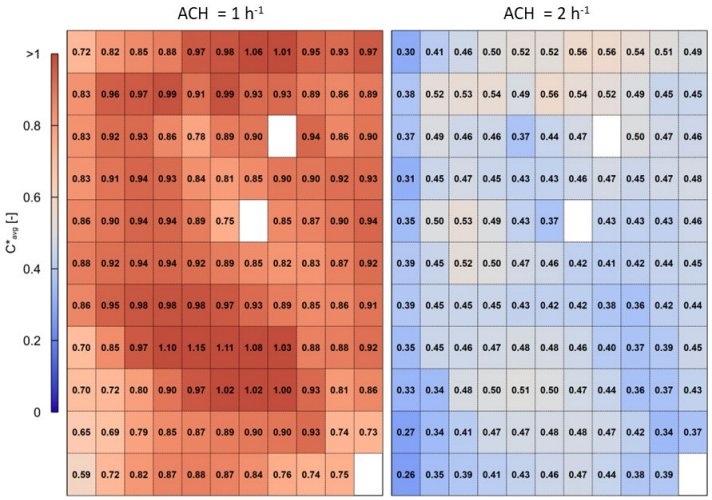

Figure 4. Average normalized concentration in the breathing plane (height 1.2 m) for the different source locations, for two different ACHs, for the case with three inlets and three outlets.

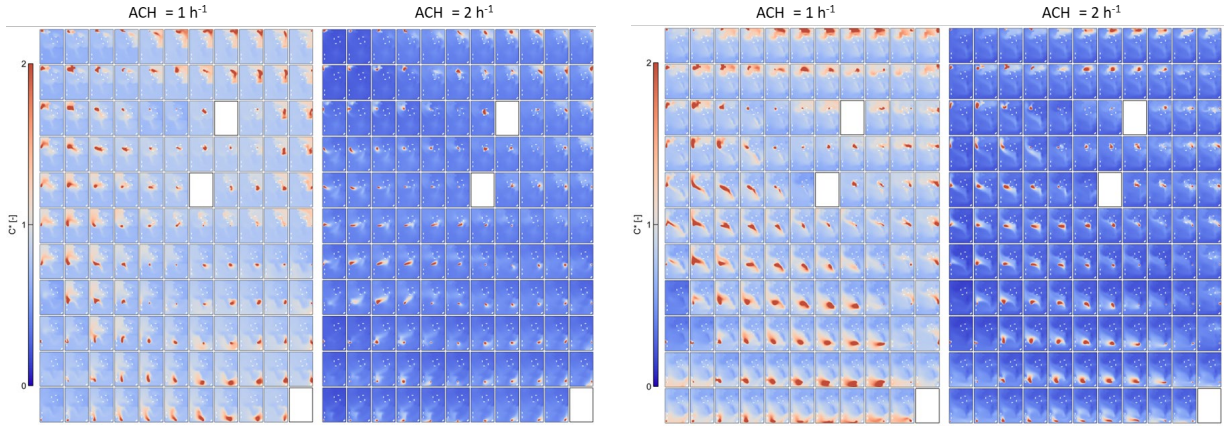

Figure 5. Normalized contaminant distribution at the breathing plane (1.2m height) as function of the source position for two different ACHs for cases with different inlet and outlet configurations.

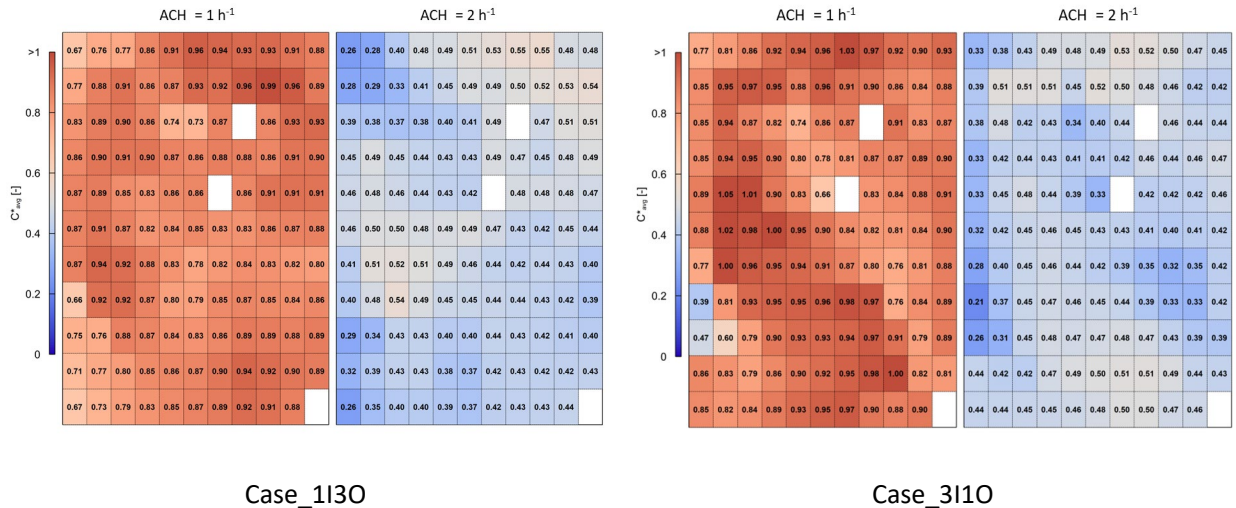

Figure 6. Average normalized concentration in the breathing plane (height 1.2 m) as function of the source position for two different ACHs for cases with different inlet and outlet configurations.

Figure 5 and Figure 6 present similar results as for Figure 3 and Figure 4, but now for the other ventilation configurations that were investigated. Though, overall, a similar behavior of the flow can be identified, the use of one inlet and three outlets shows a slightly better overall performance in case of ACH = 1 h^{-1}. This can also be shown when boxplots are determined from the average concentration values. For ACH = 2 h^{-1} the difference is less obvious, as is also shown in the boxplot in Figure 7. Two clear conclusions can be drawn from the figure. On average, a higher ventilation rate is the most effective measure for reducing exposure to aerosols. However, for the variants investigated with different ventilation rates, it appears that there are source positions that can (partially) negate the effect of an increased ventilation rate. Overall, as the concentration is normalized with the concentration for a perfectly mixed situation, the conditions in the breathing plane generally are better than a fully mixed assumption, both for ACH = 1 and 2 h^{-2}.

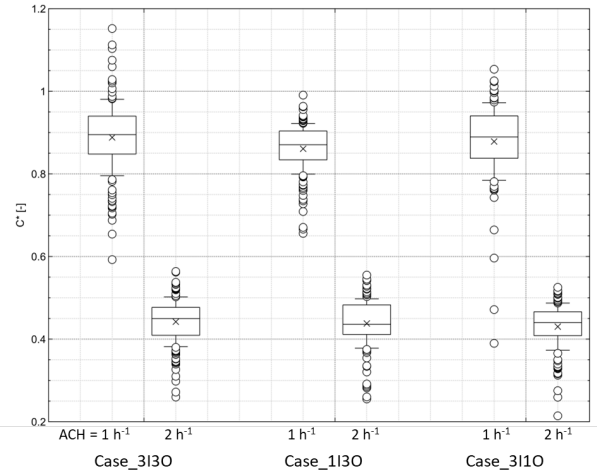

Figure 7. Boxplots of the average normalized concentration values for the different source locations, for different inlet and outlet configurations and different ACH.

The complete results for all variants there were investigated are summarized in the 'Handelingsperspectief Systeemconfiguratie'.

2.2. Publication: Ventilation and air cleaning in the context of infection risk – results from two large Dutch research projects

Within P3Venti a new approach for assessing the performance of a ventilation system was developed. An example for a complex LTCF case was described in paragraph 2.1. With this approach it is possible to identify how well a contaminant (e.g. pathogen) that is produced in the breathing zone is removed from the breathing zone in the room (i.e. cannot be inhaled). The approach allows an in-room analysis of the ventilation performance, as in the context of pathogen exposure, the source and receiver are located in the room. In order to have the assessment procedure assessed by peers, a conference article was prepared and presented for the Healthy Buildings Europe 2025 conference. At the time of writing the example in paragraph 2.1 was not yet available. In this paper also the test procedure for portable air cleaners was discussed with respect to room size and experimental approach and analysis. The reference information is:

Loomans, M. G. L. C., Xia, L., Peng, Q., & van Hooff, T. (2025). Ventilation and air cleaning in the context of infection risk: results from two large Dutch research projects. In O. H. Wallevik, V. E. Merida, & S. D. Sigurjonsdottir (Eds.), Healthy Buildings Europe 2025 Proceedings of an ISIAQ International conference (pp. 138-144). Reykjavik University.

The abstract of the published manuscript is provided below, including some representative figures (Figure 8-9).

Abstract: Ventilation and air cleaning are two important means of supporting indoor air quality in the context of the risk of exposure to pathogens. This paper presents two results, from Dutch research projects, related to expressing ventilation effectiveness and portable air cleaner performance. A new test facility was used in this research. The results show that in-room performance indicators like the source-specified surface-

averaged concentration add to the understanding of ventilation performance in the context of contaminant exposure. For portable air cleaners, the standardized clean air delivery rate (CADR) assessment procedure is relatively robust, but local variations in a large room are better captured by the so-called practical CADR assessment procedure.

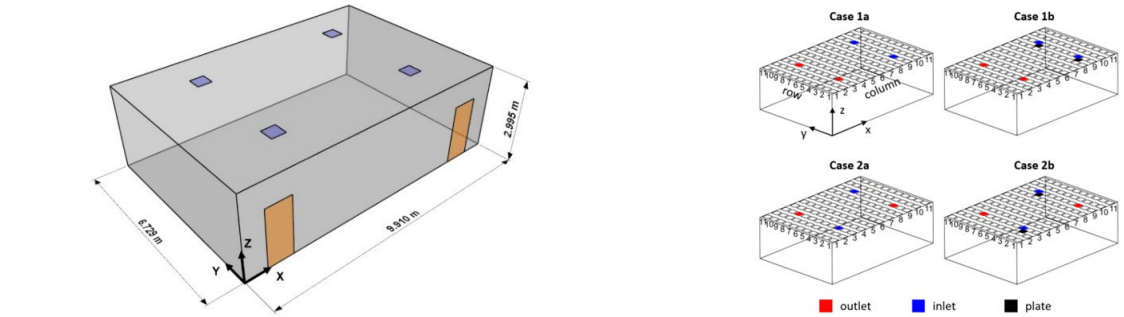

Figure 8. Schematic drawing of the test facility, including its dimensions (left). Investigated cases with different supply and exhaust configurations (right).

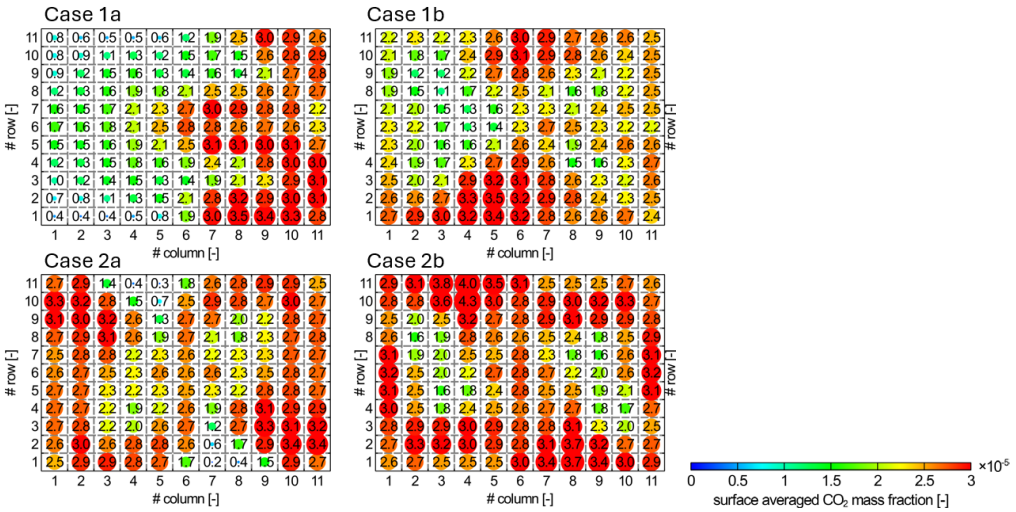

Figure 9. Surface averaged CO_2 mass-fraction at a horizontal plane at 1.2 m height for four different ventilation configurations. Sources are positioned at a 11×11 uniform grid (each cell represents one case).

2.3. Publication: Experimental and numerical analysis of particle distribution in a well-controlled mock-up: Impact of source conditions

The simplified test case setup with nine heat sources which was measured and analysed in PLIII provided the first real opportunity to perform a CFD study of the test facility and to validate the model. Apart from the validation, this model was also used to in more detail analyse the effect of breathing/speaking/singing (momentum and direction) on the contaminant distribution in the room . The validation work has been summarized in a paper, and was COBEE 2025. That COBEE paper has not been published, as it was intended to part of the content for a journal publication. A journal article in which also the detailed analysis was described was prepared in parallel. This journal article was accepted for publication on June 23rd 2025 (online June 27th), just before the COBEE conference. The reference information is:

Qin, P., de Lange, A., van Hooff, T., Traversari, R. and Loomans, M. 2025. Experimental and CFD analysis of particle distribution in a controlled test facility: Impact of exhalation flow velocity and direction. *Building and Environment*. https://doi.org/10.1016/j.buildenv.2025.113328

Qin, P. Qin, P., de Lange, A., van Hooff, T., Traversari, R. and Loomans, M. 2025. CFD validation of airflow and particle distribution in a controlled test facility. 6th International Conference on Building Energy and Environment (COBEE). Eindhoven

The abstract of the published journal article is provided below, including some representative figures (Figure 10-11).

Abstract: The dispersion of exhaled particles in indoor environments is significantly influenced by the airflow conditions. Constant human respiration conditions are widely employed in experiments and CFD simulations for indoor particle transmission studies. However, it remains challenging to reach a definitive consensus on how the exhalation flow velocity/rate and direction interact with the indoor airflow pattern and influence the indoor particle distributions. The goal of this study is to systematically investigate the impact of constant source conditions, specifically the exhalation flow velocity (EFV) and direction (EFD) at the source, on the particle distribution in a controlled test facility by experiments and CFD simulations. First, the velocity, temperature and concentration results obtained from CFD simulations, employing the RNG k-ε turbulence model, are validated with experimental results. Next, the validated computational setup is used for CFD simulations of the same test facility, incorporating two mixing ventilation configurations. Under each ventilation configuration, three different EFV (i.e. 2.33, 4.65, and 9.30 m/s), each with three EFD (i.e. positive y, negative y, and positive x), and a reference case with no EFV/EFD at the source are considered. The effect of the variation of EFV and EFD on the surface-averaged concentration (C_{avg}) on the breathing height plane (z = 1.2 m) generally remains below 5.8%, compared to the reference cases (no EFV/EFD). However, when considering the C_{avg} over a central area near the source, the C_{avg} deviation can reach up to 29.9%. This study enhances the understanding of indoor particle transmission and its dependency on the EFV and EFD.

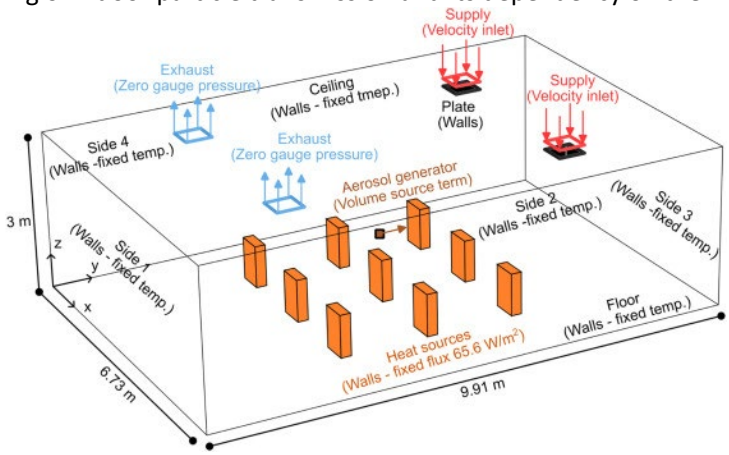

Figure 10. Computational domain with the indication of the boundary conditions (Type A; Note that for Type B, the supply and exhaust are positioned diagonally).

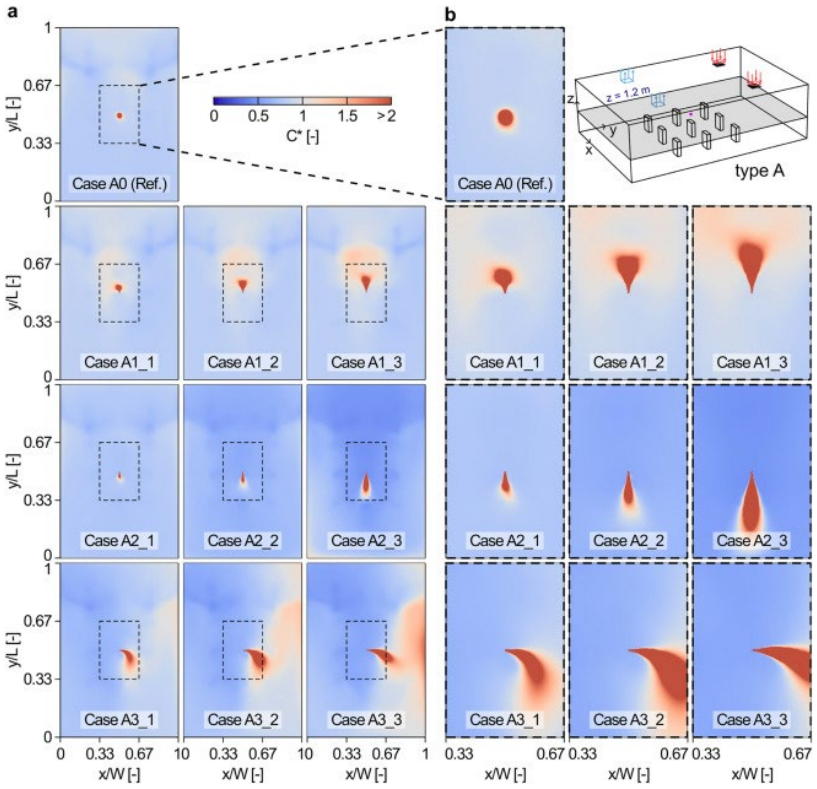

Figure 11. Comparison of normalized mean concentration (C*) contours of dp0.3 [particles with 0.3µm diameter] in the horizontal plane at z = 1.2 m for (a,b) Case A0, Case A1_1-3, Case A2_1-3, and Case A3_1-3, and (c,d) Case B0, Case B1_1-3, Case B2_1-3, and Case B3_1-3. Note that (b) and (d) are localized enlargements of (a) and (c), respectively, with x/W and y/L in the range of 0.33 and 0.67.

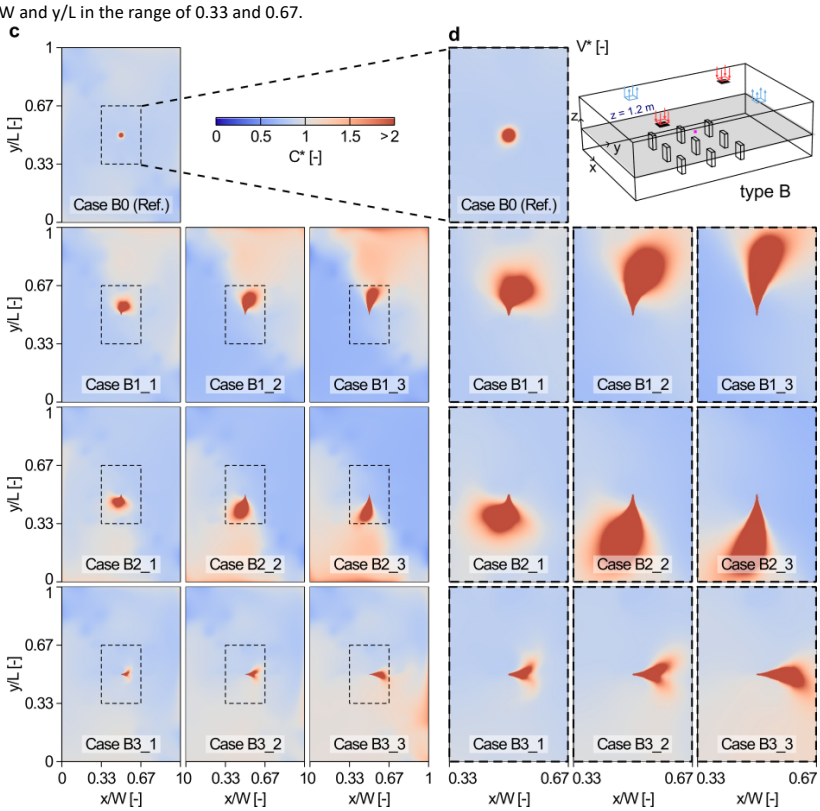

Figure 11. Continued.

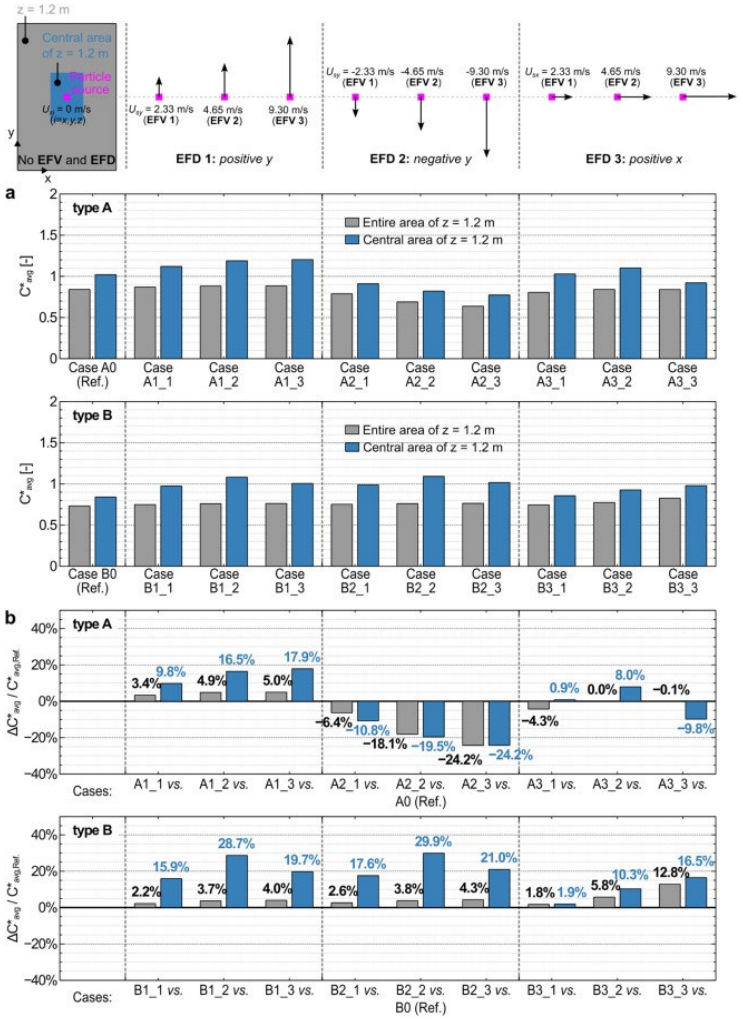

Figure 12. (a) Surface-averaged normalized concentration (C^*_{avg}) at z = 1.2 m, considering both the entire area and the central area, for cases with different exhalation flow velocities and directions (i.e. EFV and EFD) under ventilation types A and B. (b) Deviation ratio of relative differences in C^*_{avg} (ΔC^*_{avg}) between specific cases (Case A/B_{m_n}, m,n=1,2,3) and the reference case (Case A0/B0), normalized by C^*_{avg} of the reference case ($C^*_{avg,Ref}$).

3. Public presentations and publications of results related to P3Venti (2025)

Several publications presenting the results of work carried out in the context of P3Venti were realized in 2025. Additionally, the results were communicated to a wider public, peers and policymakers in conference presentations.

- ***Conference paper***: Loomans, M. G. L. C., Xia, L., Peng, Q., & van Hooff, T. (2025). Ventilation and air cleaning in the context of infection risk: results from two large Dutch research projects. In O. H. Wallevik, V. E. Merida, & S. D. Sigurjonsdottir (Eds.), *Healthy Buildings Europe 2025 Proceedings of an ISIAQ International conference* (pp. 138-144). Reykjavik University.
- ***Presentation***: Loomans, M. G. L. C., Xia, L., Peng, Q., & van Hooff, T. (2025). Ventilation and air cleaning in the context of infection risk: results from two large Dutch research projects. In O. H. Wallevik, V. E. Merida, & S. D. Sigurjonsdottir (Eds.), *Healthy Buildings Europe 2025 Proceedings of an ISIAQ International conference*
- ***Journal article***: Qin, P., de Lange, A., van Hooff, T., Traversari, R. and Loomans, M. 2025. Experimental and CFD analysis of particle distribution in a controlled test facility: Impact of exhalation flow velocity and direction. *Building and Environment*. https://doi.org/10.1016/j.buildenv.2025.113328
- ***Conference paper***: Qin, P. Qin, P., de Lange, A., van Hooff, T., Traversari, R. and Loomans, M. 2025. CFD validation of airflow and particle distribution in a controlled test facility. 6th International Conference on Building Energy and Environment (COBEE). Eindhoven (not published – added to Appendix)
- ***Presentation***: Qin P. 2025. CFD validation of airflow and particle distribution in a controlled test facility. Presented at the 6th International Conference on Building Energy and Environment (COBEE). Eindhoven. The Netherlands.
- ***Presentation***: Loomans, M.G.L.C. 2025. Pandemic Preparedness the relevance of air quality. Presented at the 6th International Conference on Building Energy and Environment (COBEE). Eindhoven. The Netherlands.
- ***Journal article***: Mamulova, E., Loomans, M., & van Hooff, T. (2025). RANS-based fast computational methods for indoor flows: a framework-driven performance assessment for a simple benchmark. Developments in the Built Environment, 23, Article 100716. https://doi.org/10.1016/j.dibe.2025.100716

Appendix

A.1. PDFs of publications and presentations

a. Loomans, M. G. L. C., Xia, L., Peng, Q., & van Hooff, T. (2025). Ventilation and air cleaning in the context of infection risk: results from two large Dutch research projects. In O. H. Wallevik, V. E. Merida, & S. D. Sigurjonsdottir (Eds.), *Healthy Buildings Europe 2025 Proceedings of an ISIAQ International conference* (pp. 138-144). Reykjavik University**. (full paper + presentation)**
b. Qin, P., de Lange, A., van Hooff, T., Traversari, R. and Loomans, M. 2025. Experimental and CFD analysis of particle distribution in a controlled test facility: Impact of exhalation flow velocity and direction. *Building and Environment*. https://doi.org/10.1016/j.buildenv.2025.113328 *(***journal article** - *open access, not included in the Appendix)*
c. Loomans, M.G.L.C. 2025. Pandemic Preparedness the relevance of air quality. Presented at COBEE 2025. Eindhoven. The Netherlands. **(presentation)**
d. Qin, P., de Lange, A., van Hooff, T., Traversari, R. and Loomans, M. 2025. Experimental and CFD analysis of particle distribution in a controlled test facility: Impact of exhalation flow velocity and direction. Presented at COBEE 2025. Eindhoven. The Netherlands. **(full paper + presentation)**
e. Mamulova, E., Loomans, M., & van Hooff, T. (2025). RANS-based fast computational methods for indoor flows: a framework-driven performance assessment for a simple benchmark. Developments in the Built Environment, 23, Article 100716. https://doi.org/10.1016/j.dibe.2025.100716 *(***journal article** - *open access, not included in the Appendix)*
f. Qin, P., A., van Hooff, T., and Loomans, M. 2025. Toward an accurate CFD modeling of air distribution in the near zone of a realistic supply ventilation terminal: Sensitivity analysis of computational and physical parameters. (**concept journal article** - *not included in the Appendix)*

Ventilation and air cleaning in the context of infection risk – results from two large Dutch research projects

Marcel G.L.C. Loomans [1,*], Lili Xia[1], Qin Peng[1], Twan van Hooff[1]

[1] Eindhoven University of Technology, Eindhoven, The Netherlands

[*] *Corresponding email: M.G.L.C.Loomans@tue.nl*

SUMMARY

Ventilation and air cleaning are two important means of supporting indoor air quality in the context of the risk of exposure to pathogens. This paper presents two results, from Dutch research projects, related to expressing ventilation effectiveness and portable air cleaner performance. A new test facility was used in this research. The results show that in-room performance indicators like the source-specified surface- averaged concentration add to the understanding of ventilation performance in the context of contaminant exposure. For portable air cleaners, the standardized clean air delivery rate (CADR) assessment procedure is relatively robust, but local variations in a large room are better captured by the so-called practical CADR assessment procedure.

KEYWORDS

Exposure; Ventilation effectiveness; Air cleaning; CFD; Measurements.

INTRODUCTION

The Covid-19 pandemic has been a reminder of what the impact can be when we are in contact with airborne pathogens to which we don't yet have resistance. This pandemic was able to change a persistent dogma of the last ~100 years that airborne infection was not an important means of disease transmission (Jimenez et al., 2022). As a result, more attention is being paid to the quality of indoor air.

Although source control is the best strategy to improve the indoor air quality, it is often not feasible. Therefore, since Covid-19, more attention is paid to ventilation and air cleaning (Morawska et al. 2020). Also in the Netherlands, several research projects have been initiated to improve our understanding of the effectiveness of ventilation and (portable) air cleaning in the context of pathogen removal (P3Venti; www.p3venti.nl; CLAIRE; claireproject.nl). In these projects, general research questions to be answered relate to how to assess the performance of a ventilation design and how portable air cleaners perform in realistic situations. This paper presents two results of novel work done to support the answers to these general research questions, one concerning the ventilation effectiveness and one related to the performance of a portable air cleaner.

METHODS

As part of answering the research questions, a large test facility was designed and built at the Eindhoven University of Technology (see Figure 1, left). This large room is assumed to be representative of a classroom or living room in a long-term care facility. The room is used for airflow research, to provide validation data for CFD simulations, and to test the performance of portable air cleaners.

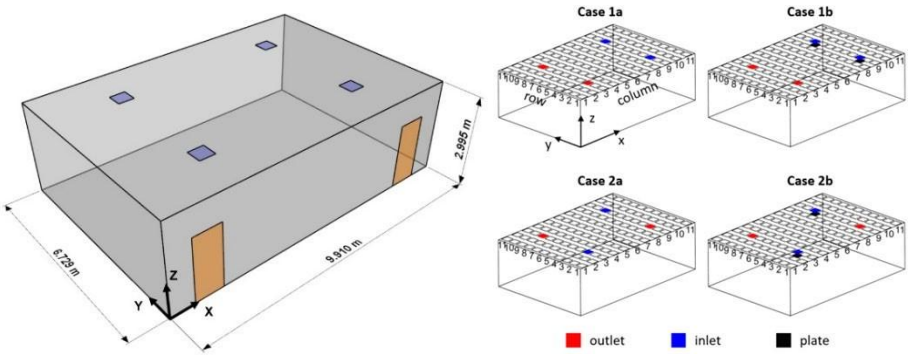

Figure 1. Schematic drawing of the test facility, including its dimensions (left). Investigated cases with different supply and exhaust configurations (right).

The test facility is equipped with an HVAC system capable of supplying conditioned HEPA-filtered air up to an air change rate of 6 h^{-1}. The room is airtight, resulting in an infiltration rate of 0.01 h^{-1}.

Ventilation effectiveness

As part of the design process, the test facility was analyzed using Computational Fluid Dynamics (CFD) to study the flow field. This analysis has been published elsewhere (Kang et al., 2024). Figure 1 (right) shows the cases studied as part of that analysis. It is an isothermal case with two supply and two exhaust grilles in the ceiling. The supply was designed as a perforated grille. For cases 1b and 2b, a plate was fixed 100 mm below the grille to force the air horizontally into the room. An air exchange rate of 3 h^{-1} was assumed for each case.

The CFD simulations in this study use the same computational domain, grid, boundary conditions, and solver settings as in the study by Kang et al. (2024). In addition, a total of 121 source locations at the breathing height (i.e. 1.2 m height), instead of the two source locations studied by Kang et al. (2024), are considered here to further investigate and visualize the ventilation effectiveness for different source locations. The developed procedure assumes a constant contaminant source that is released consecutively in a horizontal and regular grid (11×11) across the room. No momentum is assumed for the release of the contaminant. This assumption allows the flow field in the CFD simulations to be fixed and only the contaminant distribution in the room to be calculated. This is done for each source location on the grid. Next, the results are presented as an average pollutant concentration for a selected plane in the space. Since the interest is in human pathogen emissions, the grid of sources is assumed at the level of the mouth (0.1 m diameter sphere with CO_2 emission rate of 0.001 kg/m^3/s at 1.2m height). Similarly, assuming that breathing takes place at a similar height, the interest is in the

concentration field at breathing height. Therefore, the average concentration in the room as a function of the source location is calculated for this height.

Portable air cleaner performance

The performance of portable air cleaners (PACs) was also tested in the large test facility. A comparison was made between analyzing the performance of a PAC according to the ANSI/AHAM standard (ANSI/AHAM, 2020), which should be performed in a ~28 m^3 room, and the performance in a realistically sized room (large test facility ~200 m^3). The performance is expressed in Clean Air Delivery Rate (CADR [m^3/h]). The resulting CADR is referred to as the theoretical CADR ($CADR_{th}$). An alternative approach following another standard (DIN/TS 67506; Deutsches Institut für Normung, 2022) was investigated as well. The resulting CADR from this analysis is called the practical CADR ($CADR_{pr}$).

The DIN/TS 67506 method is almost identical to ANSI/AHAM. Both compare a situation with only natural decay of aerosols and a situation with the PAC on. However, for the DIN/TS 67506 method the fans in the room are switched off at the start of the decay measurements. So air movement in the room then is limited for natural decay measurements, or only the result from the active PAC. In the ANSI/AHAM standard the fans are kept running during both decay measurements. In this paper the effect of the room size and difference in outcome for the two standards are presented for a specific PAC. Figure 2 shows a schematic of the type of PAC studied and the set-up in the ANSI/AHAM test room and the large test facility (Xia et al. 2024). All measurements were repeated three times.

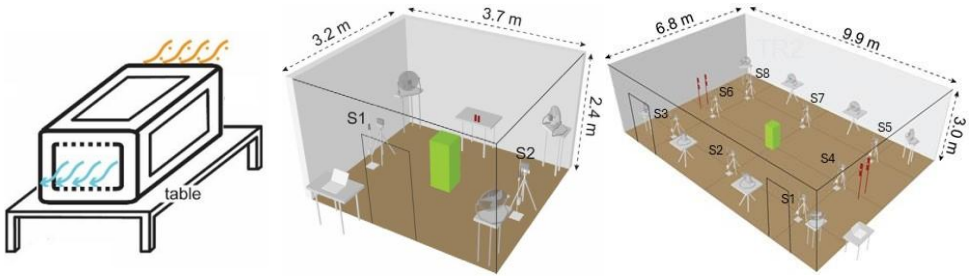

Figure 2. Schematic of the investigated PAC (left). Lay-out of the measurement set- up in the 28 m^3 test room (middle) and large test facility (right). S1-2/S1-8 represent the positions of the particle counters. Fans are visualized as well. The green box represents the position of the PAC.

The results are presented as $CADR_{th}$ and $CADR_{pr,}$ for the particle sizes monitored. In the analysis, the sensitivity towards the time interval used for calculating the decay rate was also investigated. Comparisons are made in terms of CADR for the relative $CADR_{th}$ difference between the ANSI/AHAM standard room size and the large room size of the test facility (D_{th}), the relative difference between the $CADR_{th}$ from the ANSI/AHAM standard room size and $CADR_{pr}$ from the large room ($D_{pr\text{-}th,\ TR1}$) and the relative difference between $CADR_{th}$ and $CADR_{pr}$, both for the large room ($D_{pr\text{-}th,\ TR2}$). Such comparisons have not been presented earlier.

RESULTS AND DISCUSSION

Ventilation effectiveness

Figure 3 shows results of the airflow in the room for the four cases presented in Figure 1. The velocity path lines clearly show the effect of the plates on the flow field in the room (case 1b and 2b). Figure 4 shows the surface-averaged mass fraction of the pollutant at a height of 1.2 m for a grid of 11×11 uniformly distributed source positions, for the four cases studied. Note that in this case the pollutant (CO_2) is a gaseous pollutant. Assuming, for example, the drift-flux model, it is possible to account for aerosols and calculate their distribution similarly.

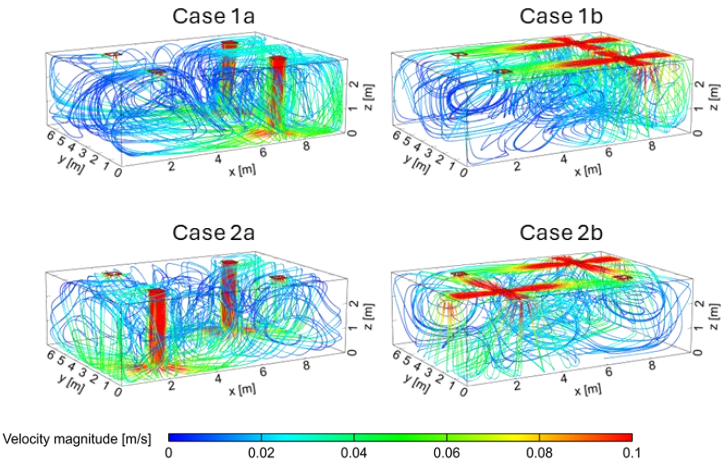

Figure 3. Velocity path lines for the different cases.

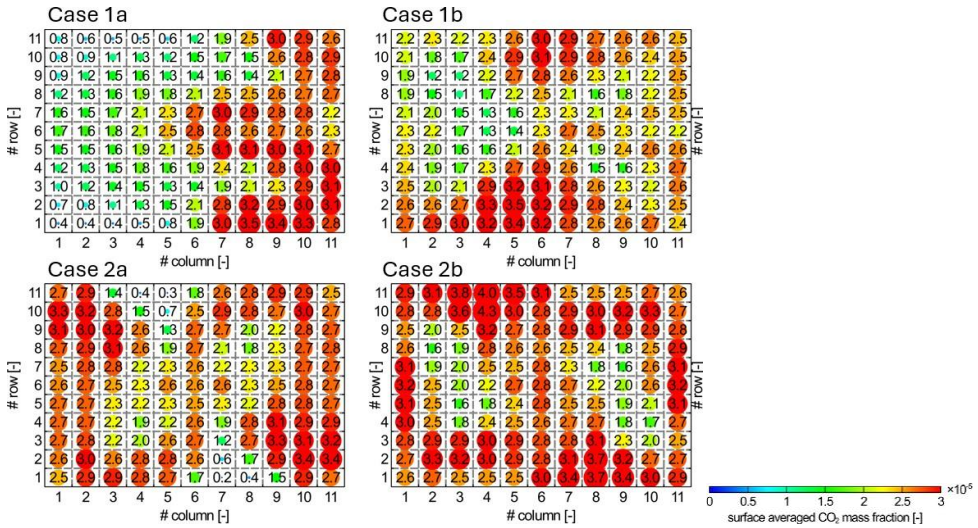

Figure 4. Surface averaged CO_2 mass-fraction at a horizontal plane at 1.2 m height. Sources are positioned at a 11×11 uniform grid (each cell represents one case).

The results show that the design of the supply and the position of the supply and exhaust influence the removal of contaminants in a room. The developed procedure differs from the analysis of the air change efficiency (REHVA, 2004) in that individual source locations are examined. Although the absolute results are shown in Figure 4, the procedure has a clear resemblance to the assessment of the contaminant removal effectiveness. In this case, the

capabilities of CFD are used to calculate the distribution of the contamination in the room. Only average results are shown in the example. Nevertheless, the available information can be used to identify the distribution of the contamination. For example, the standard deviation, assuming a normal distribution, or a box plot can provide an indication of the concentration variation throughout the plane. The visualization then has to be updated. Alternatively, areas can be selected to focus the results, rather than an area average for the entire room. This would allow a better assessment of the risk of exposure within a room when the location of the source is not known.

Portable air cleaner performance

Table 1 shows the $CADR_{th}$ for the two rooms and $CADR_{pr}$ for the large room. The results are presented as a function of the number of data points (time interval) that have been used to analyse the decay, and the particle size. A larger number of data points improves the evaluation of the CADR.

Table 1. $CADR_{th}$, $CADR_{pr}$, and the relative difference for the investigated air cleaner across various particle sizes (0.25, 0.25-0.5, 0.5-3, 3-10 μm), data points (related to time interval) and rooms (TR1: small room; TR2: large room).

Parameter	Data points	PM0.25	PM0.25-0.5	PM0.5-0.3	PM3-10
$CADR_{th,TR1}$ (m^3/h)	12	334	342	351	368
$CADR_{th,TR2}$ (m^3/h)	9	302	309	321	434
	12	319	325	333	433
	19	329	333	339	422
$CADR_{pr,TR2}$ (m^3/h)	12	364	371	388	439
	30	355	360	374	447
	50	366	370	382	457
D_{th} (%)	12 TR1, 19 TR2	-2	-3	-3	15
$D_{pr\text{-}th,\ TR1}$ (%)	12 TR1, 50 TR2	10	8	9	24
$D_{pr\text{-}th,\ TR2}$ (%)	19 TR2, 50 TR2	11	11	13	8

From Table 1 it can be concluded that for larger particles (PM3-10) the CADR for the large room is in the order of 20% larger than that for the smaller room. This is similar when compared to the smaller particle sizes for the large room. It is assumed that deposition contributes to the CADR obtained. It is noteworthy that the difference $D_{pr\text{-}th,TR2}$ is similar for all particle sizes. This indicates that, due to the way the CADR is determined, the deposition is not really affected by the additional air movement caused by the fans, as applied for determining $CADR_{th}$. Not shown in Table 1, but identified from the individual results of the particle counters (S1-S8; Figure 2), the situation without the fans operating ($CADR_{pr}$) results in more variation between the particle counters, up to an order of 100%, especially for larger particles (PM3-10). So, while the averages at room level between a theoretical assessment according to ANSI/AHAM and a practical assessment according to DIN don't show much differences, locally it can be expected that $CADR_{pr}$ gives more realistic performance levels for the air cleaner.

CONCLUSION

The paper presents two results from ongoing research as part of two large Dutch research projects focussed at the mitigation of pathogen exposure through ventilation and air cleaning.

For ventilation, the proposed methodology to investigate the contaminant distribution in a room extends the option to assess the performance of a ventilation design. It provides an insightful assessment of the effectiveness with which contaminant with an unknown source location can be removed from a room. The rich CFD data can be used to extend the assessment, e.g., to fine-tune the analysis to zones in the room.

For air cleaners, different evaluation methods (room size/standards) were tested to assess their impact on the performance of a PAC. For the PAC studied, the room size is most important, especially for the larger particle sizes (PM3-10). Evaluation of the CADR with fans on (theoretical approach) or fans off (practical approach) shows relatively small differences. Results from the practical approach, however, do show local variations of the CADR throughout the investigated room.

Research on extensions of the analysis of the ventilation performance continues. Among other things, the effect of a momentum source in the release of a contaminant is being investigated. Air cleaner performance tests are extended by including the effect of the position of the air cleaner in the room and combining it with ventilation.

ACKNOWLEDGEMENT

The research presented received funding from the Pandemic Preparedness Programme and Ventilation (P3Venti Program) coordinated by the Netherlands Organization for Applied Scientific Research TNO and funded by the Dutch Ministry of Health, Welfare and Sport and the collaboration project CLAIRE (LSHM22032), co-funded by the PPP Allowance made available by Health~Holland, Top Sector Life Sciences & Health, to stimulate public-private partnerships (https://www.health- holland.com/).

REFERENCES

ANSI/AHAM. 2020. *ANSI/AHAM AC-1-2020: Method for Measuring Performance of Portable Household Electric Room Air Cleaners*. Washington, DC: Association of Home Appliance Manufacturers (AHAM).

DIN. 2022. *DIN/TS 67506: Disinfection of indoor air using UV-C secondary air units*.

Deutsches Institut für Normung.

Jimenez, J. L., Marr, L. C., et al. 2022. What were the historical reasons for the resistance to recognizing airborne transmission during the COVID-19 pandemic? *Indoor Air*, 32(8), Article e13070. https://doi.org/10.1111/ina.13070.

Kang, L., Qin, P., Diepens, J., van Hooff, T., & Loomans, M. G. L. C. 2024. CFD-aided ventilation design for a large experimental chamber to study aerosol dispersion and removal. 1-8. In: *Proceedings RoomVent 2024*, Stockholm, Sweden.

Morawska, L., Tang, J. W., et al. 2020. How can airborne transmission of COVID-19 indoors be minimised? *Environment International*, 142, Article 105832. https://doi.org/10.1016/j.envint.2020.105832.

REHVA. 2004. *Ventilation effectiveness*, REHVA Guidebook No 2. Brussel, Belgium: Federation of European Heating and Air-conditioning Associations.

Xia, L., Diepens, J., Loomans, M. G. L. C., & van Hooff, T. (2024). Testing and comparing of portable air cleaners for indoor aerosol particle removal in laboratory environments. 1-7. In: *Proceedings RoomVent 2024*, Stockholm, Sweden.

SS 554 (2016) *Code of practice for indoor air quality for air-conditioned buildings*.

WHO (2010) *Guidelines for indoor air quality: selected pollutants*, *World Health Organization. Regional Office for Europe.* Geneva: World Health Organization.

WHO (2021) *Global air quality guidelines: Particulate matter (PM2.5 and PM10), ozone, nitrogen dioxide, sulfur dioxide and carbon monoxide*. Geneva: World Health Organization.

Wong, N.H. and Huang, B. (2004) 'Comparative study of the indoor air quality of naturally ventilated and air-conditioned bedrooms of residential buildings in Singapore', *Building and Environment*, 39(9), pp. 1115–1123.

Xu, X. *et al.* (2021) 'Environmental factors affecting sleep quality in summer: a field study in Shanghai, China', *Journal of Thermal Biology*, 99(April), p. 102977.

CLAIRE | CLEAN AIR FOR EVERYONE

p3 venti

Ventilation and air cleaning in the context of infection risk

results from two large Dutch research projects

Marcel Loomans
Lili Xia
Peng Qin
Twan van Hooff

Healthy Buildings Europe 2025

TU/e

Credits

We are grateful to the funding agencies and the partners in the projects, whose contributions made the research presented possible.

p3 venti

Rijksoverheid

CLAIRE | CLEAN AIR FOR EVERYONE

NL Health~Holland
SHARED CHALLENGES, SMART SOLUTIONS

And of course thanks to all TU/e colleagues that contributed to this work!

TU/e

The issue (pathogens)

Keep distance

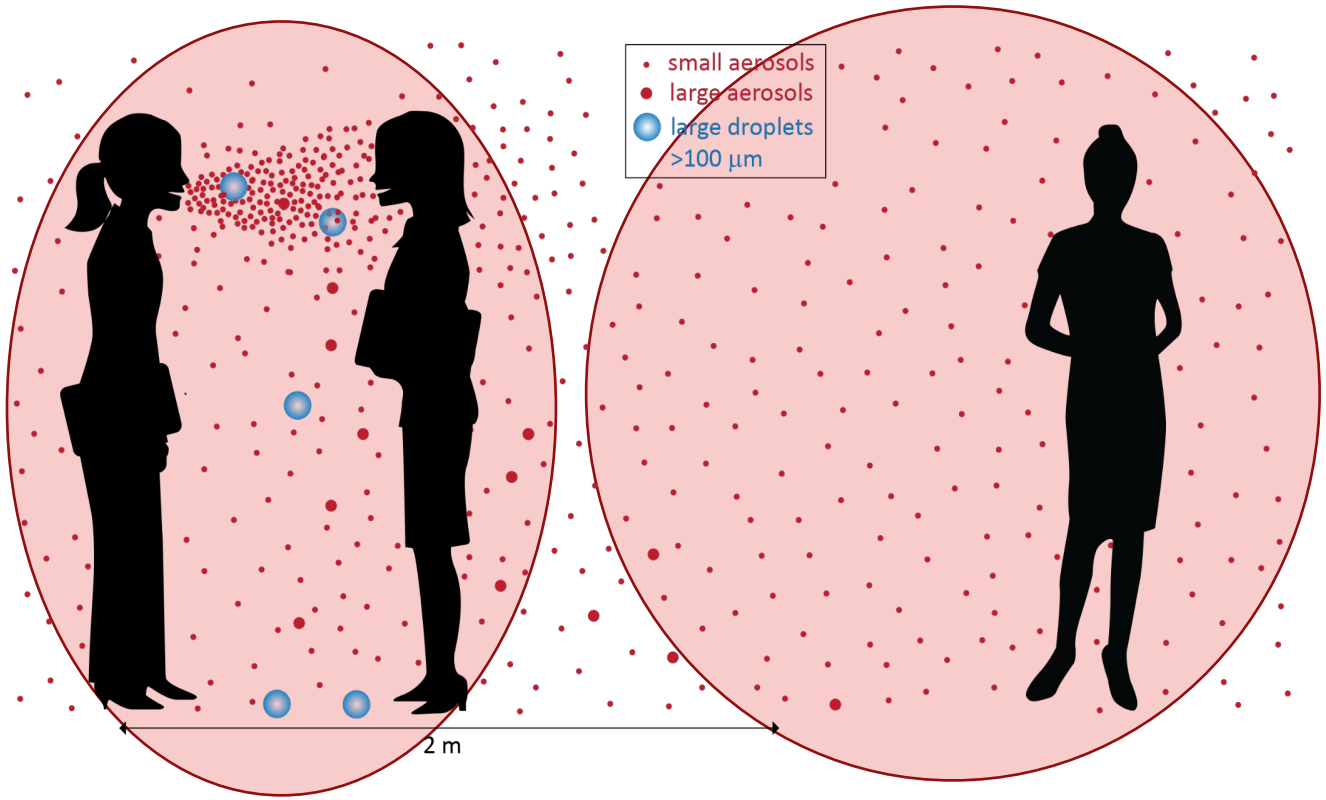

Dilution (ventilation, air cleaning)

Jimenez JL, Marr LC, Randal K, Ewing ET, Tufekci Z, Greenhalgh T, et al. 2022. What Were the Historical Reasons for the Resistance to Recognizing Airborne Transmission during the COVID-19 Pandemic? Indoor Air; Vol. 32, Iss.8

TU/e

Introduction

Need for more research on

- Ventilation and air cleaning (portable air cleaners [PAC])

Main research question (paper):

How to assess the (realistic) performance of a (1) ventilation design or (2) portable air cleaner in the context of exposure to pathogens?

CLAIRE | CLEAN AIR FOR EVERYONE p3 venti TU/e

Method

Development of large test facility

Dimensions: ~7x10x3 m
HEPA filtered supply air
0.5-6 ACH
Temperature controlled
Free placement of supply and exhaust grilles

CLAIRE | CLEAN AIR FOR EVERYONE
p3 venti
TU/e

Method (1)

Effect different designs supply and position supply and exhaust
CFD analysis contaminant distribution for grid of sources

Ventilation effectiveness

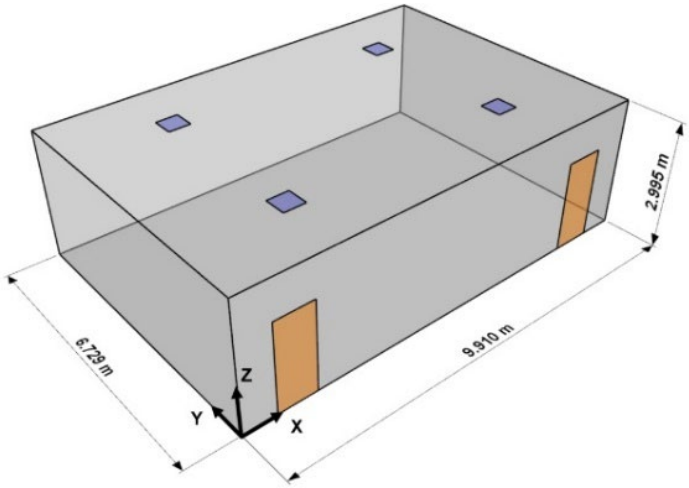

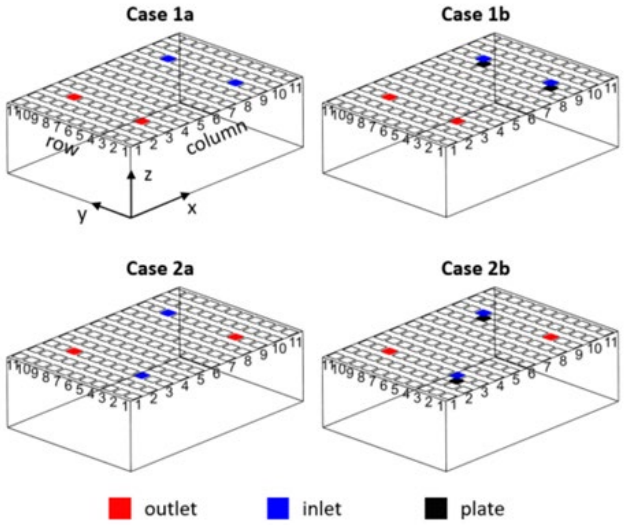

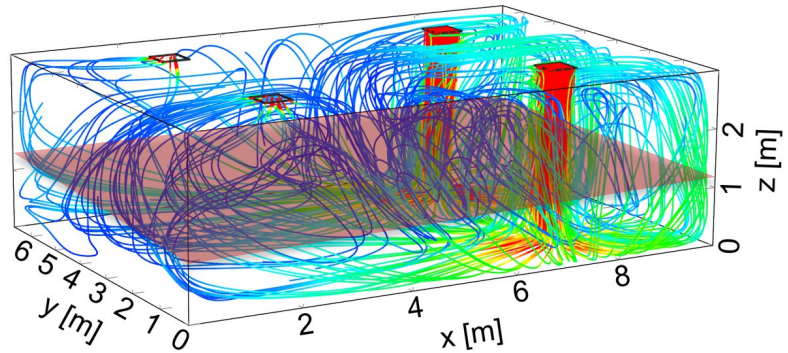

CLAIRE CLEAN AIR FOR EVERYONE p3 venti TU/e

Results and discussion (1)

Ventilation effectiveness

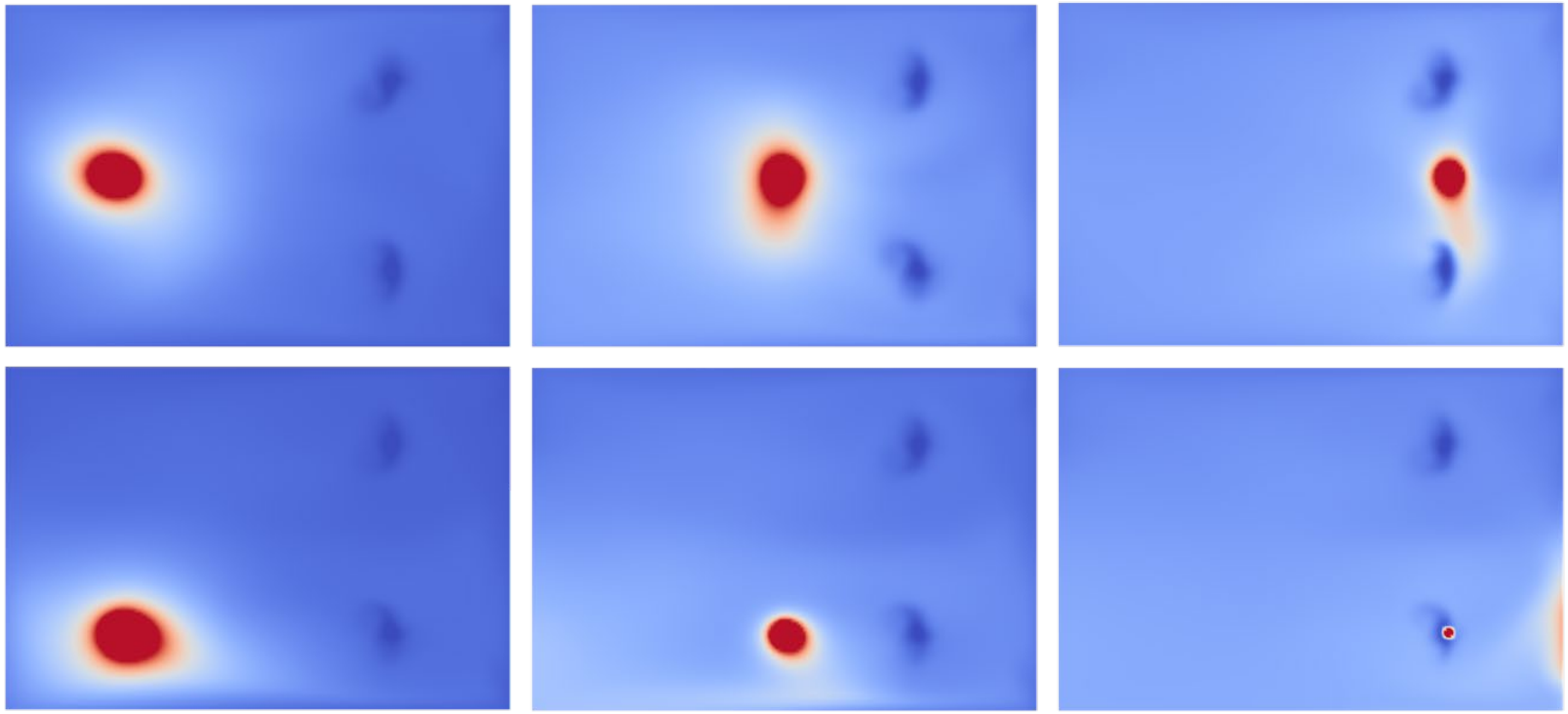

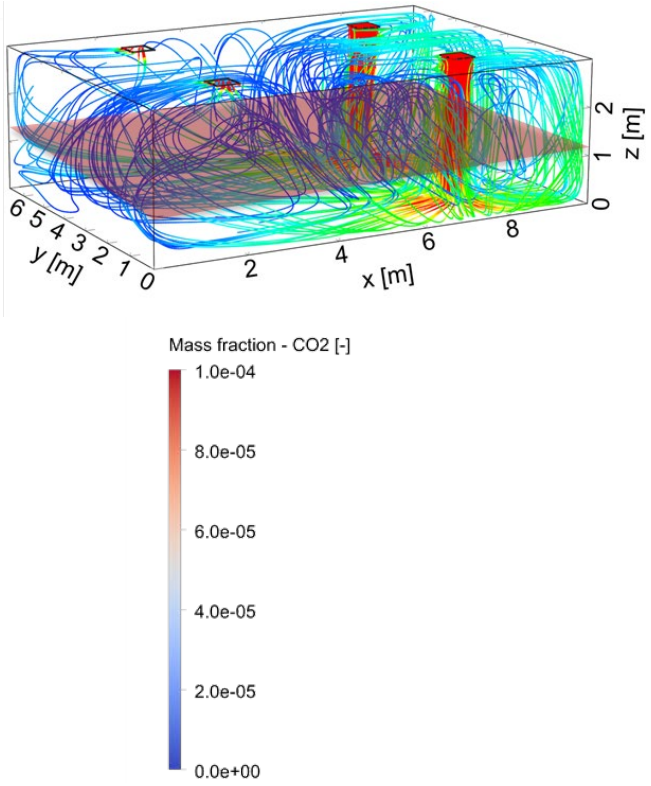

CLAIRE CLEAN AIR FOR EVERYONE p3 venti TU/e

Results and discussion (1)

Position of source affects average concentration

Effectivity ventilation improved by positioning sources near exhaust

Ventilation effectiveness

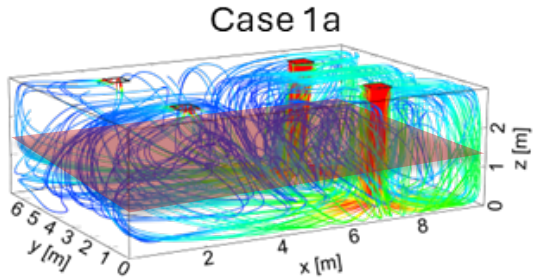

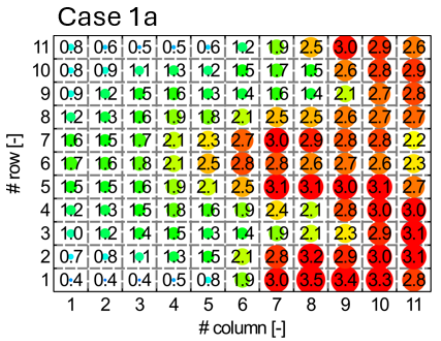

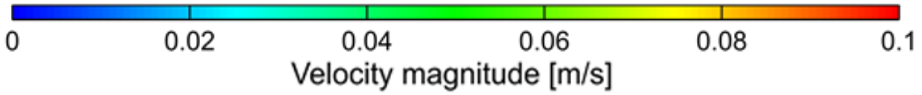

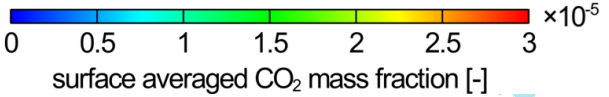

CLAIRE CLEAN AIR FOR EVERYONE p3 venti TU/e

Method (2)

PAC performance according to ANSI/AHAM standard [mixing fans]: **$CADR_{th}$**
Effect of room size
Effect of PAC performance practical application [DIN; no mixing fans]: **$CADR_{pr}$**

Portable Air Cleaner (PAC) performance

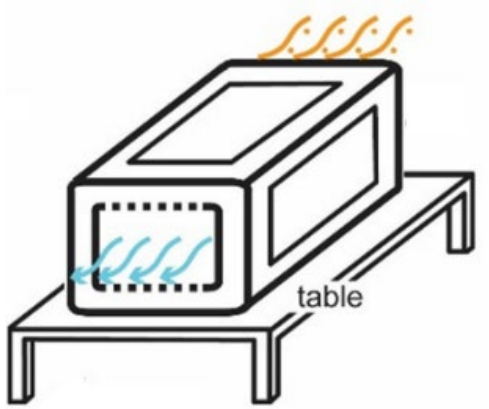

Air cleaner schematic

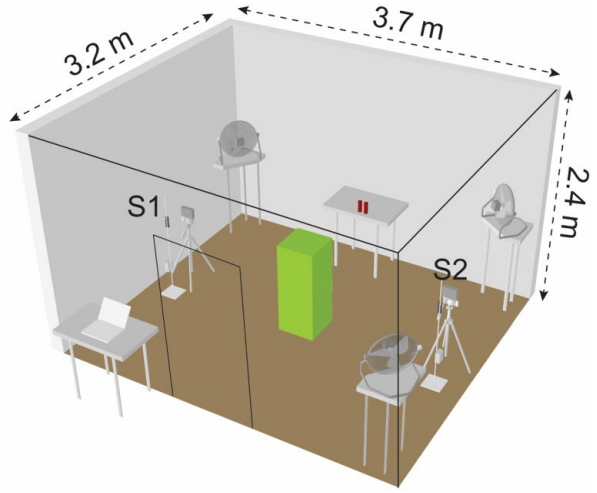

$CADR_{th,TR1}$
TR1: Test room ANSI/AHAM

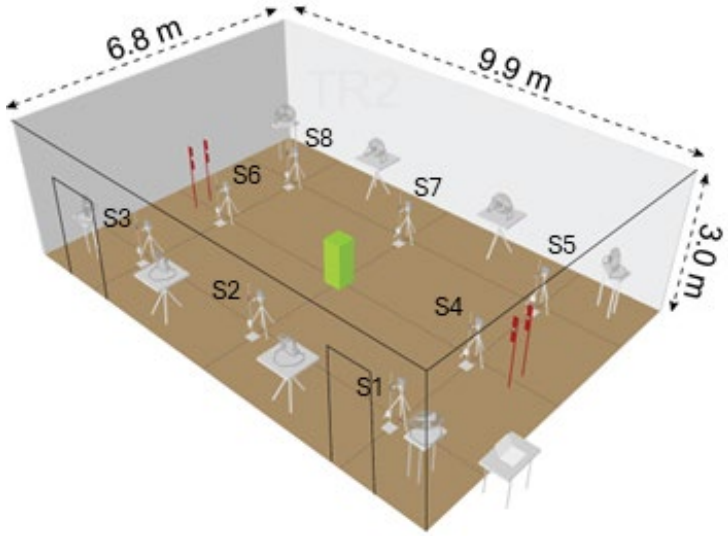

$CADR_{th,TR2}$ $CADR_{pr,TR2}$
TR2: Set-up large test facility

CADR = Clean Air Delivery Rate [m^3/h]

CLAIRE CLEAN AIR FOR EVERYONE p3 venti TU/e

Results and discussion (2)

Portable Air Cleaner (PAC) performance

Parameter	PM0.25	PM0.25-0.5	PM0.5-0.3	PM3-10
$CADR_{th,TR1}$ (m^3/h)	334	342	351	368
$CADR_{th,TR2}$ (m^3/h)	329	333	339	422
$CADR_{pr,TR2}$ (m^3/h)	366	370	382	457
$Difference_{th,\ TR1\text{-}TR2}$ (%)	-2	-3	-3	15
$Difference_{pr\text{-}th,\ TR2}$ (%)	11	11	13	8

th: theory – according to ANSI/AHAM (mixing fans during decay)
pr: practice – according to DIN (no mixing fans during decay)

TR1

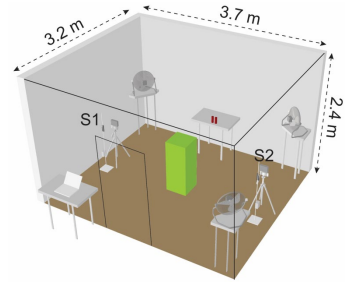

TR2

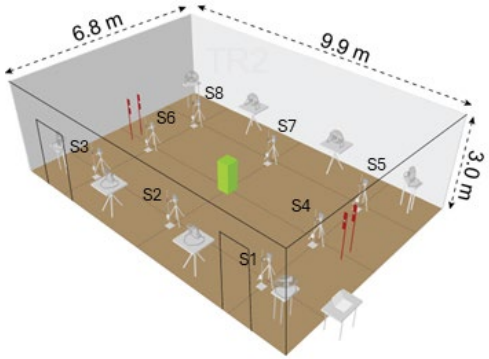

CLAIRE CLEAN AIR FOR EVERYONE p3 venti TU/e

Conclusions

(0) Test facility useful for ventilation research

- Several tests performed for different ventilation configurations, and air cleaners
- Validation data for CFD simulations

(1) Grid of sources + analysis of breathing zone provides info on in-room ventilation effectiveness

- Extension possible: info on variation, attention to local areas

(2) For PAC assessment, room size important consideration (PM3-10)

- Local variations in the room with practical approach ($CADR_{pr}$)

CLAIRE | CLEAN AIR FOR EVERYONE p3 venti TU/e

Thank you

More info

P3Venti; www.p3venti.nl

CLAIRE; www.claireproject.nl

Pandemic Preparedness the relevance of air quality

Marcel Loomans

Credits

We are grateful to the funding agencies and the partners in the projects, whose contributions made the research presented possible.

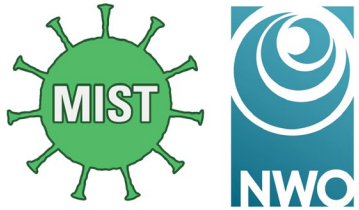

And of course thanks to all TU/e colleagues that contributed to this work!

The issue (pathogens)

Keep distance

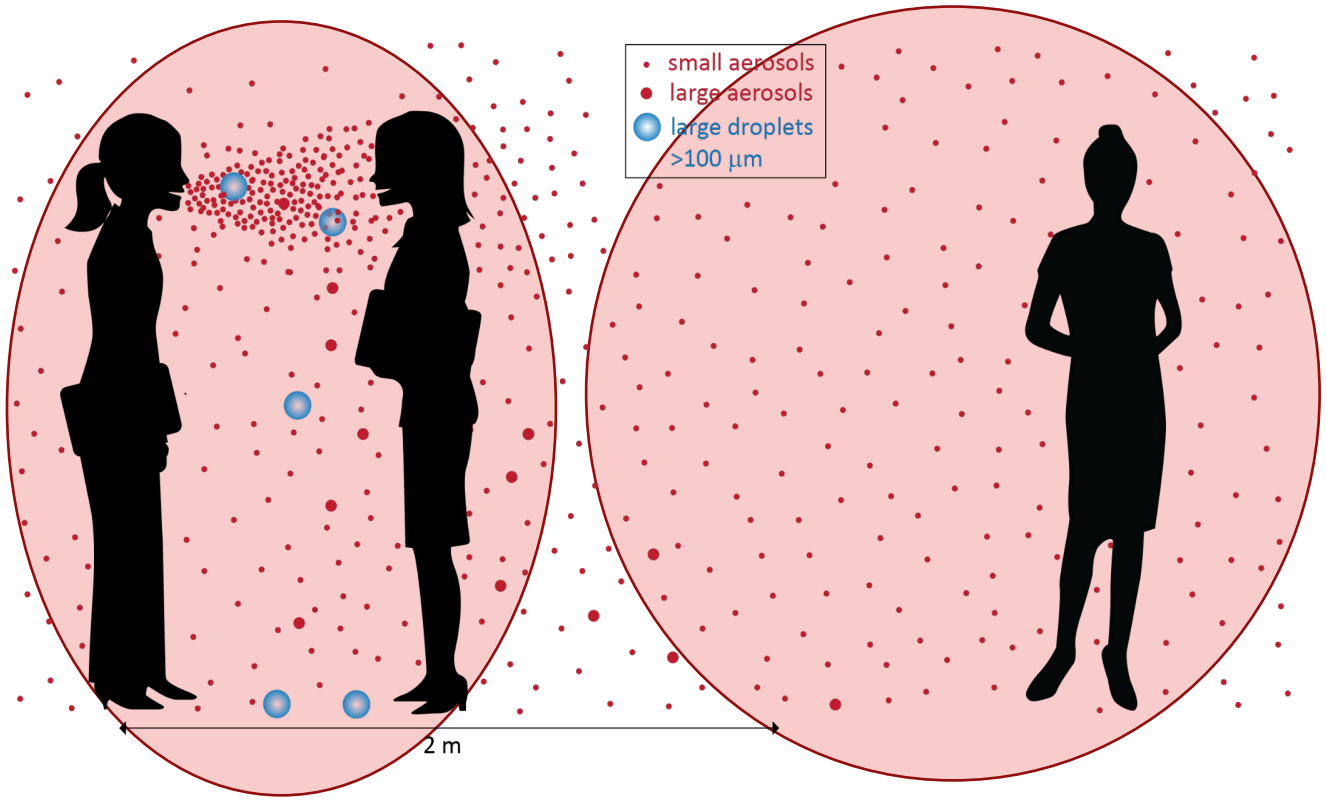

Dilution (ventilation, air cleaning)

Airborne transmission

History…

-Miasma theory ('bad air')

*-2nd half 19th century: **germ the***

-Start 20th century: Charles Cho

-1910-1962: No natural diseas

-1962-2020: Reluctancy to acce

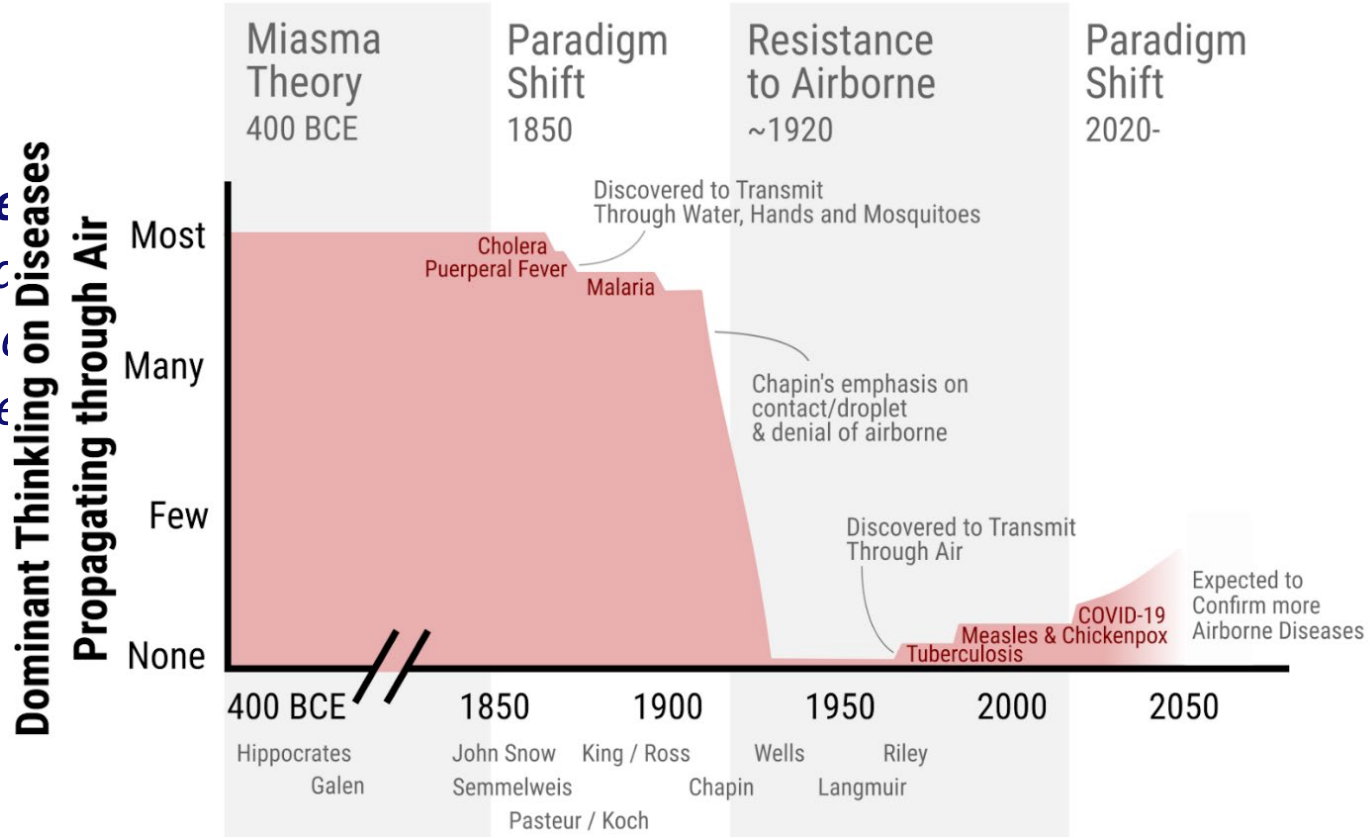

Jimenez JL, Marr LC, Randal K, Ewing ET, Tufekci Z, Greenhalgh T, et al. What Were the Historical Reasons for the Resistance to Recognizing Airborne Transmission during the COVID-19 Pandemic? Indoor Air 2022; Under Review.

Real-life evidence

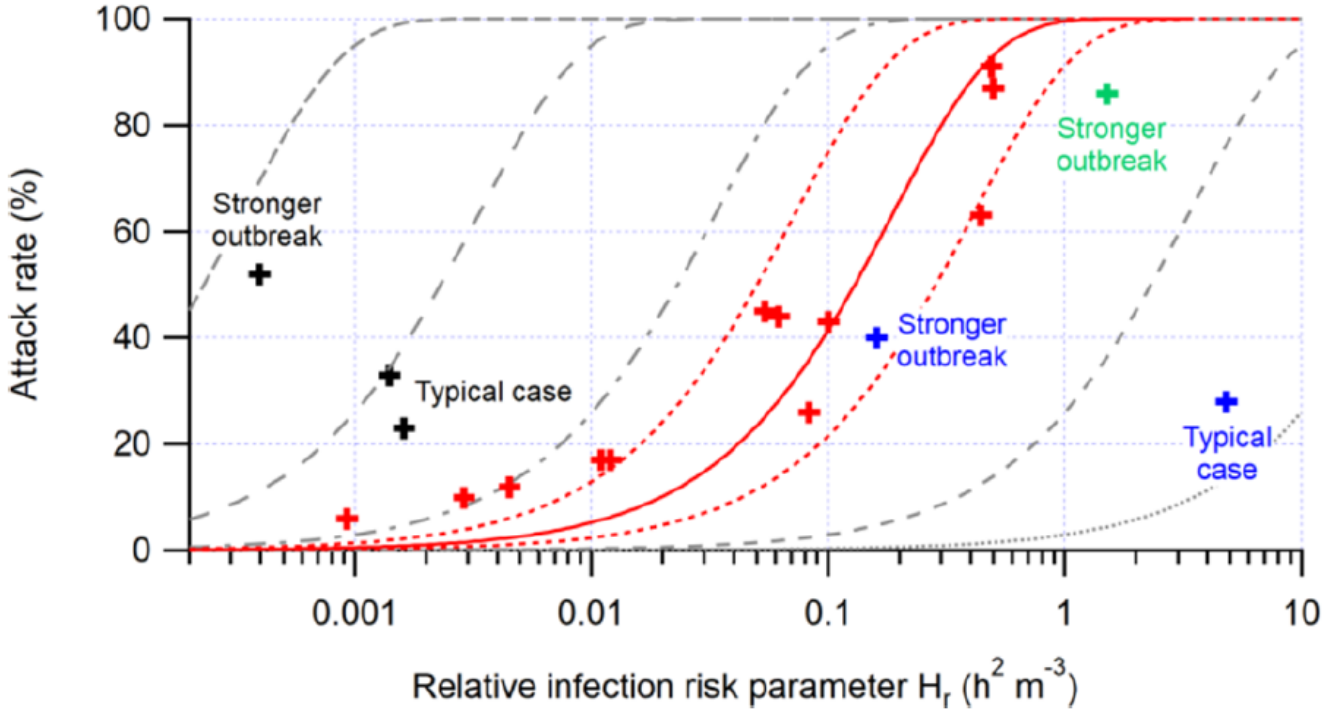

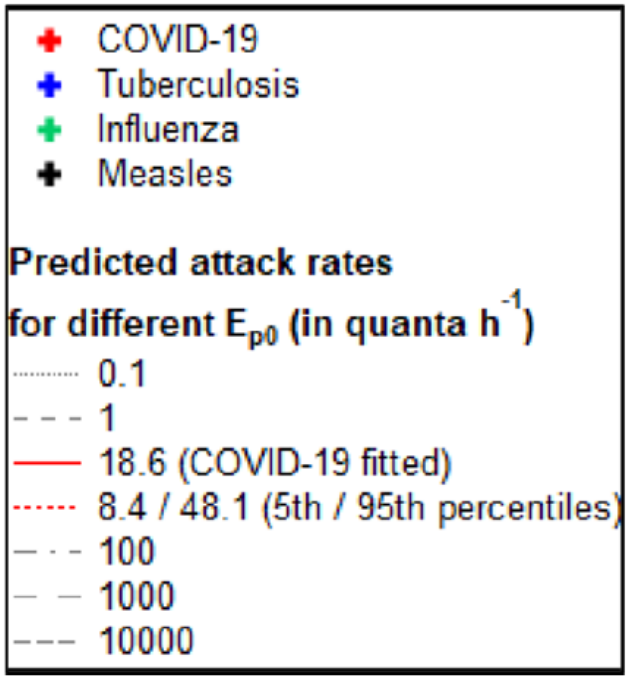

Based on Wells-Riley infection risk model

$$H_r = r_{ss} r_E r_B f_e f_i D/(V\lambda)$$

D: exposure duration
V: volume of the room
λ: sink term (ventilation, decay, deposition, …)
r: related to emission, breathing, transient effects
f: effect mask

Peng et al. 2022. Practical Indicators for Risk of Airborne Transmission in Shared Indoor Environments and Their Application to COVID-19 Outbreaks. Environ. Sci. Technol. 2022, 56, 1125−1137

CLAIRE CLEAN AIR FOR EVERYONE p3 venti MIST TU/e

Pandemic Preparedness

Air quality is relevant

Difference between CO_2 and a virus

What happens if you lower the occupancy rate?

CO_2

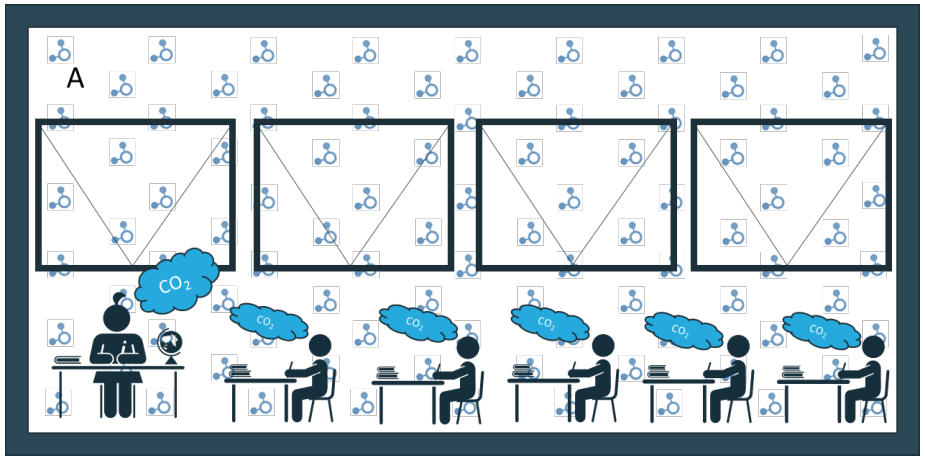

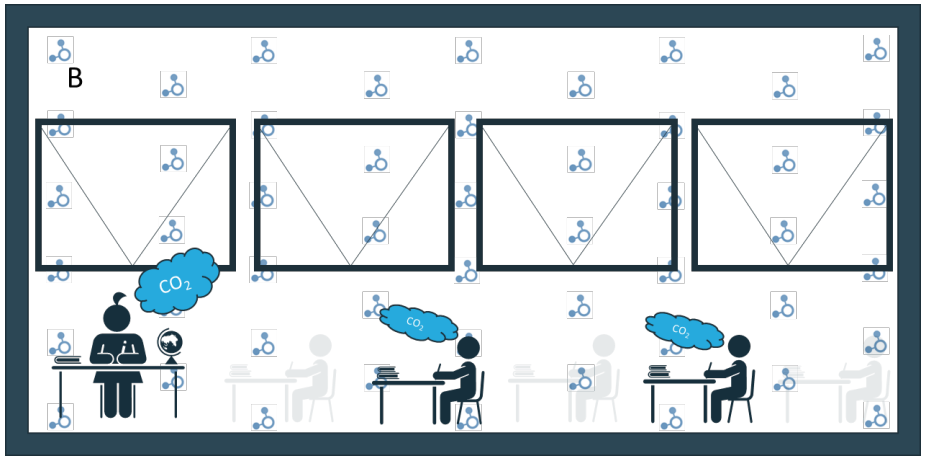

virus

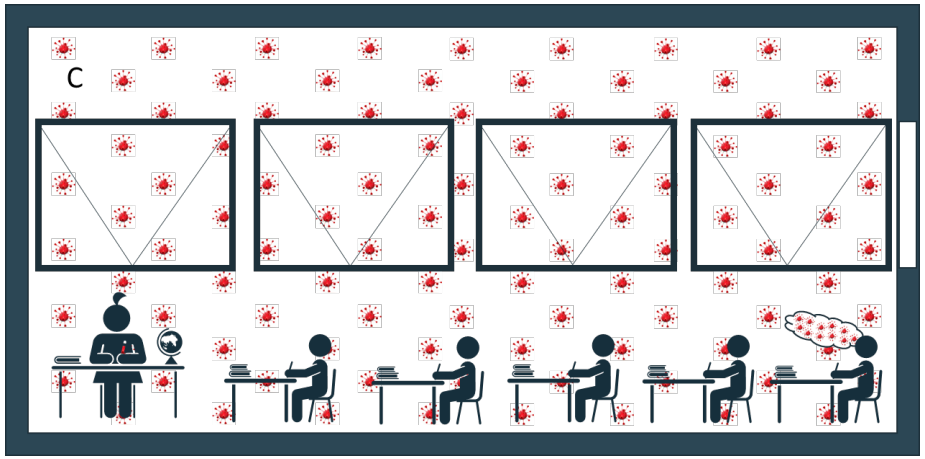

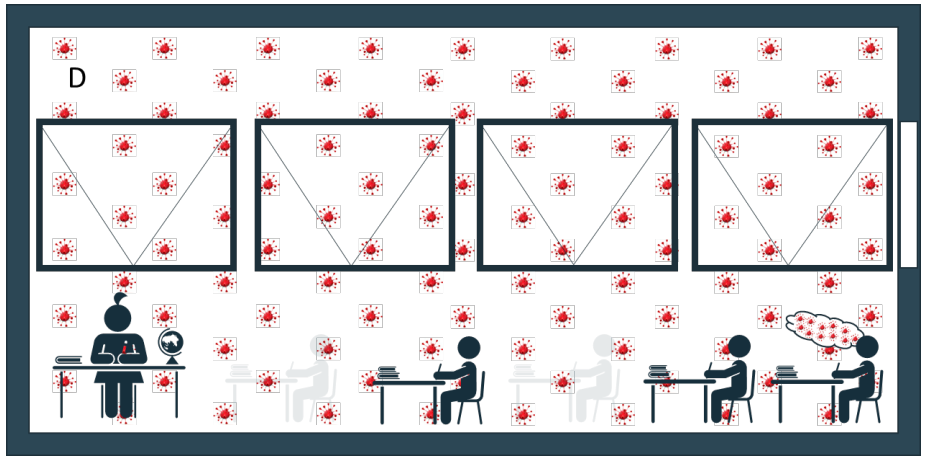

Franchimon, F. en Loomans, M.G.L.C. 2021. CO2 als indicator voor ventilatiekwaliteit versus CO2 als ontwerpcriterium. TVVL Magazine, 6, pp.42-46.

CLAIRE | CLEAN AIR FOR EVERYONE

p3 venti

MIST

TU/e

Purging?

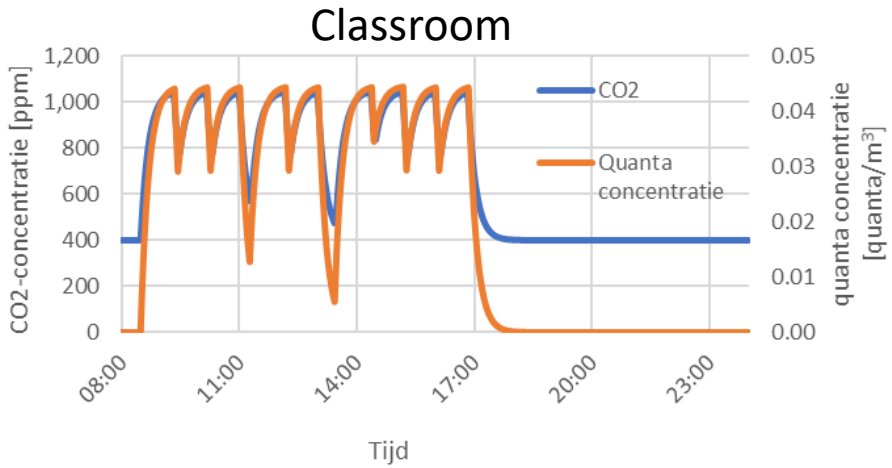

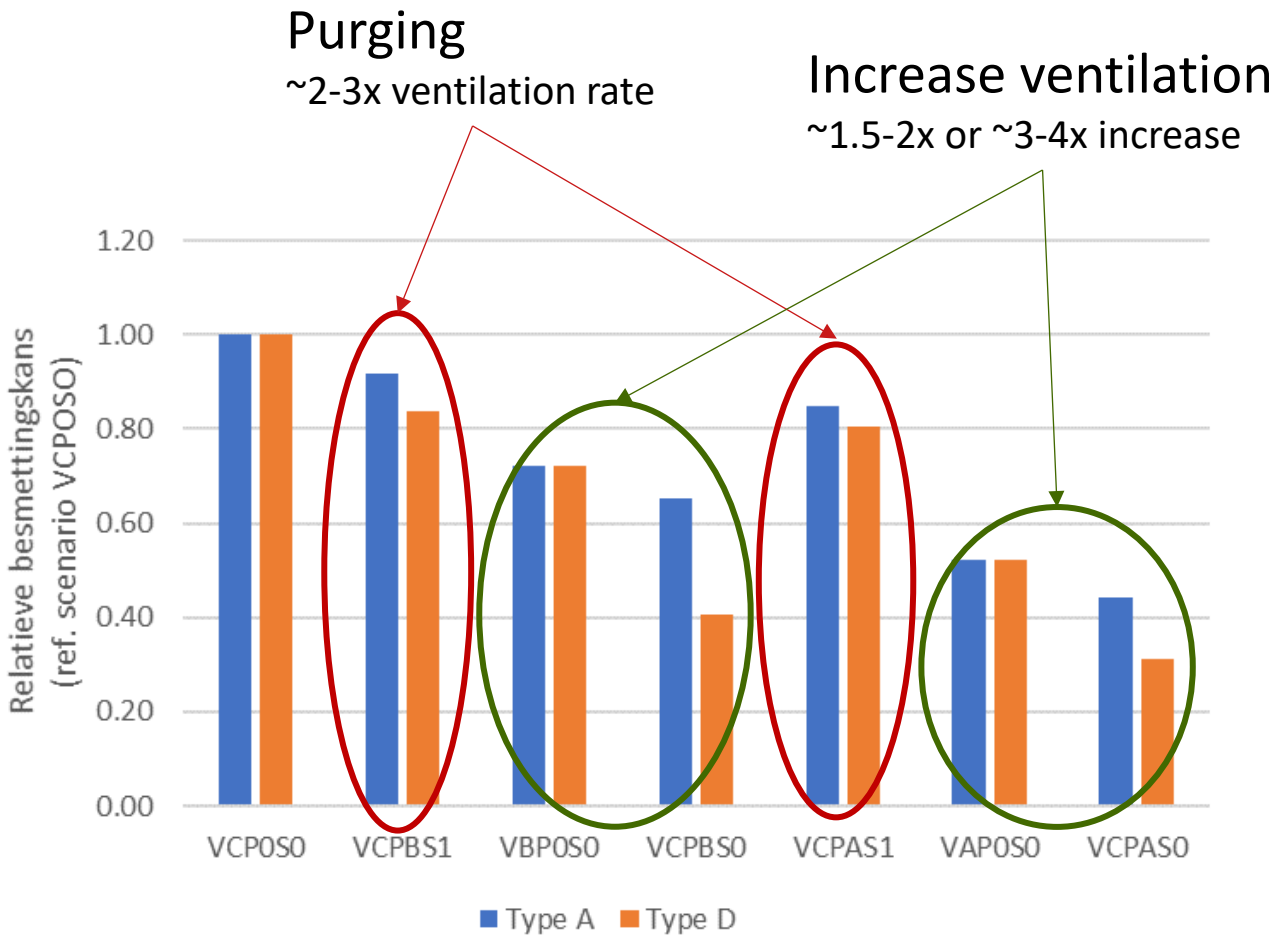

Sufficient ventilation is to be preferred…

Loomans, M.G.L.C., Staassen, M.M. en Loonen, R.C.G.M. 2022. Scholen, Ventilatie, Energie en Besmettingskans - En de zin en onzin van spuien. . TVVL Magazine, 4.

Air change rate versus ventilation effectiveness

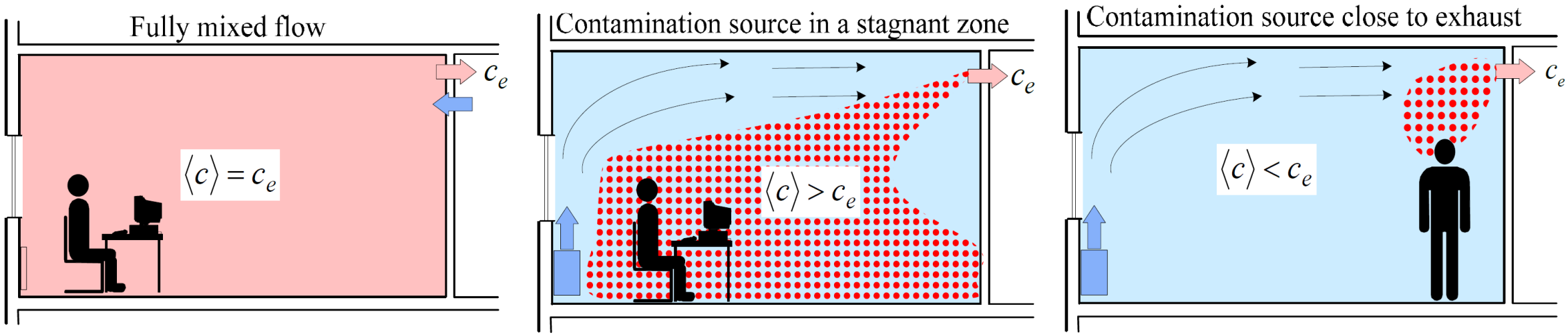

Mundt et al. 2004. Ventilation Effectiveness. REHVA Guidebook No. 2. REHVA. Brussel. België

Research

Large test facility

Dimensions: ~7x10x3 m
HEPA filtered supply air
0.5-6 ACH
Temperature controlled
Free placement of supply and exhaust grilles

Research

Ventilation effectiveness different ACH, designs supply and position supply and exhaust

Numerical CFD

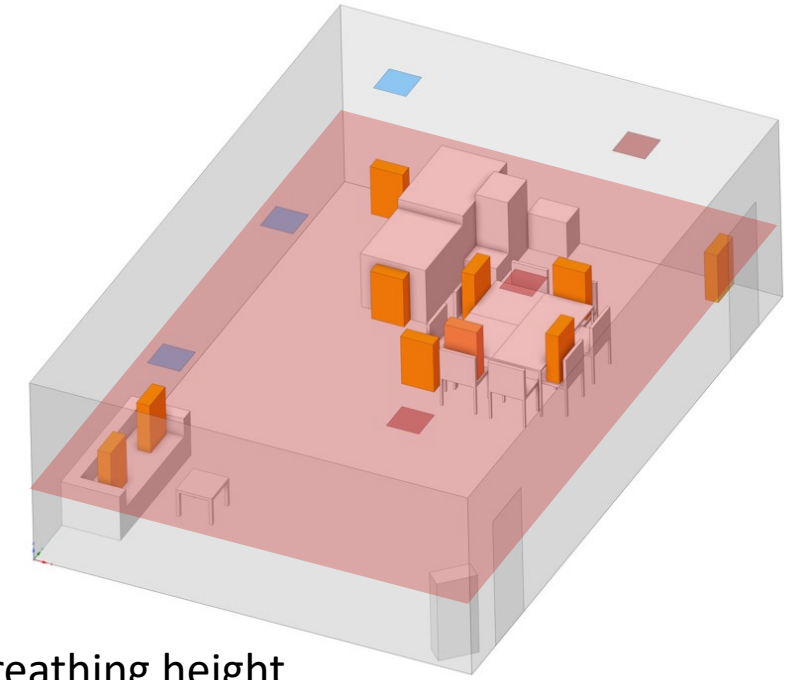

Breathing height

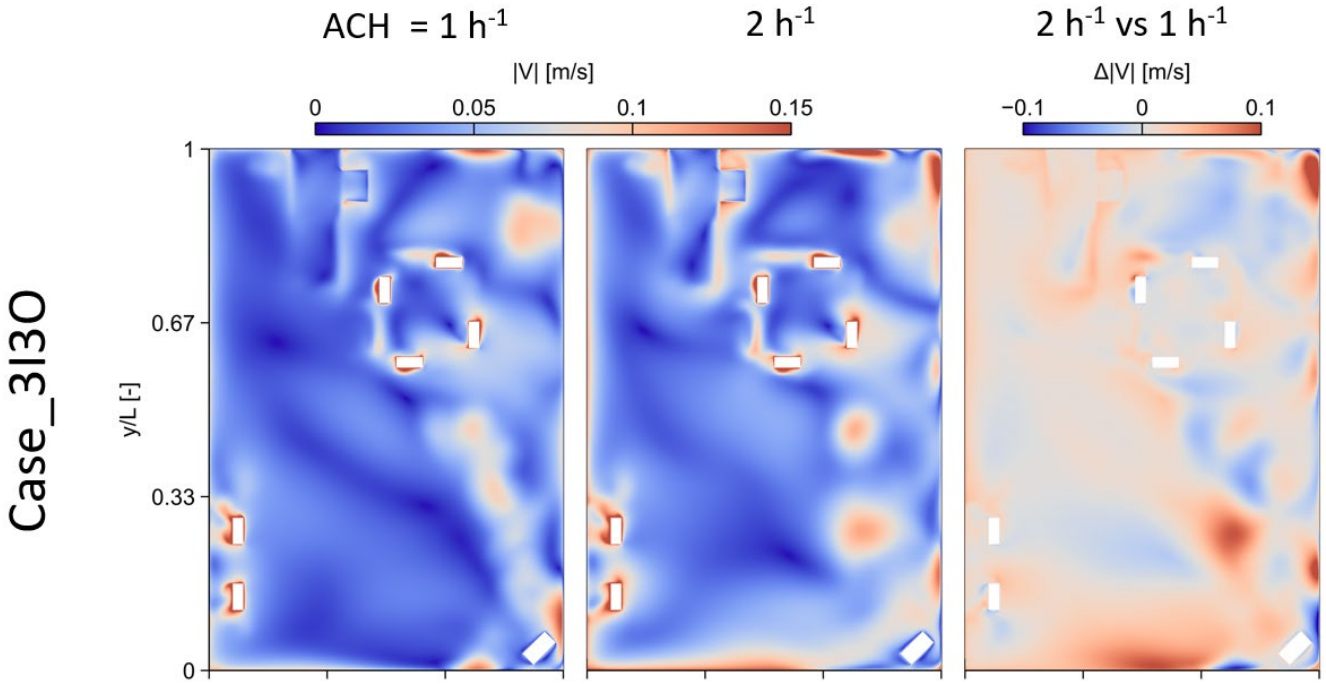

Research

Numerical CFD

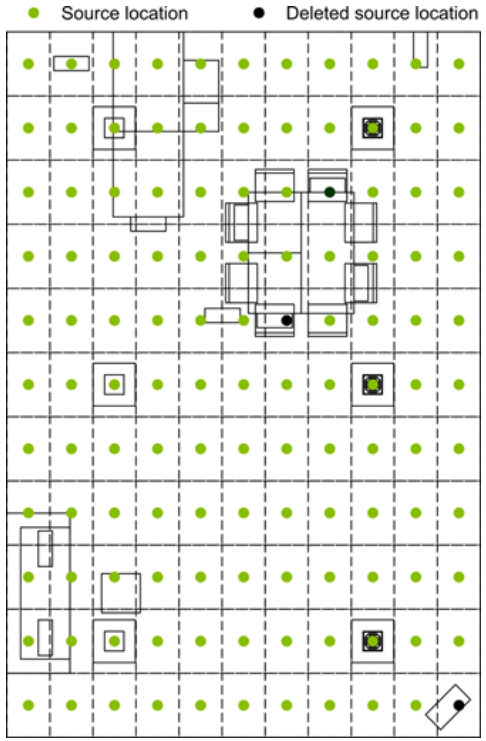

Breathing height

CFD analysis contaminant distribution for grid of sources

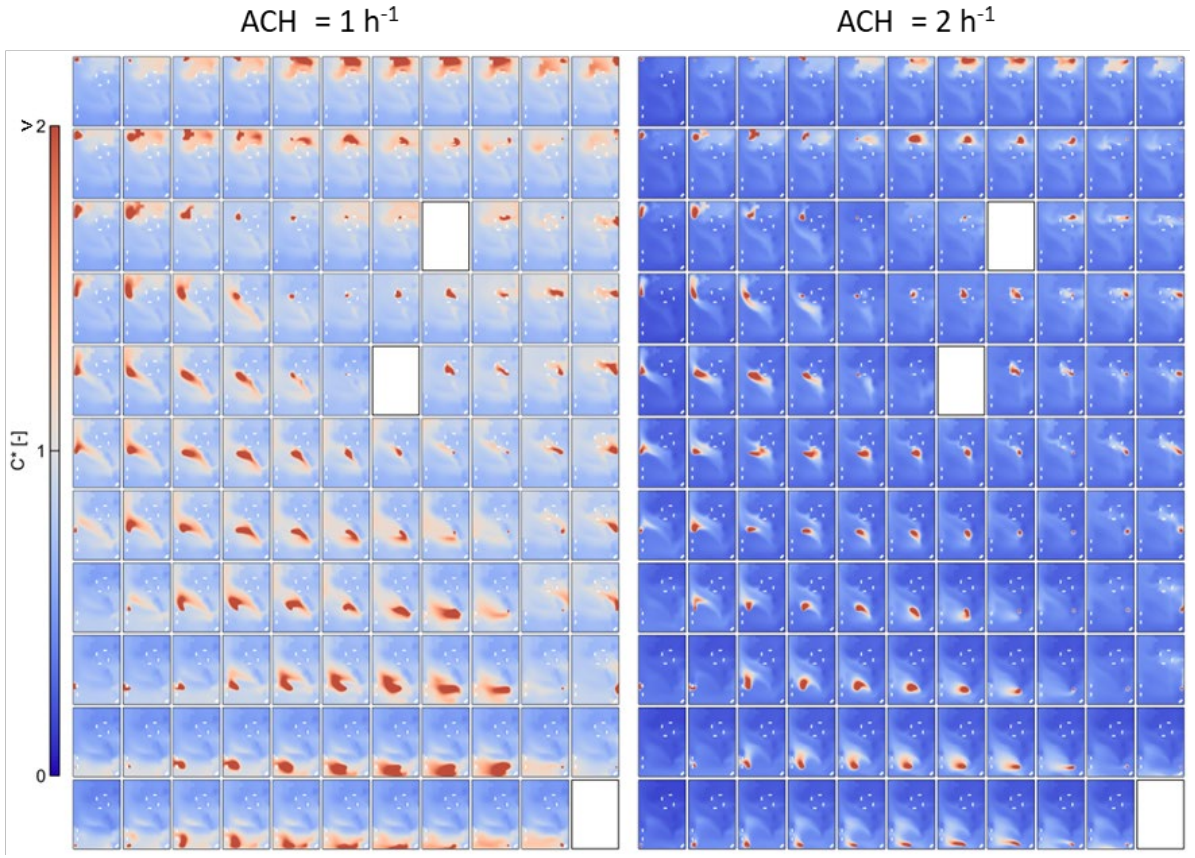

Research

Numerical CFD

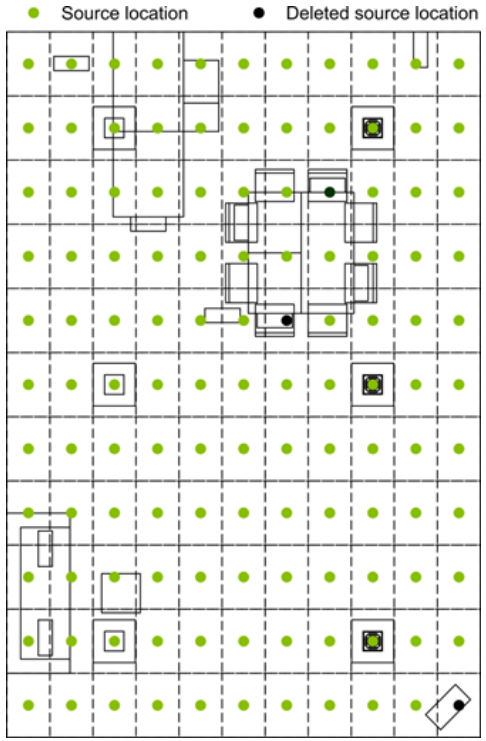

Breathing height

CFD analysis contaminant distribution for grid of sources

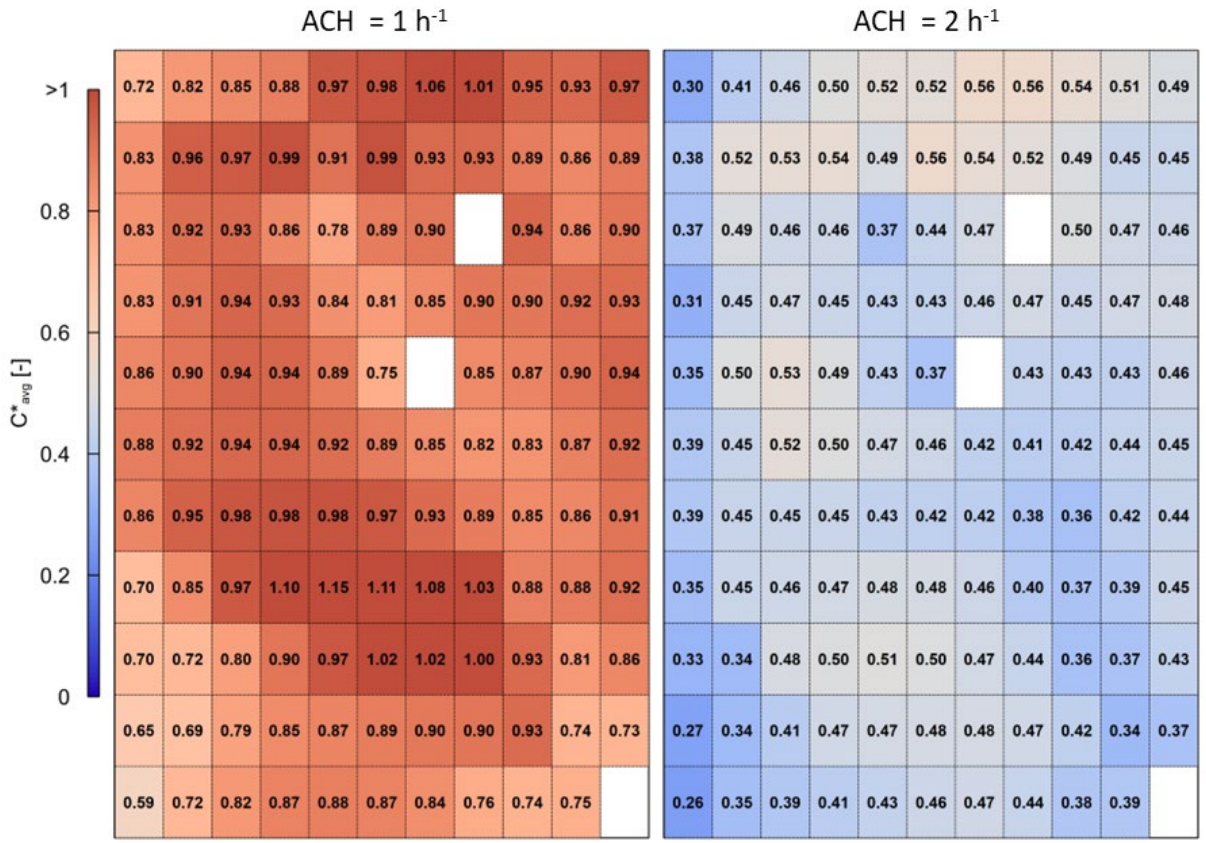

Research

large test facility

Research

PAC performance according to ANSI/AHAM standard [mixing fans]: **$CADR_{th}$**
Effect of room size
Effect of PAC performance practical application [DIN; no mixing fans]: **$CADR_{pr}$**

Experimental: Portable Air Cleaner (PAC) performance

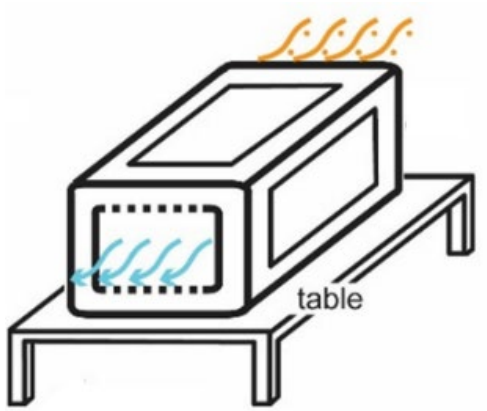

Air cleaner schematic

CADR = Clean Air Delivery Rate [m^3/h]

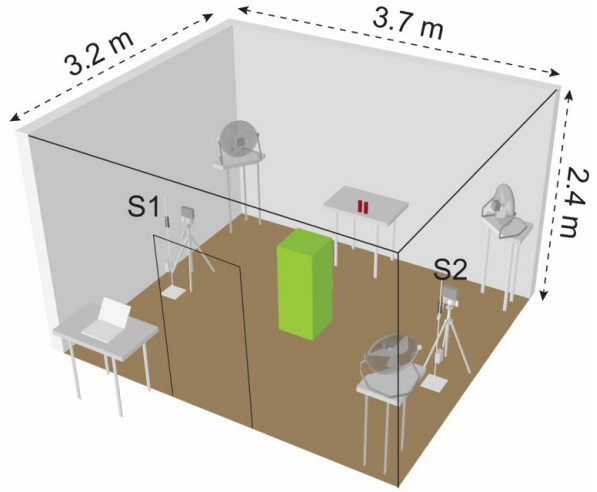

$CADR_{th,TR1}$
TR1: Test room ANSI/AHAM

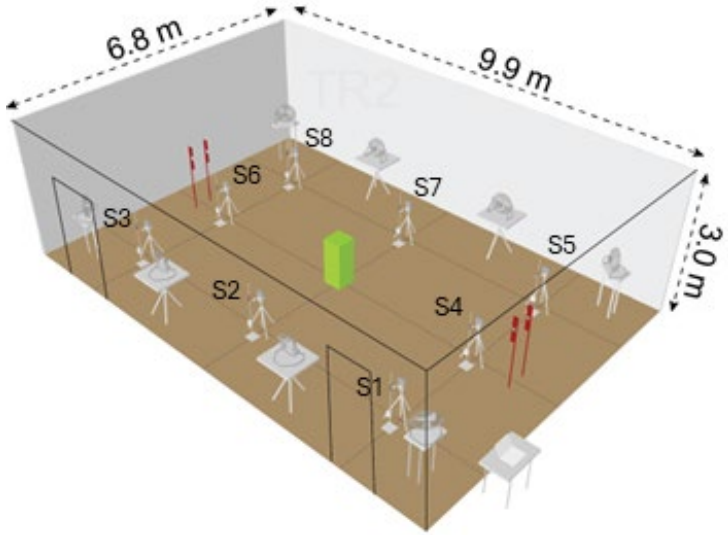

$CADR_{th,TR2}$ $CADR_{pr,TR2}$
TR2: Set-up large test facility

Research

- *Depends on PAC type*
- *Effect of position and ventilation configuration on performance also investigated*

Portable Air Cleaner (PAC) performance

Parameter	PM0.25	PM0.25-0.5	PM0.5-3	PM3-10
$CADR_{th,TR1}$ (m^3/h)	334	342	351	368
$CADR_{th,TR2}$ (m^3/h)	329	333	339	422
$CADR_{pr,TR2}$ (m^3/h)	366	370	382	457
$Difference_{th,\ TR1\text{-}TR2}$ (%)	-2	-3	-3	15
$Difference_{pr\text{-}th,\ TR2}$ (%)	11	11	13	8

TR1

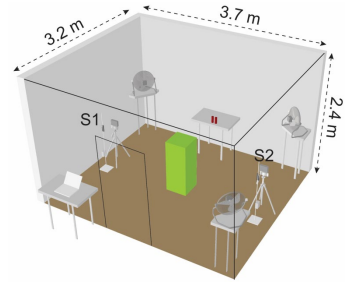

TR2

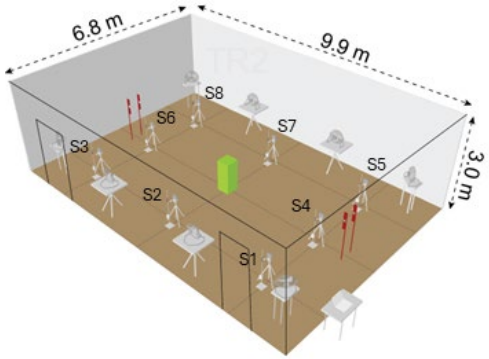

th: theory – according to ANSI/AHAM (mixing fans during decay)
pr: practice – according to DIN (no mixing fans during decay)

CLAIRE | CLEAN AIR FOR EVERYONE p3 venti MIST TU/e

Research

In-situ

https://www.pzc.nl/brugge/bibberen-in-de-klas-met-die-open-ramen-en-deuren-onze-verwarming-draait-overuren-ecologisch-is-dat-een-ramp-en-de-factuur-zal-wel-volgen~ad86c18a/?referrer=https%3A%2F%2Fwww.google.com%2F

Research

Portable Air Cleaner performance in primary schools

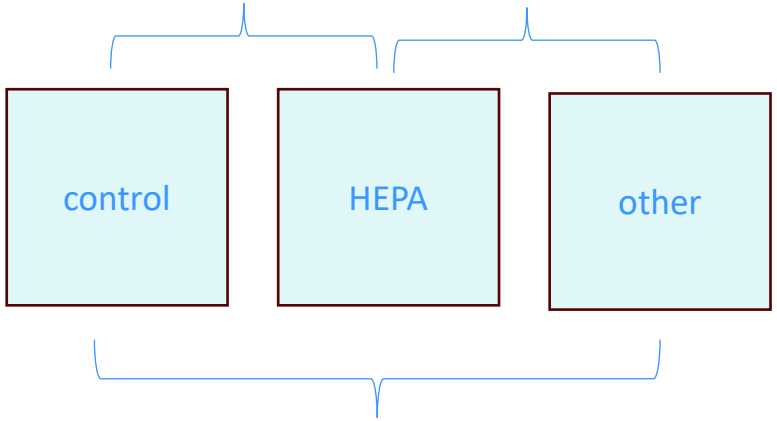

- ~180 classrooms
- ~60 class groups (control, HEPA, other)
- ~ 3 months (partly 2 years)
- IAQ measurements (PM, CO_2)
- Bio aerosol measurements / sick leave
- User experience

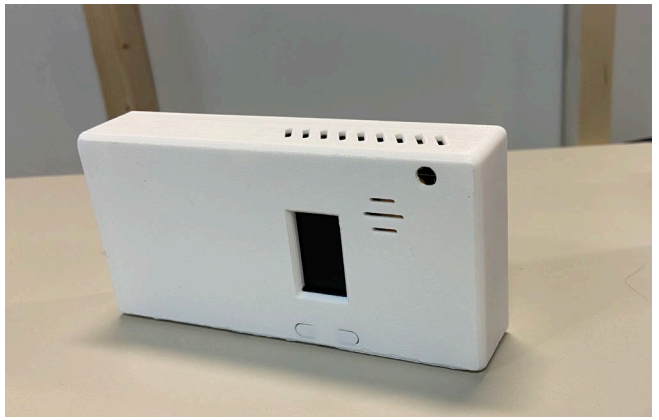

Research

Portable Air Cleaner performance

(very) Preliminary results!

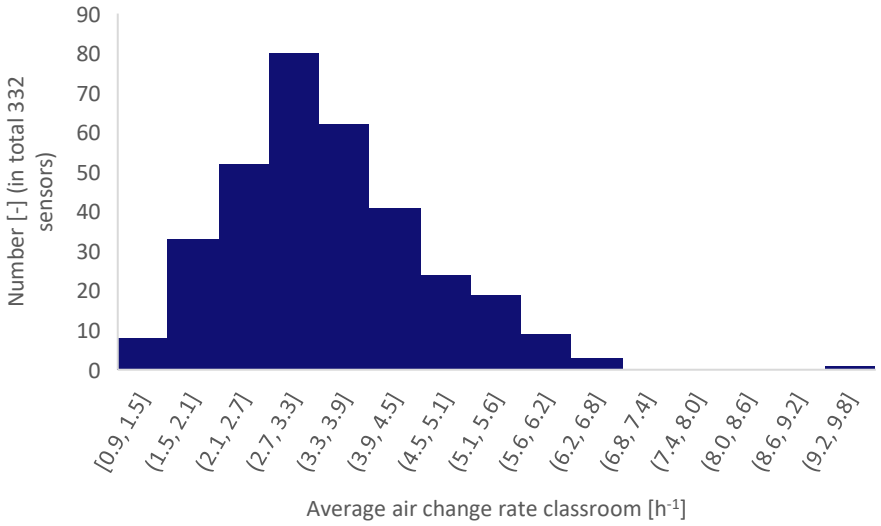

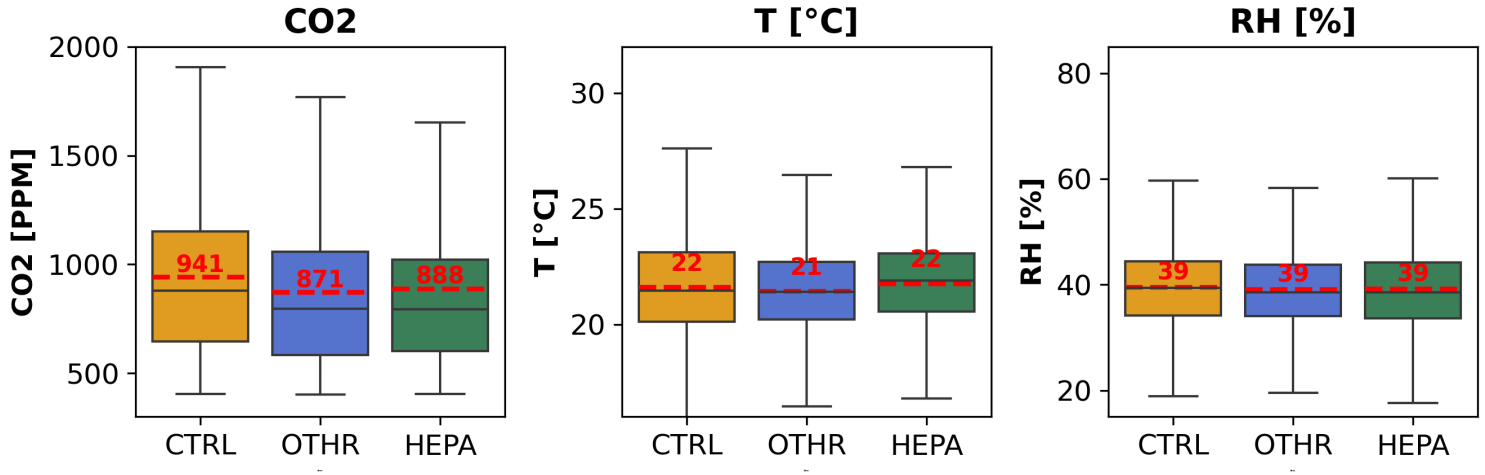

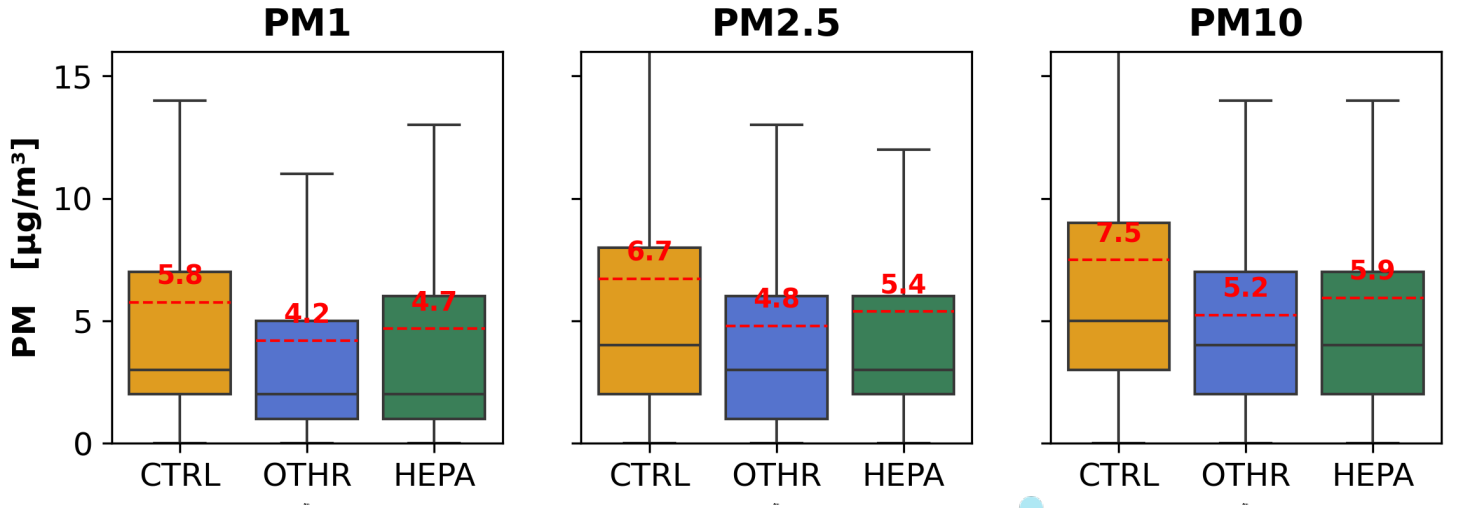

Conclusions

- Covid-19 put the focus (again?) on a part of air quality that we appeared to have forgotten

- Ventilation and air cleaning performance should go beyond the air change rate
- Research is still ongoing
  - Numerical (e.g. modelling particles, fast CFD methods)
  - Experimental (e.g. local ventilation solutions)

Thank you

More info

P3Venti; www.p3venti.nl

CLAIRE; www.claireproject.nl

MIST; https://www.mist-project.nl/

TU/e

6th International Conference on Building Energy and Environment
Eindhoven University of Technology, The Netherlands
6 - 10 July 2025

CFD validation of airflow and particle distribution in a controlled test facility

Peng Qin [1], Anneloes de Lange [2], Twan van Hooff [1], Roberto Traversari [2], Marcel Loomans [1]

[1]*Physics and Services, Department of the Built Environment, Eindhoven University of Technology, Eindhoven, The Netherlands, p.qin@tue.nl - t.a.j.v.hooff@tue.nl - m.g.l.c.loomans@tue.nl*
[2]*Physics and Systems, TNO Netherlands Organization for Applied Scientific Research, Delft, The Netherlands, anneloes.delange@tno.nl - roberto.traversari@tno.nl*

SUMMARY
Indoor airflow and particle distribution are of great importance for estimating indoor air quality and the potential contaminant exposure in rooms. However, there is a lack of detailed room-scale experimental data in the literature, especially with respect to aerosol particle concentrations, which could be used for CFD validation studies. To address this, this paper first presents detailed room-level measurements, conducted in a controlled test facility with mixing ventilation. Next, the CFD simulations closed by the RNG k-ε turbulence model were performed to predict the airflow and particle distributions in this test facility. The particle dispersion was modeled by the Drift-flux model. The computational grid was obtained based on grid-sensitivity analysis. A good agreement in terms of normalized air velocity (V^*), air temperature (T^*) and particle concentrations (C^*) between the CFD results and the measured data was arrived at, as indicated by FAC2 values of 0.889 for V^*, 1.0 for T^*, and 0.708 for C^*. However, some discrepancies were still observed between the two datasets.

Keywords: room-level measurement, CFD, particle distribution

1. INTRODUCTION

Airborne viruses, generated by human respiratory activities, can remain airborne and be inhaled by others in the room, posing a risk of exposure, also beyond 1-2 meters from an infected individual (e.g. Morawska et al., 2009). Therefore, a good understanding of the transmission of droplets/particulate matter in indoor environments is essential for estimating exposure and developing effective control measures. Experiments and computational fluid dynamics (CFD) simulations are two most commonly used methods for investigating indoor airborne transmission (e.g. Brink et al, 2022; Thysen et al., 2022). Experimental studies can provide real-case empirical evidence on the effects of building ventilation and environmental factors on airborne transmission indoors. However, experimental studies involve limitations such as the limited number of experimental scenarios and sampling points (e.g. Blocken, 2015). These limitations in experiments support the need for complementary approaches, such as CFD, to enhance understanding of particle dispersion indoors. Although CFD simulations can provide high-resolution whole-field flow and particle concentration data, high-quality validation and uncertainty evaluations of CFD simulations are indispensable. For this reason, combining CFD with experimental data can enhance understanding and improve predictive capabilities regarding particle transmission in indoor environments. However, the literature lacks detailed room-scale experimental data, particularly concerning aerosol particle concentrations, suitable for CFD validation. The goal of this study is to provide a benchmark by combining experimental data with a validation and

evaluation of CFD simulations for predicting airflow and particle distribution in a well-controlled test facility.

2. METHODOLOGY

2.1. Description of the experiments

Figure 1 shows a schematic view of the experimental setup in a test facility. This test facility, constructed at Eindhoven University of Technology, has dimensions of 9.91 m in length (L), 6.73 m in width (W), and 3 m in height (H), which generally represents a typical room configuration, such as a living room in a long-term care facility or a classroom.

The ventilation system consisted of two supply vents and two exhaust vents close to each side of the room. In addition, two solid plates were placed beneath the supply vents. All the supply vents, exhaust vents, and the plates were square with an edge length of 0.50 m. The air change rate (ACH) was set at 3 h^{-1} during the entire experiment. Nine cardboard boxes were used to mimic the thermal plumes generated by human bodies in a room. Each cardboard box measured 0.5 m in length, 0.2 m in width, and 0.8 m in height, placed on the floor. An 80 W lightbulb was placed inside each cardboard box to serve as the heat source. The distance between the two adjacent cardboard boxes in x-direction and y-direction was 1.68 m (center of the box).

In the experiments, the velocity and temperature, and particle measurements were conducted separately. For brevity, the velocity and temperature measurements were hereafter referred to as Exp1, and the particle measurements were referred to as Exp2:

- In Exp1, ClimaCube 3D acoustic sensors were used to measure the velocity and temperature in space. These sensors have a velocity measurement range of 0.03 m/s to 3 m/s with an accuracy of ±0.03 m/s, and a temperature measurement range of 10°C to 40°C with an accuracy of ±0.1°C. They were placed at nine locations (GP1-GP9) in the test facility, and at each location, data for velocity and temperature were collected at eight different heights: 0.17 m, 0.56 m, 1.20 m, 1.60 m, 1.91 m, 2.22 m, 2.52 m and 2.84 m. The sampling period was set to 180 s with data recorded at a frequency of 1 Hz.
- In Exp2, the TOPAS GmbH atomizer aerosol generator ATM 228 was used to generate particles, with the particle exhaust positioned above the center carboard box at a height of 1.2 m (Fig. 1). Paraffin oil was selected as the aerosol substance. In addition, an air pump was included with an airflow rate of 14 L/min, corresponding to a jet velocity of about 4.65 m/s at the particle exhaust. Six Lighthouse Handheld (LH) sensors and eight Grimm particle counters were used to measure particle concentrations. During the particle measurement, concentrations for particle sizes of 0.3, 0.5, 0.7, 1.0, 2.0, and 5.0 μm were recorded, hereafter referred to as dp0.3, dp0.5, dp0.7, dp1, dp2, and dp5, respectively. The data recording frequency for both LH and Grimm particle counters was set to 0.067 Hz and sampled continuously throughout the entire process. Note that in Epx2, the combination of the aerosol generator and the air pump introduced a particle emitting velocity (i.e. 4.65 m/s) at mouth height (sitting position: 1.2m), which was absent in the Exp1.

In both Exp1 and Exp2, five thermal sensors were installed on each wall of the test facility to measure the wall surface temperatures. The average temperature reading from these five sensors was used to represent the surface temperature of each wall. These temperature values are presented in Section 2.2 as the thermal boundary conditions of the test facility in CFD simulations.

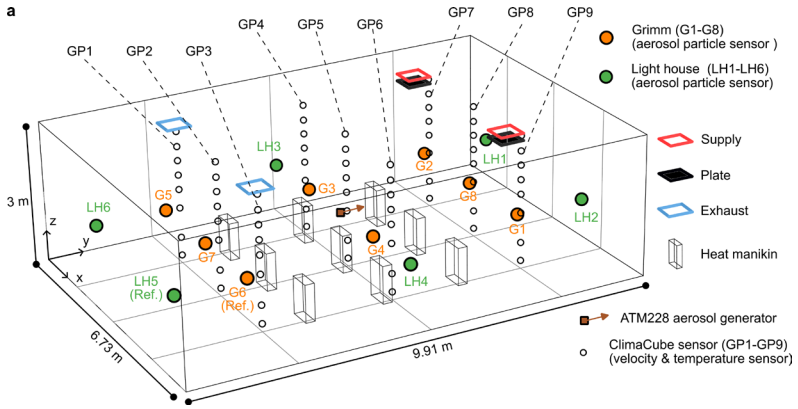

Figure 1. Schematic view of the experimental setup.

2.2. CFD simulations: computational settings and parameters

2.2.1. Computational domain and grid

The computational domain used in this study is a replication of the aforementioned test facility (Fig. 1), with dimensions of 9.91 m × 6.73 m × 3.00 m. The supply vents, exhaust vents and the cardboard boxes were explicitly modeled in the computational domain to closely reproduce the experimental setup. However, the aerosol generator and the measurement sensors were omitted to simplify the CFD simulations. The origin of the computational domain was set at the corner, in line with the experimental setup. A non-conformal computational grid and hexahedral cells with a stretching ratio between 1.01 and 1.20 were used to discretize the entire computational domain. Finally, the computational domain was divided into two subdomains: (*i*) cell refinement subdomains where manual grid adaptation was applied and (*ii*) the bulk subdomain. For brevity, the computational grid details and grid-sensitivity analysis results were not included in this paper. Overall, the grid-sensitivity analysis resulted in two computational grids, one for validating velocity and temperature (~ 8.4 million cells) and the other for particle concentration (~ 8.5 million cells).

2.2.2. Boundary conditions and other numerical settings

At the supply vents, the velocity inlet boundary condition was imposed, with each inlet having a supply velocity of 0.333 m/s perpendicular to the inlet surface, corresponding to a total ACH of 3 h^{-1}. At the exhaust vents, zero static-gauge pressure was imposed. The cardboard box surfaces were set as heat sources, with a surface heat flux of 65.6 W/m^2. Note that in CFD only the five air-exposed surfaces of cardboard box were explicitly modeled; the bottom surface, not in contact with the airflow, was omitted. For this reason, the surface heat flux was slightly adjusted to maintain the total power input of 80 W per box as in Exp1 and Exp2. At the sides, ceiling, and floor of the test facility, no-slip wall boundary conditions and constant temperature conditions were used. Details of the surface temperature on each wall, supply, and exhaust vents are provided in Table 1. All wall surfaces were set to have an internal emissivity of 0.9.

3D steady Reynolds-averaged Navier-Stokes (RANS) simulations were performed with the RNG k-ε turbulence model (Yakhot et al., 1992). Low-Reynolds number modeling was adopted to solve the flow down to the laminar sublayer ($y^* < 5$). To this end, enhanced wall treatment with a two-layer model was employed in this study, whereas in the viscosity-affected near-wall region the one-equation model of Wolfshtein (1969) was used. The surface-to-surface (S2S) radiation model

was used to account for the radiative heat transfer. Drift-flux model was used to account for particle dispersion. An additional moment source term was included at the particle source position in the CFD simulations to reproduce the particle emitting velocity in Exp2. For each particle size (e.g. dp0.3), one user-defined scalar (UDS) was assigned in ANSYS Fluent (Ansys Inc., 2022), resulting in six UDSs (dp0.3, dp0.5, dp0.7, dp1, dp2, dp5). For pressure-velocity coupling, the pseudo-transient under-relaxing algorithm was used. Pressure interpolation was solved with a staggered scheme using PRESTO!. Second order discretization schemes were used for both the convection and viscous terms of the governing equations. The incompressible ideal gas law was used to account for the buoyancy effects. Convergence was assumed to be reached when all the monitoring mean velocities/concentrations show negligible changes. To achieve convergence, the simulations were initially run for 6000 iterations, followed by averaging over the subsequent 6000 iterations to obtain a statistically steady solution. All the simulations were performed with ANSYS Fluent 2023R1 (Ansys Inc., 2022).

Table 1. Surface temperature boundary conditions for CFD simulations replicating Exp1 and Exp2.

CFD simulations replicating	Supply [K]	Exhaust [K]	Ceiling [K]	Floor [K]	Side walls [K]
Exp1	293.90	294.15	295.15	296.70	294.75
Exp2	292.85	294.20	295.95	294.65	293.85

2.2.2. Data analysis

To evaluate the overall agreement between the predicted (CFD) and the measured (Exp1/Exp2) results, three performance indicators were used: the average absolute difference of normalized data for the velocity (V*), temperature (T*) and particle concentration (C*), the quantile-quantile (QQ) plot, and validation metrics. The normalized velocity V^* and temperature T^* are calculated as follows:

$$V^* = \frac{|V|}{V_{in}} \tag{3}$$

$$T^* = \frac{T - T_{in}}{T_{out} - T_{in}} \tag{4}$$

where $|V|$ is the mean velocity magnitude, V_{in} is the mean velocity at the inlet faces, T is the mean temperature measured/calculated at the specific location in the room, T_{in} and T_{out} are the mean temperature at the inlet and outlet faces. The normalized particle concentration C^* is calculated as the ratio of the mean particle concentration (C) to the reference particle concentrations (C_{ref}). However, it should be noted that, as two types of particle counters were used, the particle concentration (C_{G6}) at G6 (see Figure 1) was selected as the C_{ref} for the Grimm particle counters, while the particle concentration (C_{LH5}) at LH5 was selected as the C_{ref} for the Lighthouse particle counters. This selection of C_{ref} was to avoid potential measurement deviations arising from the use of different types of particle counters.

For the validation metrics, the fraction of data within a factor of 1.5 (FAC1.5) and within a factor of 2 (FAC2) were adopted, calculated using Equations 1 and 2:

$$FAC1.5 = \frac{1}{N}\sum_{i=1}^{N} n_i \quad with \quad n_i = \begin{cases} 1 & for \quad 0.67 \le \dfrac{P_i}{O_i} \le 1.5 \\ 0 & else \end{cases} \tag{1}$$

$$FAC2 = \frac{1}{N}\sum_{i=1}^{N} n_i \quad with \quad n_i = \begin{cases} 1 & for \;\; 0.5 \le \dfrac{P_i}{O_i} \le 2 \\ 0 & else \end{cases} \tag{2}$$

where O_i and P_i are the observed (experimental) and predicted (CFD) values for the i-th sample and N is the total number of measured positions in the experiments.

3. RESULTS

3.1. Comparison of velocity and temperature data between CFD and Exp1

Figure 2 compares the vertical profiles of normalized mean velocity (V^*) and normalized mean air temperature (T^*) along the vertical lines at nine GP positions between CFD and Exp1. In general, symmetry of V^* and T^* profiles is observed in the CFD results at GP7 and GP9, GP4 and GP 6, and GP1 and GP3. However, compared to the CFD results, the V^* and T^* profiles from Exp1 are less symmetrical. This discrepancy may be due to unsymmetrical factors such as small differences in the supply conditions per grille and the effect of additional tripod poles and equipment boxes present in the experimental setup, which were not accounted for in the CFD simulations. The overall average absolute differences of V^* and T^* between CFD and Exp1 are 0.065 and 0.132, respectively.

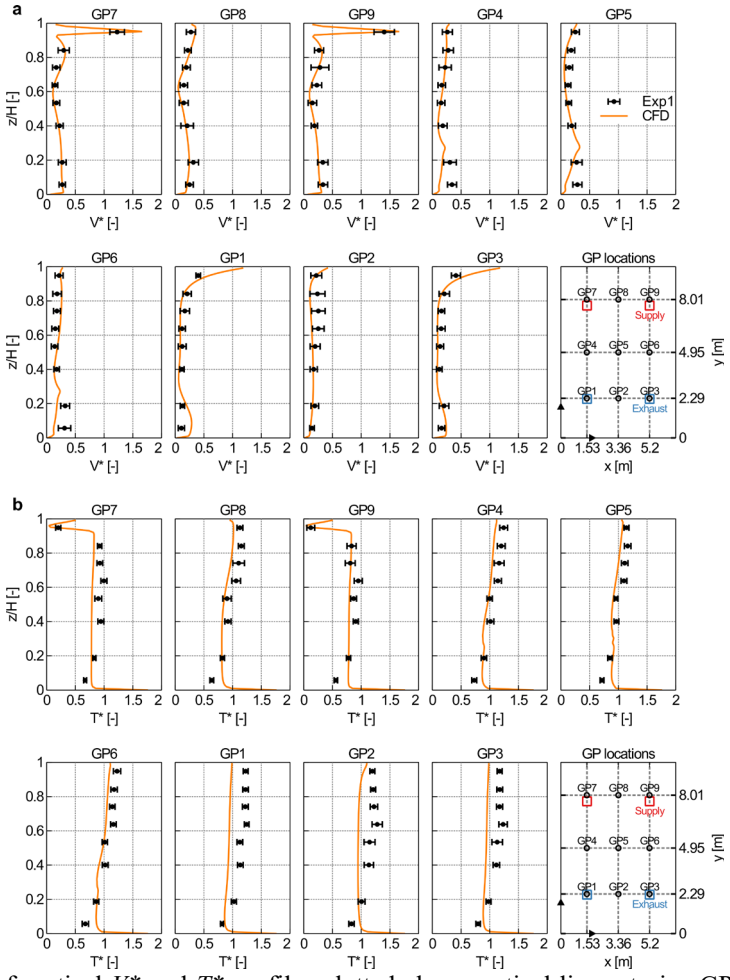

Figure 2. Comparison of vertical V^* and T^* profiles plotted along vertical lines at nine GP positions for Exp1 and CFD. The error bars indicate the measurement uncertainty of V^* and T^* in Exp1.

3.2. Comparison of particle concentration between CFD and Exp2

Figure 3 shows the comparison of CFD and Exp2 results of the normalized mean particle concentration (C^*) for dp0.3, dp0.5, dp0.7, dp1, dp2 and dp5 at 14 locations within the test facility. For all investigated particles (dp0.3-dp5), similar C^* values were obtained at different locations (e.g., G1-G8, LH1-LH6) across the test facility. This suggests a well-mixed flow for the present ventilation configuration in the test facility. In general, the CFD results of normalized mean particle concentrations closely align with the Exp2 results. However, some differences can still be observed for concentrations at some measurement locations:

- At G1, slightly lower C^* values were obtained from CFD (e.g. $C^* = 0.95$ for dp0.3) compared to those obtained from Exp2 (e.g. $C^* = 1.14$ for dp0.3), while at G3, slightly higher C^* values were obtained from CFD compared to Exp2. Notably, at G3, the difference in C^* between Exp2 and CFD progressively increased with particle size. Ideally, the C^* values at G1 and G3 should be similar for different particle sizes, as the experimental setup of Exp2 is expected to be symmetrical. However, the observed discrepancies suggest the presence of unsymmetrical factors in the experiments, similar to those found for (and induced by) V* and T* (Fig. 2).
- At G8, generally lower C^* values are obtained from CFD compared to Exp2, regardless of the particle size. As the G8 position in Exp2 faces the source injection direction, a steep C^* gradient is expected around G8. Therefore, a minor shift in the position of G8 or location of the gradient, may result in increased differences in C^* between measurements and CFD predictions.
- At LH1 and LH3 for dp = 5 μm, a large difference of C^* was observed between Exp2 and CFD results, but also when comparing these measurements results to experimental data for the other particle sizes. This appears to be a measurement error, though an objective explanation for this outcome is not available.

Figure 4 shows the QQ plot for the comparison of CFD and experimental data for V^*, T^*, and C^*, with indications of boundaries for V^*, T^* and C^* that deviate from Exp1/Exp2 by 0.15 and 0.30, respectively. For V^* (Fig. 4a), a large portion (51 out of 72) of the samples of the $V^*(CFD)$ values are lower than $V^*(Exp1)$ values, suggesting a general underprediction by the present use of RANS model coupled with the RNG k-ε turbulence model. However, approximately 90.2% (65/72) of the $V^*(CFD)$ samples are within a deviation of 0.15 from $V^*(Exp1)$, and all $V^*(CFD)$ samples are within a deviation of 0.30 from $V^*(Exp1)$. The validation metrics also confirmed a good prediction of $V^*(CFD)$ compared to $V^*(Exp1)$. In particular, FAC1.5 and FAC2 values were equal to 0.681 and 0.889, respectively, falling within the range (i.e. FAC2 > 0.5) suggested by Chang and Hanna (2005). For T^* (Fig. 7b), like $V^*(CFD)$, about 84.7% of the $T^*(CFD)$ values are lower than $T^*(Exp1)$ at the measured 72 positions. However, 99% of the $T^*(CFD)$ samples are within a deviation of 0.30 from $T^*(Exp1)$. For C^* (Fig. 4c) a tight distribution of samples around the diagonal is observed implying more mixing than the experimental data shows. 9 of 72 $C^*(CFD)$ samples deviating by more than 0.3 from $C^*(Exp2)$. The corresponding FAC1.5 and FAC2 values for C^* are equal to 0.653 and 0.708, respectively, and therefore still fall within the recommended range (i.e. FAC2 > 0.5) by Chang and Hanna (2005). The latter may result from the fact that the room is relatively well mixed, blurring some obvious differences. Nevertheless, the main distribution pattern seems to have been captured in the CFD simulations conducted, when combining the results from V^*, T^* and C^*.

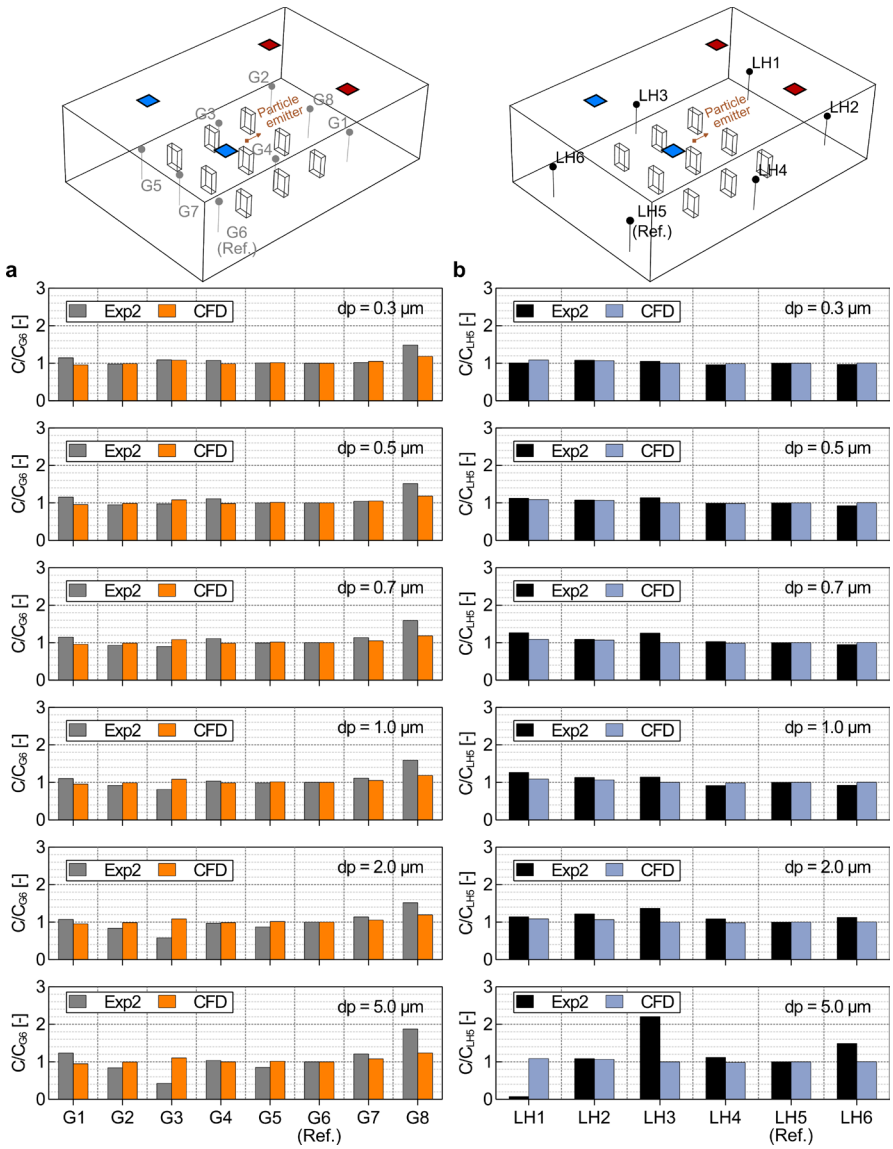

Figure 3. Comparison of CFD and Exp2 results of mean particle concentration (C) for particle sizes of 0.3, 0.5, 0.7, 1.0, 2.0 and 5.0 µm: (a) at measurement locations G1-G8, normalized to the reference particle concentration (C_{G6}) at G6 for the Grimm particle counters, (b) at measurement locations LH1- LH6, normalized to the reference particle concentration (C_{LH5}) at LH5 for lighthouse particle counters.

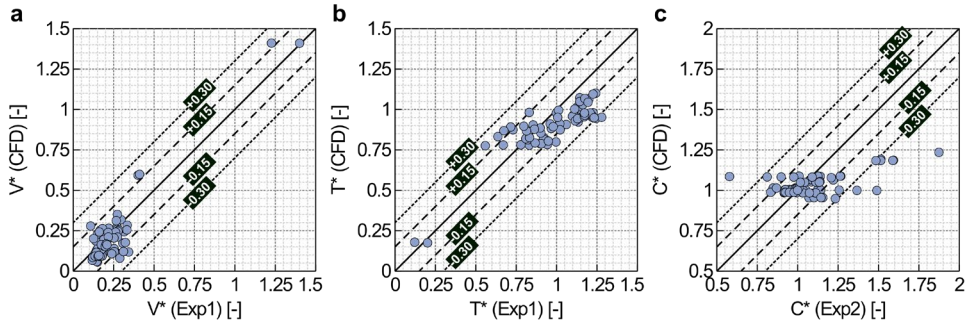

Figure 4. Quantile-quantile (QQ) plot for the comparison of CFD and experimental (i.e. Exp1/Exp2) data for (a) normalized mean velocity magnitude (V*), (b) normalized mean temperature (T*), and normalized mean concentration

(C^*). Values of V^*, T^* and C^* with deviations between CFD and Exp1/Exp2 exceeding 0.15 and 0.30, respectively, are also indicated in the figures.

4. CONCLUSIONS

This study provides a benchmark by combining experimental data with a validation and evaluation of CFD simulations for predicting airflow and particle distribution in a controlled test facility. First, a detailed room-level measurement, conducted in a controlled test facility with mixing ventilation, was described. Next, the CFD simulations closed by the RNG turbulence model were performed to predict the velocity, temperature and particle distributions in this test facility. Overall, a good agreement between CFD and Exp1/Exp2 was found for V^*, T^*, and C^*, as indicated by FAC2 values of 0.889 for V^*, 1.0 for T^*, and 0.708 for C^*, though measurement and CFD analysis of airflow velocity and particle concentrations showed to be tedious. This suggests that the RANS approach used in this study is able to capture the velocity, temperature and concentration characteristics within the test facility. Future work can investigate the impact of other factors, such as the exhalation flow velocity and direction, on the airflow pattern, and particle dispersion,

ACKNOWLEDGEMENTS

This research received funding from the Pandemic Preparedness Programme and Ventilation (P3Venti Program) coordinated by the Netherlands Organization for Applied Scientific Research TNO and funded by the Dutch Ministry of Health, Welfare and Sport. The large experimental chamber is also partly financed by the collaboration project CLAIRE (LSHM22032), co-funded by the PPP Allowance made available by Health~Holland, Top Sector Life Sciences & Health, to stimulate public-private partnerships (https://www.health-holland.com/), and by the NWO-MIST programme (MItigation STrategies for Airborne Infection Control; P20-35). The numerical part of this work was carried out on the Dutch national e-infrastructure with the support of SURF Cooperative (NWO-2021.027/L1). Dr.ir. Karin Kompatscher, Dr.ir. Philomena Bluyssen, and Ir. Robert Bezemer are acknowledged for their assistance with the measurements.

REFERENCES

ANSYS Inc., 2022. ANSYS Fluent -Theory Guide.

Blocken, B., 2015. Computational Fluid Dynamics for urban physics: Importance, scales, possibilities, limitations and ten tips and tricks towards accurate and reliable simulations. Building and Environment 91, 219–245.

Brink, H.W., Loomans, M.G.L.C., Mobach, M.P., Kort, H.S.M., 2022. A systematic approach to quantify the influence of indoor environmental parameters on students' perceptions, responses, and short-term academic performance. Indoor Air 32, e13116.

Chang, J.C., Hanna, S.R., 2005. Technical descriptions and user's guide for the BOOT statistical model evaluation software package, version 2.0. George Mason University 4400, 22030–4444.

Morawska, L., Johnson, G.R., Ristovski, Z.D., Hargreaves, M., Mengersen, K., Corbett, S., Chao, C.Y.H., Li, Y., Katoshevski, D., 2009. Size distribution and sites of origin of droplets expelled from the human respiratory tract during expiratory activities. Journal of Aerosol Science 40, 256–269.

Thysen, J.-H., van Hooff, T., Blocken, B., van Heijst, G., 2022. Airplane cabin mixing ventilation with time-periodic supply: Contaminant mass fluxes and ventilation efficiency. Indoor Air 32, e13151.

Wolfshtein, M., 1969. The velocity and temperature distribution in one-dimensional flow with turbulence augmentation and pressure gradient. International Journal of Heat and Mass Transfer 12, 301–318.

Yakhot, V., Orszag, S.A., Thangam, S., Gatski, T.B., Speziale, C.G., 1992. Development of turbulence models for shear flows by a double expansion technique. Physics of Fluids A: Fluid Dynamics 4, 1510–1520.

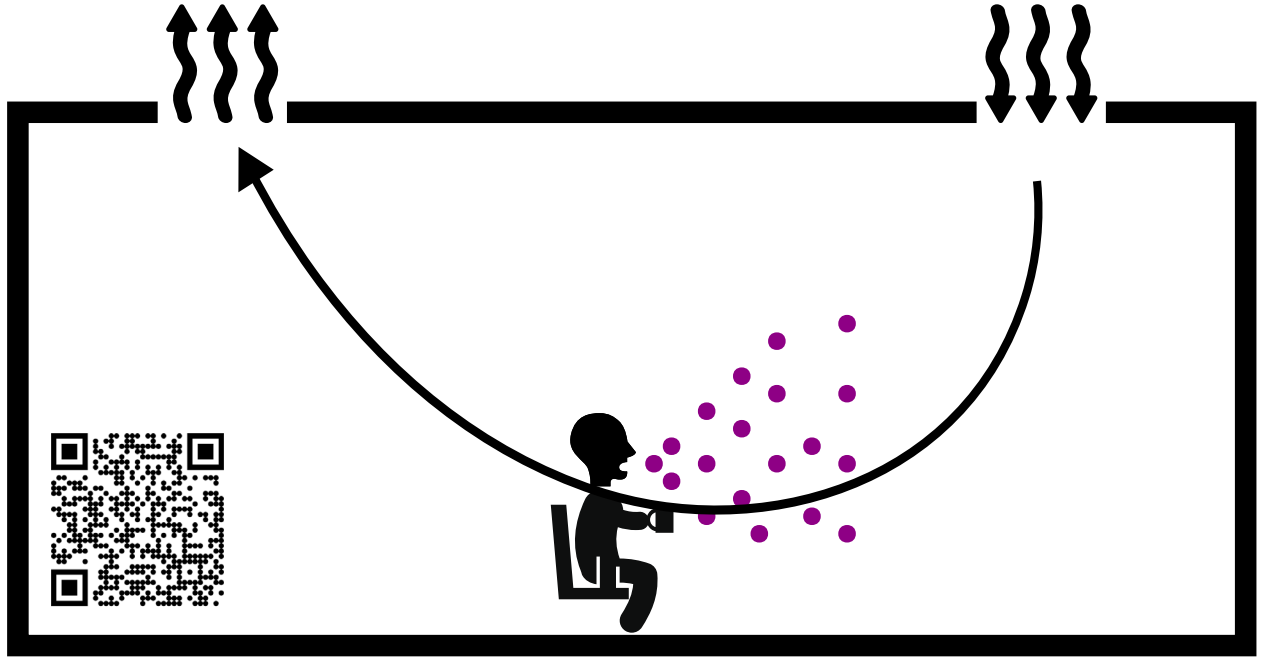

Experimental and CFD analysis of particle distribution in a controlled test facility: Impact of exhalation flow velocity and direction

Peng Qin *, [1], Anneloes de Lange [2], Twan van Hooff [1], Roberto Traversari [2], Marcel Loomans [1]

[1] Building Physics and Services, Department of the Built Environment, Eindhoven University of Technology, Eindhoven, The Netherlands

[2] Department of Buildings and Energy Systems, TNO Netherlands Organization for Applied Scientific Research, Delft, The Netherlands

* p.qin@tue.nl

Background

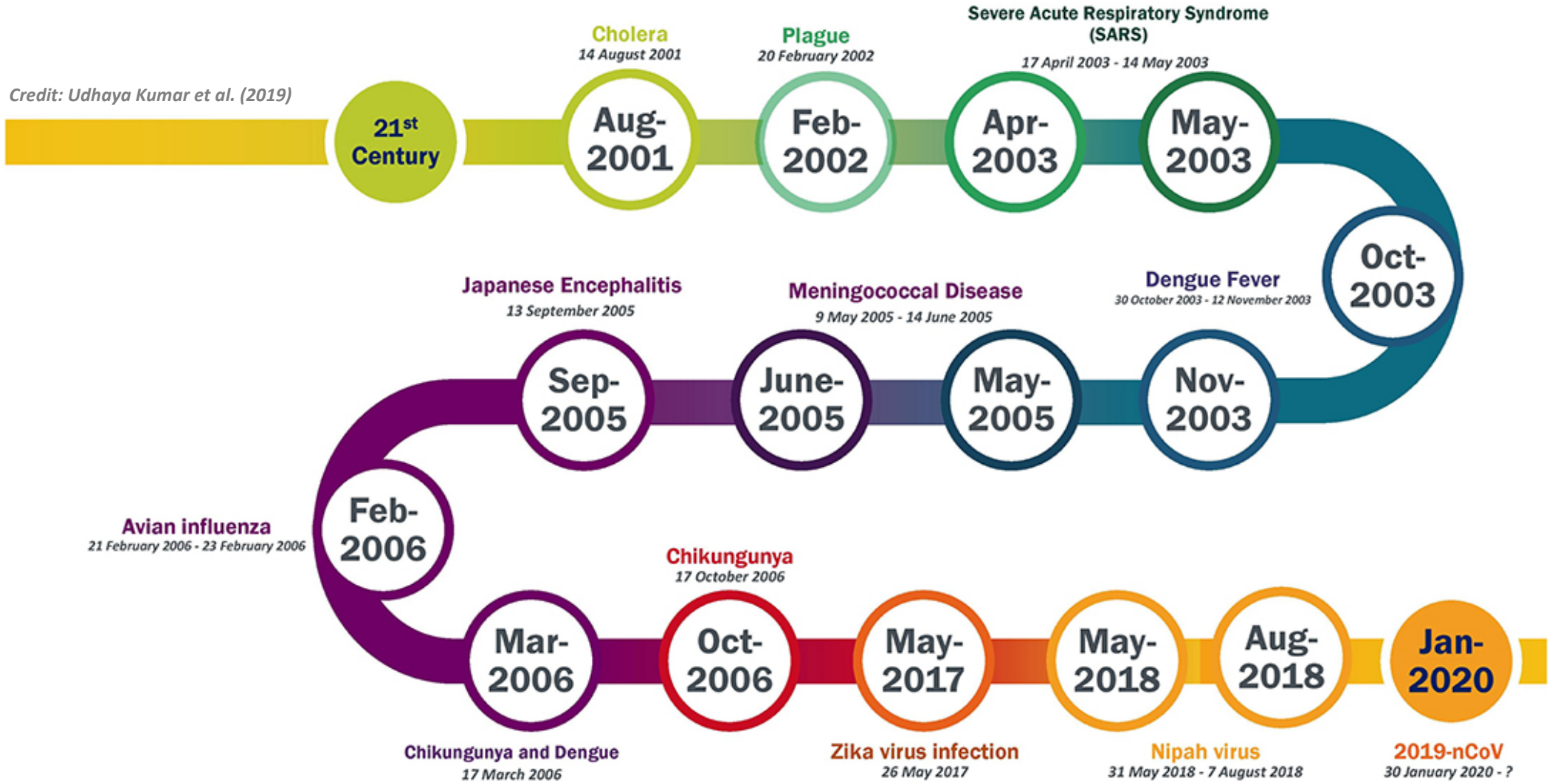

Public health emergencies of international concern in history

Background

Credit: Tellier et al. (2019)

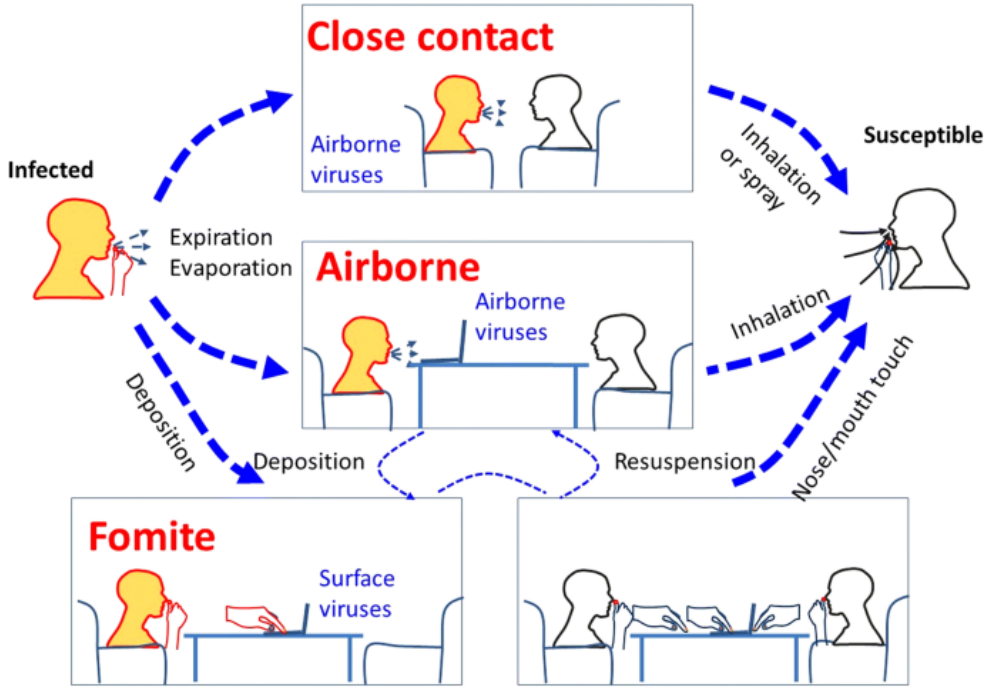

Transmission routes of respiratory infection

Credit: Wu et al. (2024)

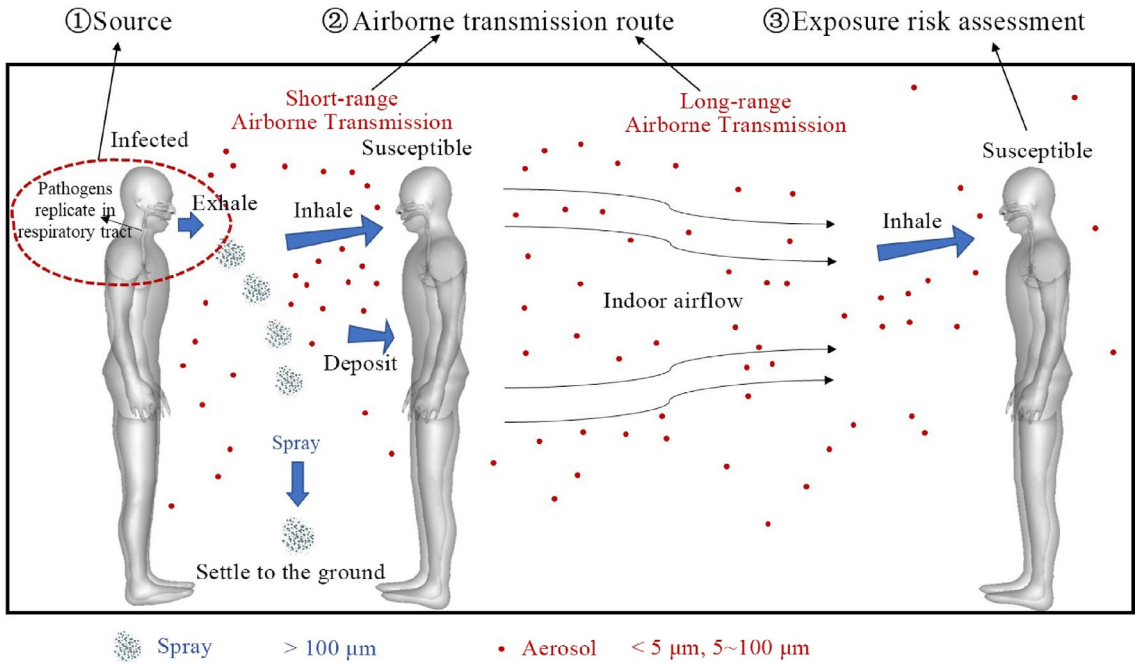

Indoor airborne transmission of respiratory infectious diseases

The understanding of aerosol transmissions indoor is crucial for estimating exposure and developing control measures.

State-of-the-art

References	Respiration	Exhalation flow rate [L/min]	Exhalation flow velocity (EFV) [m/s]	Exhalation flow direction (EFD) [-]	Particle size [µm]	Method
Qian et al. (2008)	breathing	-	0.89	PEO (mouth); 45° DW (nose)	-	Exp & CFD
Richmond-Bryant (2009)	breathing	-	0.2	-	TG	CFD
Chen and Zhao (2010)	breathing coughing sneezing	-	1 10 35	-	0.1, 1, 10, 50, 100, 200	CFD
He et al. (2011)	breathing	6	-	45° DW (mouth)	0.8; 5; 16	CFD
Villafruela et al. (2013)	breathing	6	0.01	PEO	TG	CFD
Hang et al. (2014)	breathing	-	0.107	PEO	TG	CFD
Mahyuddin et al. (2015)	breathing	8.5	1.25	45° DW (nose)	-	CFD
Zhang et al. (2017)	coughing	-	10	-	5	CFD
Ji et al. (2018)	breathing	-	1	-	10, 50, 100, 200	CFD
Duill et al. (2021)	breathing	3-11	-	-	1, 2.5, 4, 10	Exp & CFD
Auvinen et al. (2022)	breathing	14	-	PEO	< l (dry particles), 7 (wet particles)	Exp & CFD
Liu et al. (2022)	breathing	10	-	PEO	-	Exp & CFD
Luo et al. (2022)	breathing	-	1.5	PEO	5, 10, 100	Exp & CFD
Li et al. (2023)	breathing	6	0.5	PEO	1, 5, 10, 30, 50	CFD
Wei et al. (2023)	breathing talking	30 -	- 5 m/s	-	3 1-100	CFD
Won et al. (2024)	breathing	6	-	-	<1	CFD

Non-exhaustive overview of the constant respiration for indoor airborne particle transmission studies

TU/e

knowledge gap

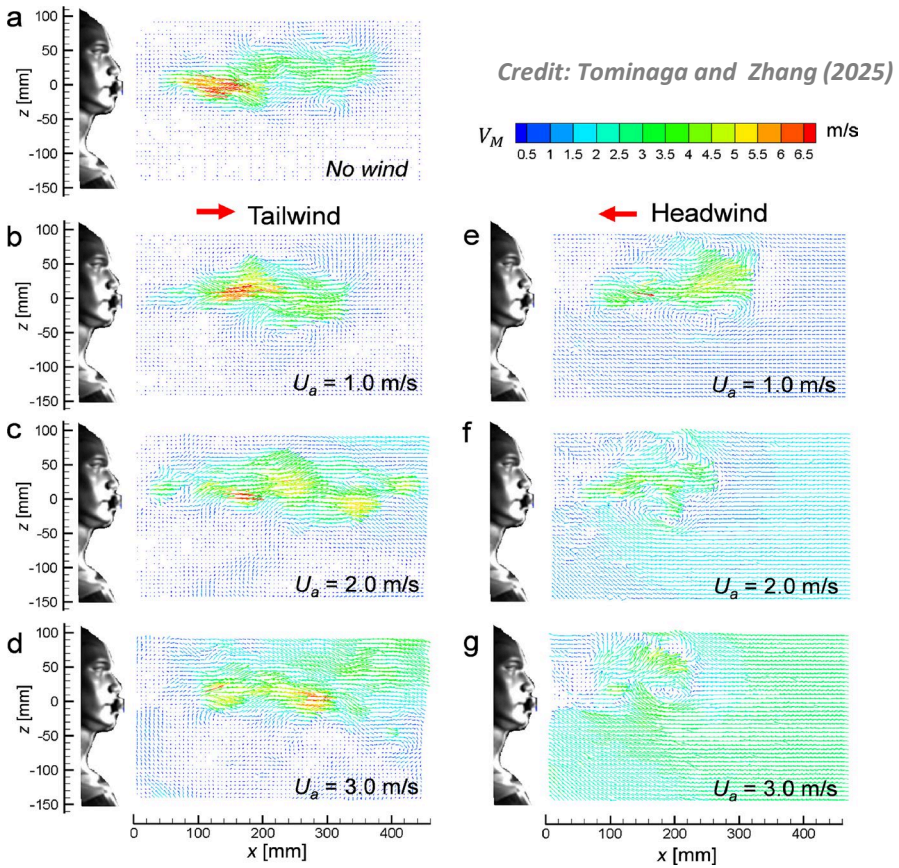

Credit: Tominaga and Zhang (2025)

Interactions between exhalation and ambient airflow

Credit: Villafruela et al. (2016)

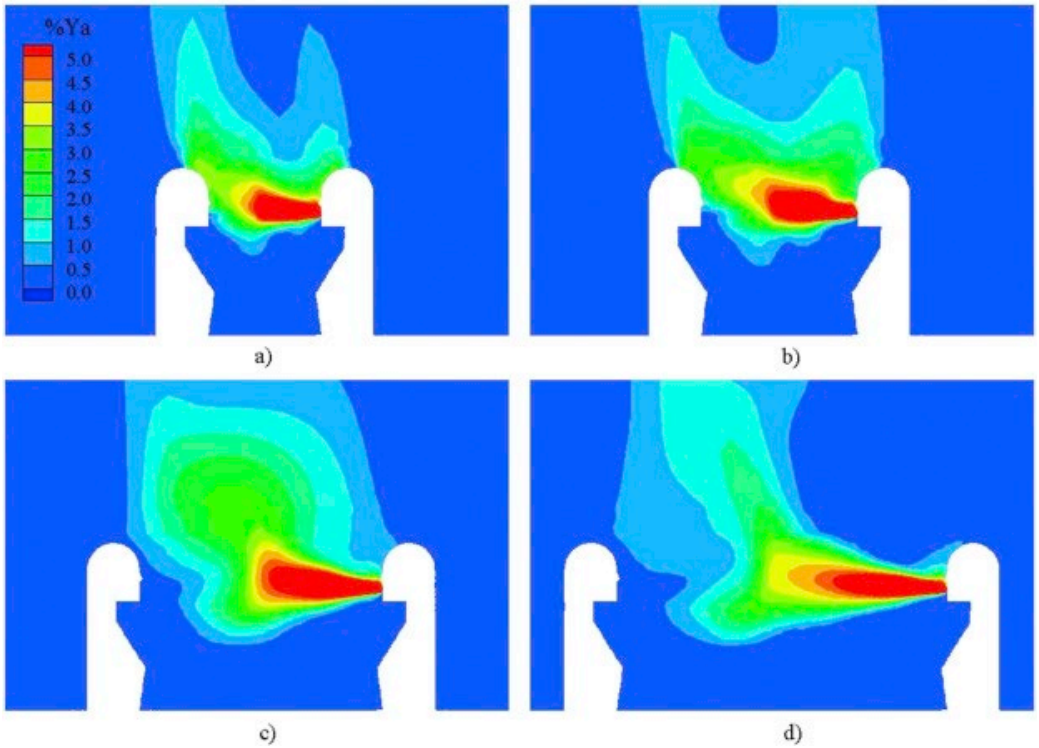

Cross-exposure involving multiple manikins

Goal and methodology

Goal: Systematical investigation of the impact of EFV and EFD, on the particle distribution in a large room with different ventilation configurations

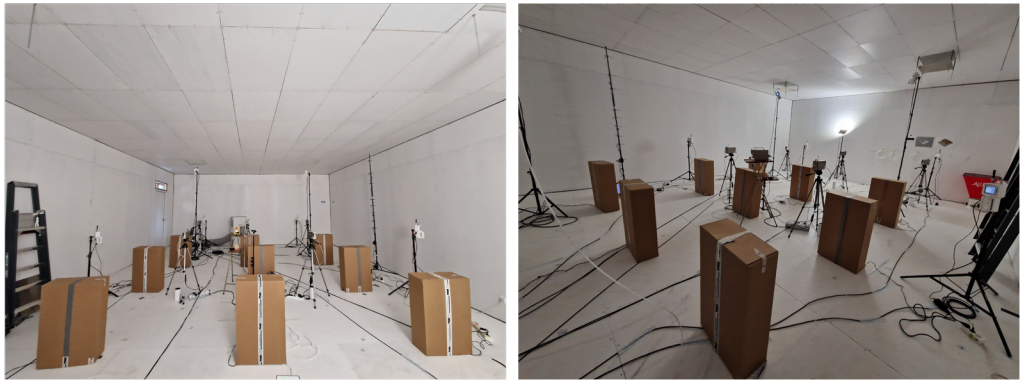

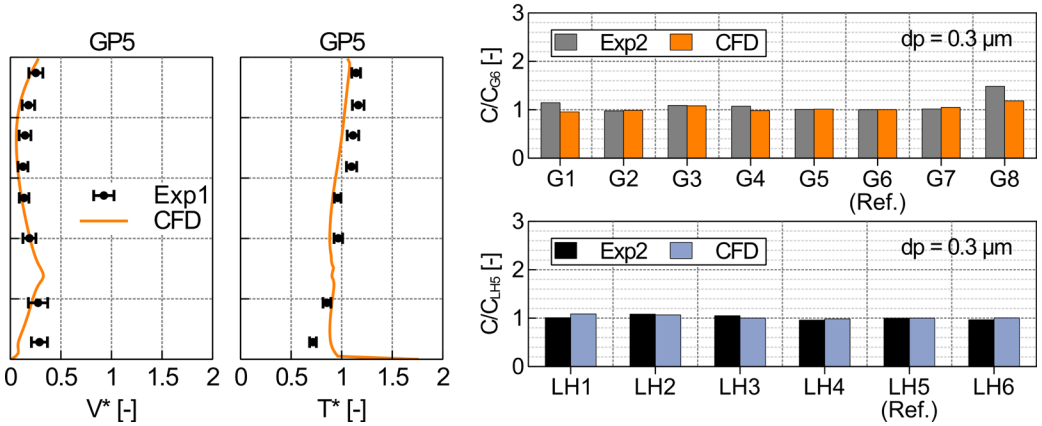

Stage 1: Experiments and validation

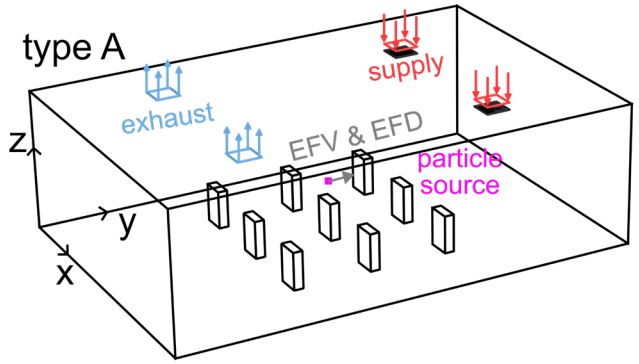

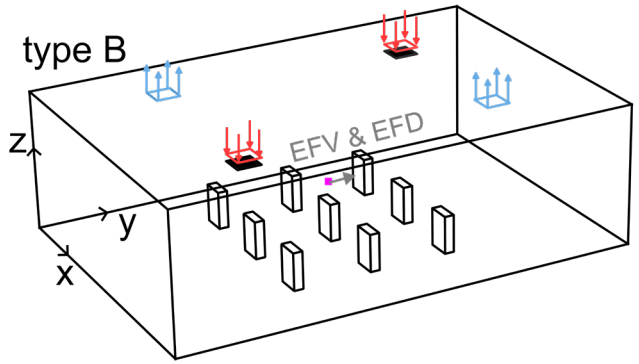

Exhalation flow velocity (EFV) *2.33 / 4.65 / 9.30 m/s*
Exhalation flow direction (EFD) *positive y / negative y / positive x*

Stage 2: Impact of EFV and EFD

Reference case: Experiments

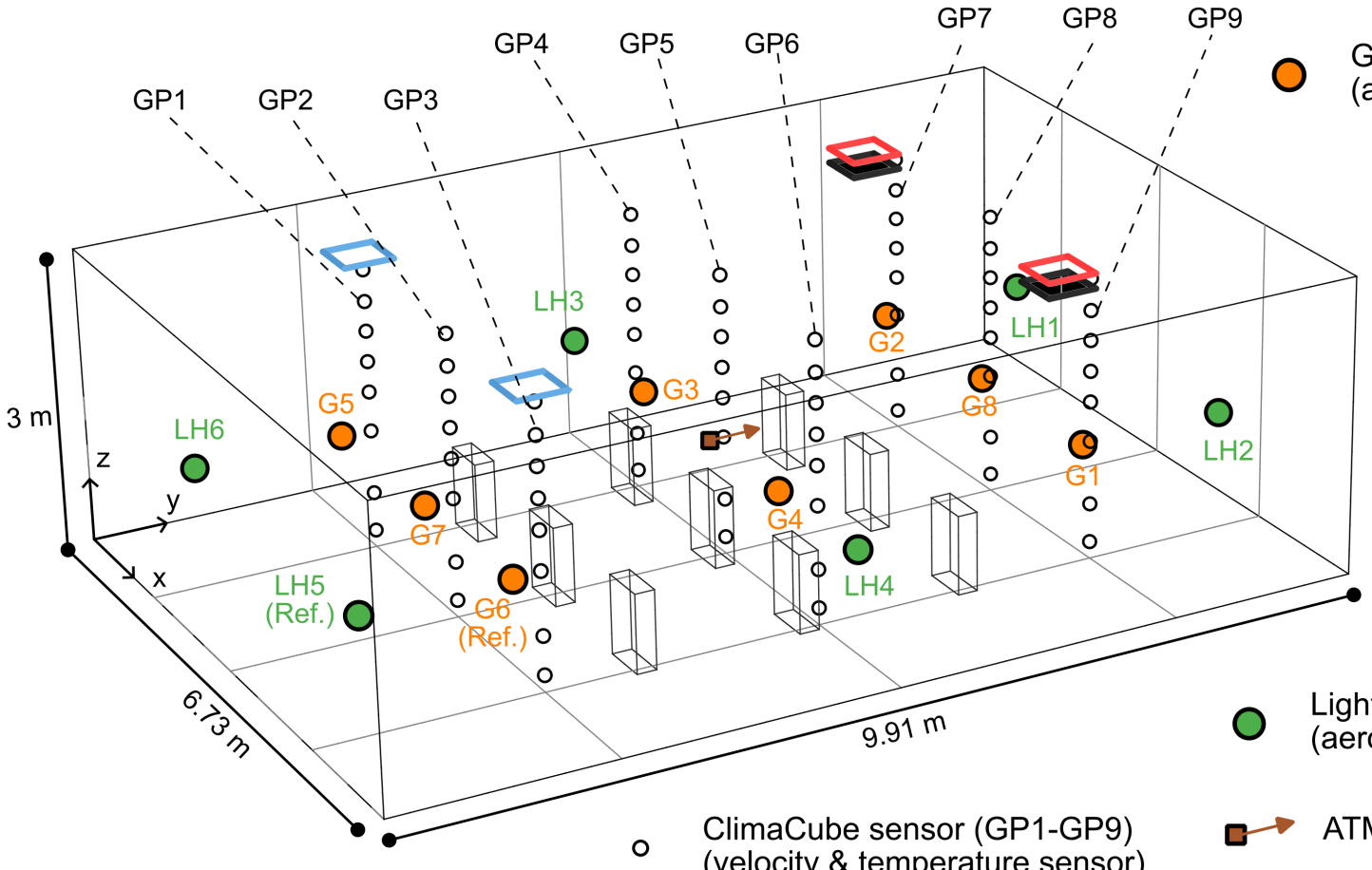

Grimm (G1-G8)
(aerosol particle sensor)

Supply

Plate

Exhaust

Heat manikin

Light house (LH1-LH6)
(aerosol particle sensor)

ClimaCube sensor (GP1-GP9)
(velocity & temperature sensor)

ATM228 aerosol generator

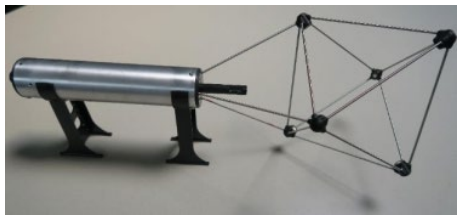

Ventilation configuration:
Type A

TU/e

Reference case: CFD simulations

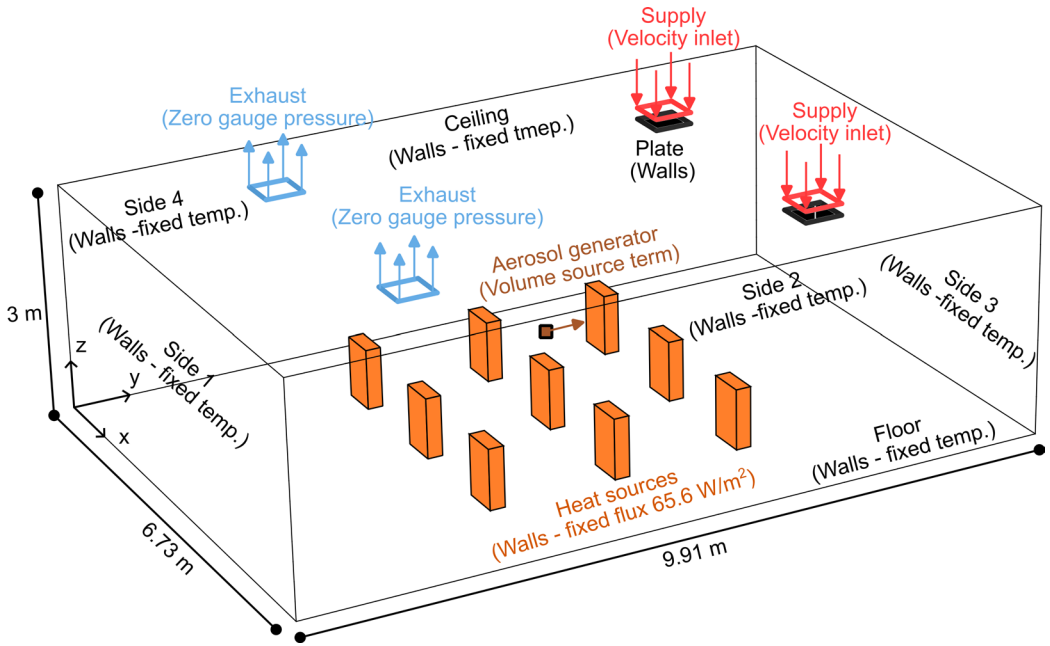

Computational domain and boundary conditions

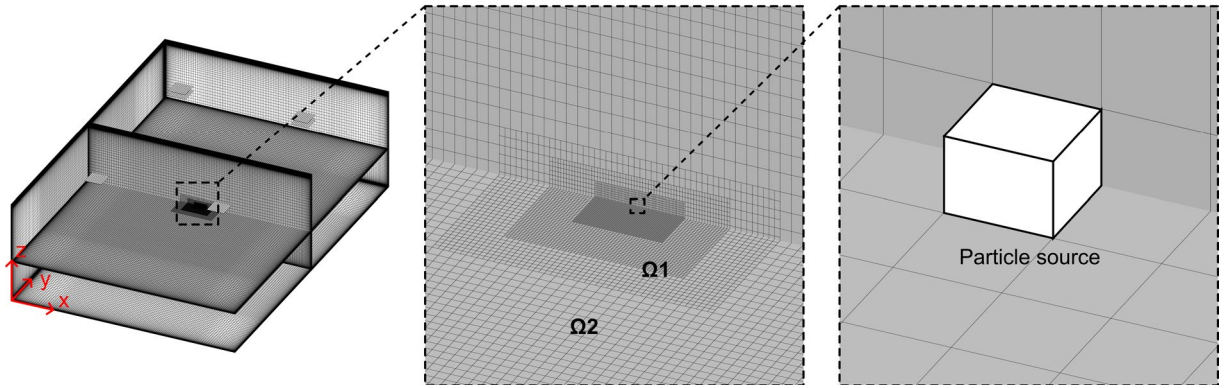

Computational grid

Other Computational settings

- 3D RANS coupled with RNG turbulence model
- Surface to surface (S2S) radiation model
- Drift-flux model for the particle dispersion
- Coupled algorithm for pressure-velocity coupling
- Second-order discretization scheme for the equations
- ANSYS Fluent 2023R1

Reference case: Validation

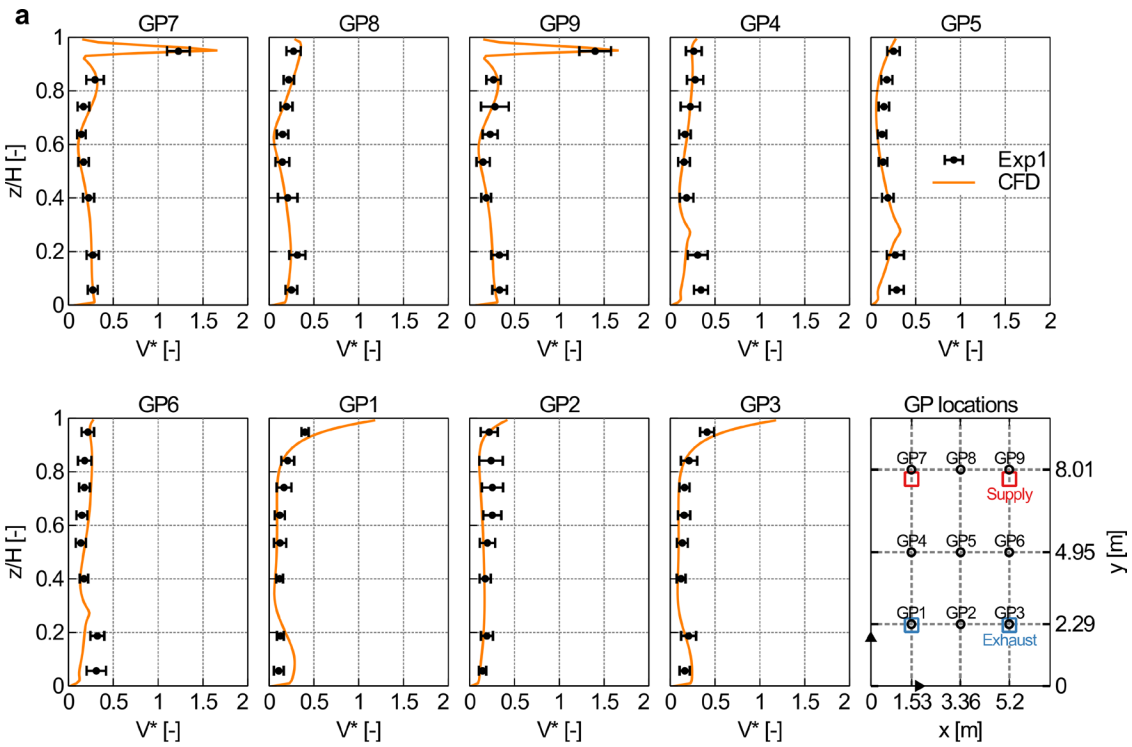

Velocity comparison between experiment and CFD

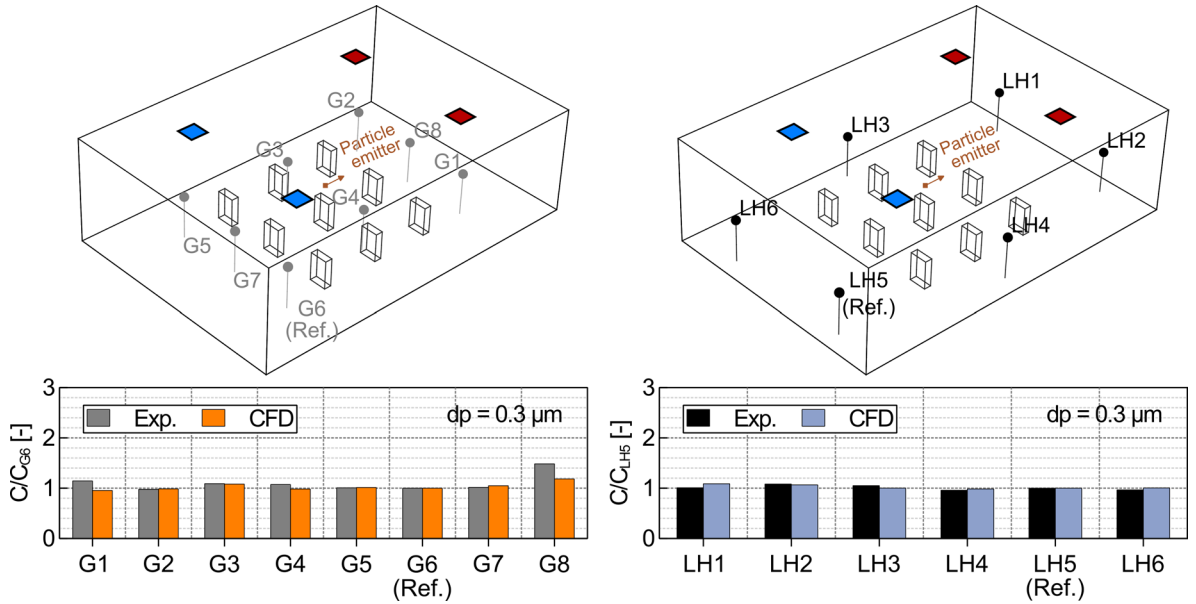

Concentration comparison between experiment and CFD

A good agreement between CFD and experiment was achieved for velocity and concentration.

Case studies: Impact of EFV and EFD

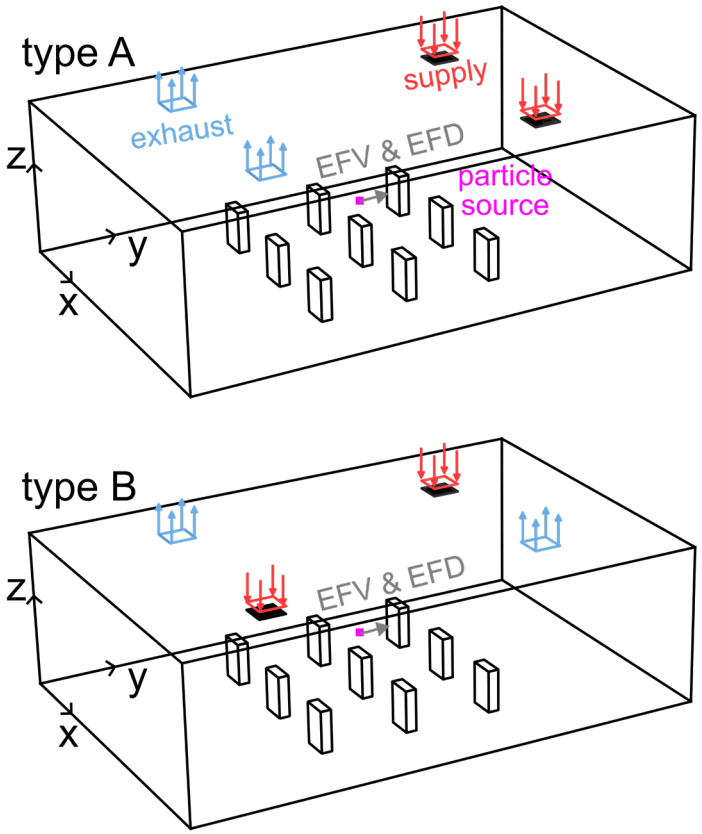

Ventilation configurations

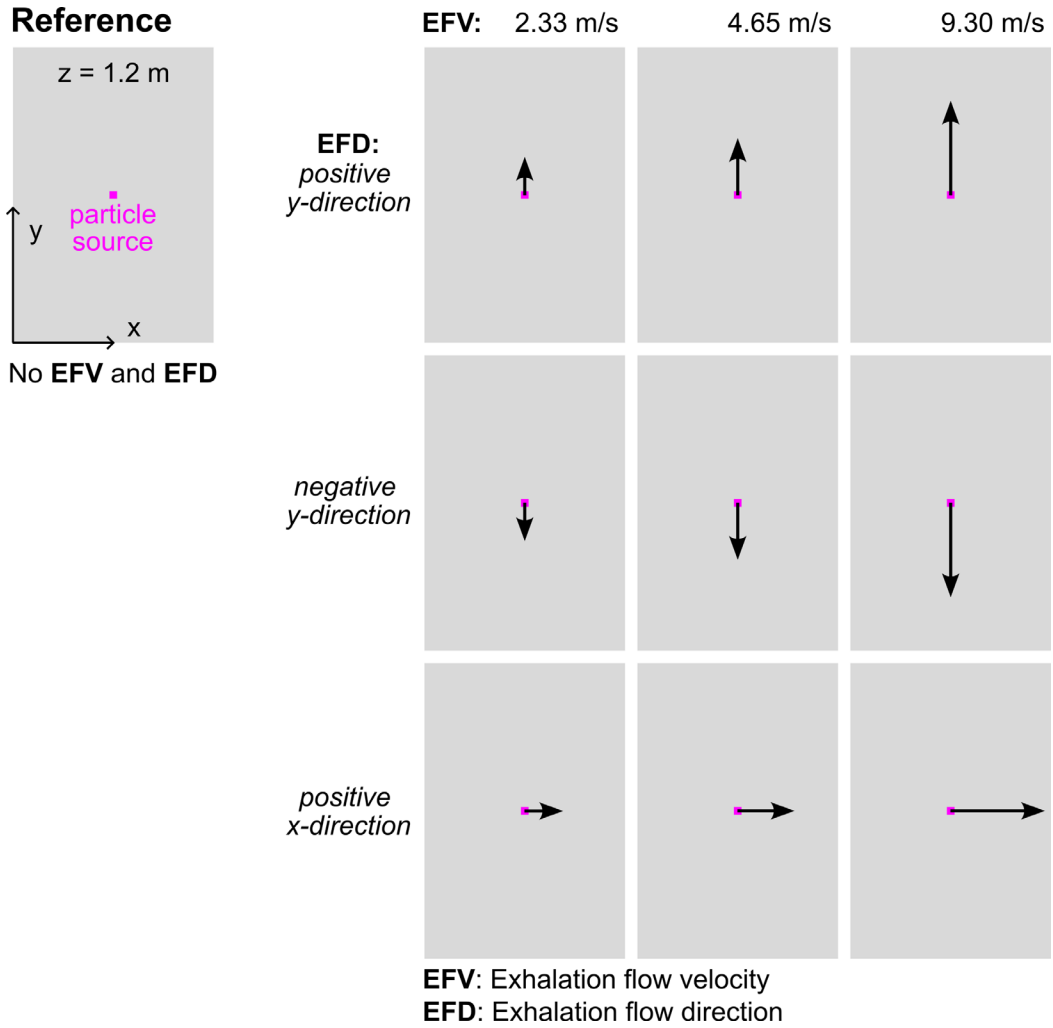

Variations of EFV and EFD

Case studies: Velocity contours

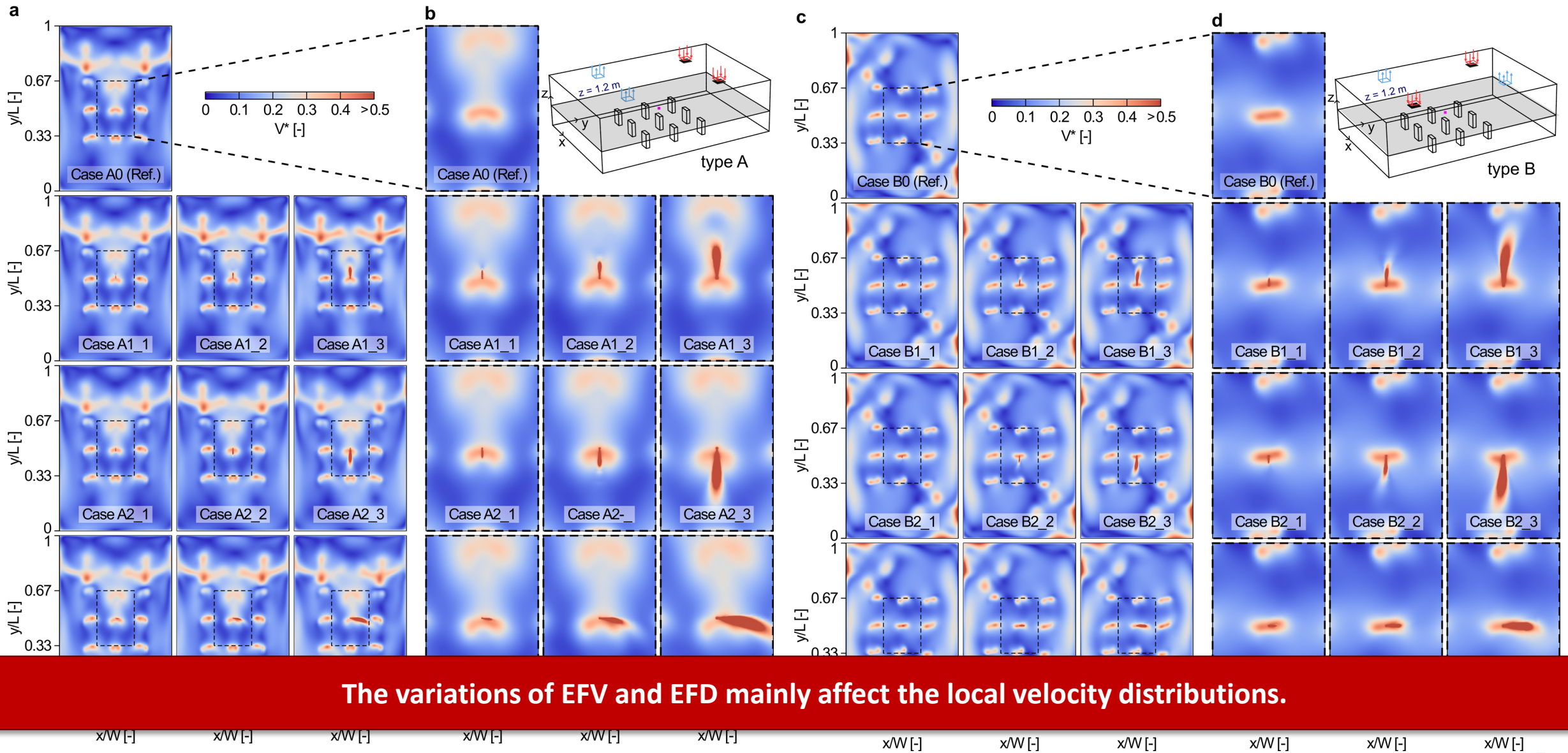

The variations of EFV and EFD mainly affect the local velocity distributions.

Case studies: Concentration contours

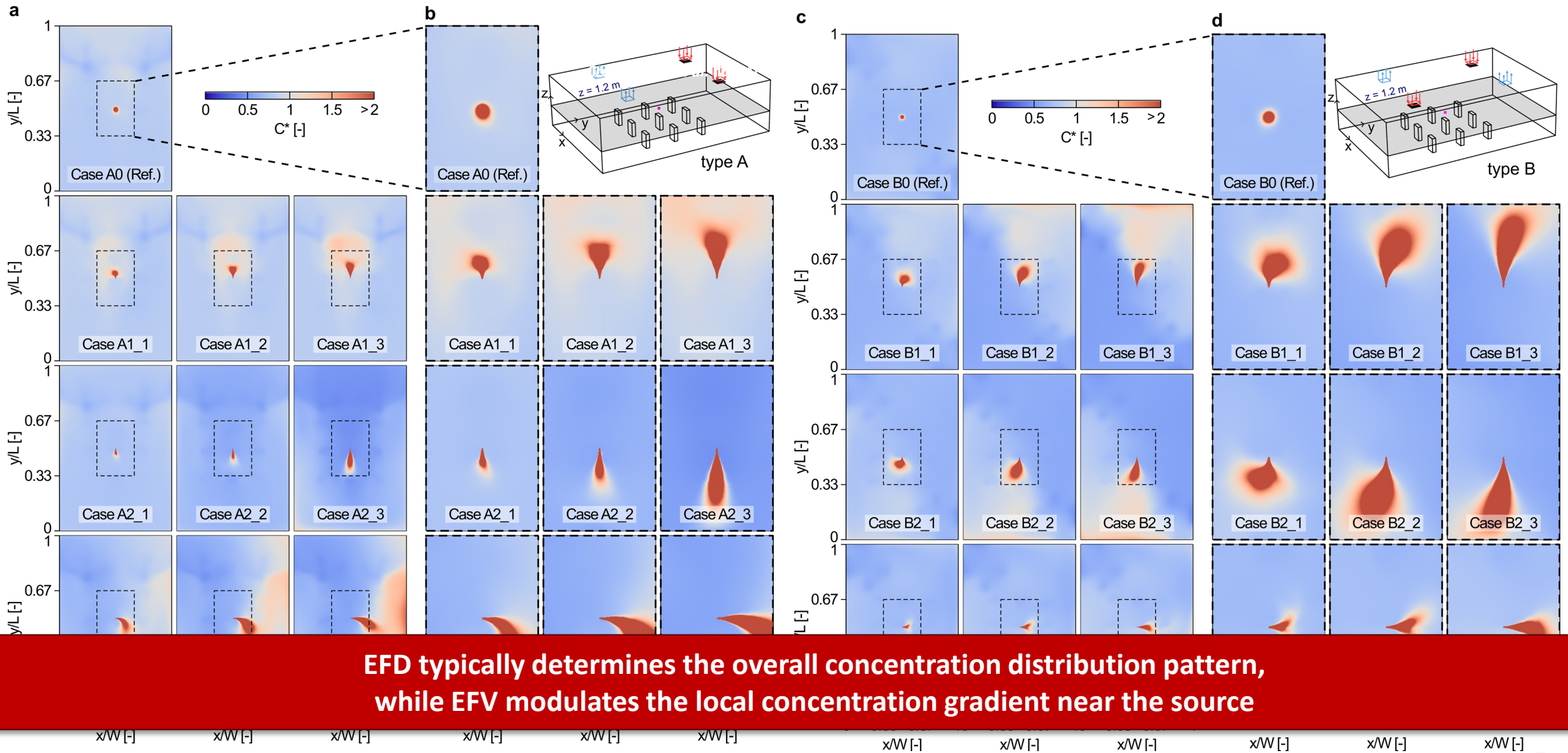

EFD typically determines the overall concentration distribution pattern, while EFV modulates the local concentration gradient near the source

Case studies: Surface-averaged concentration

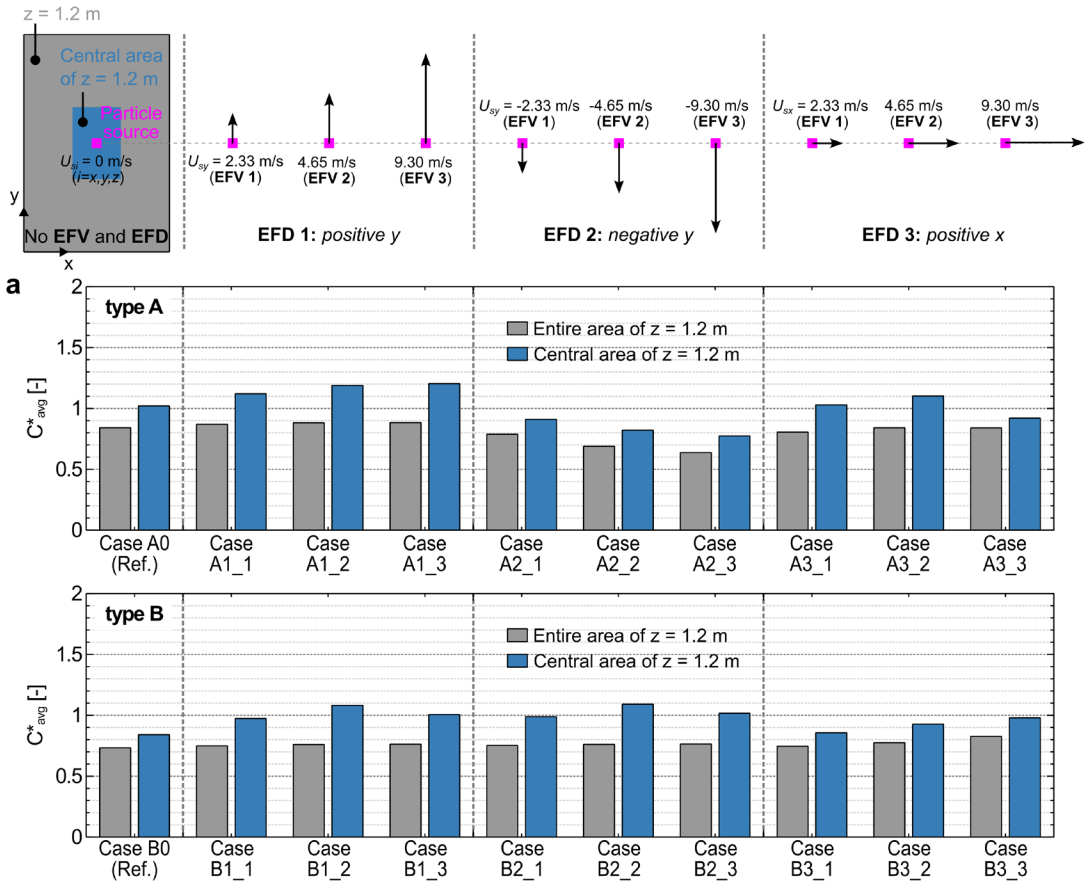

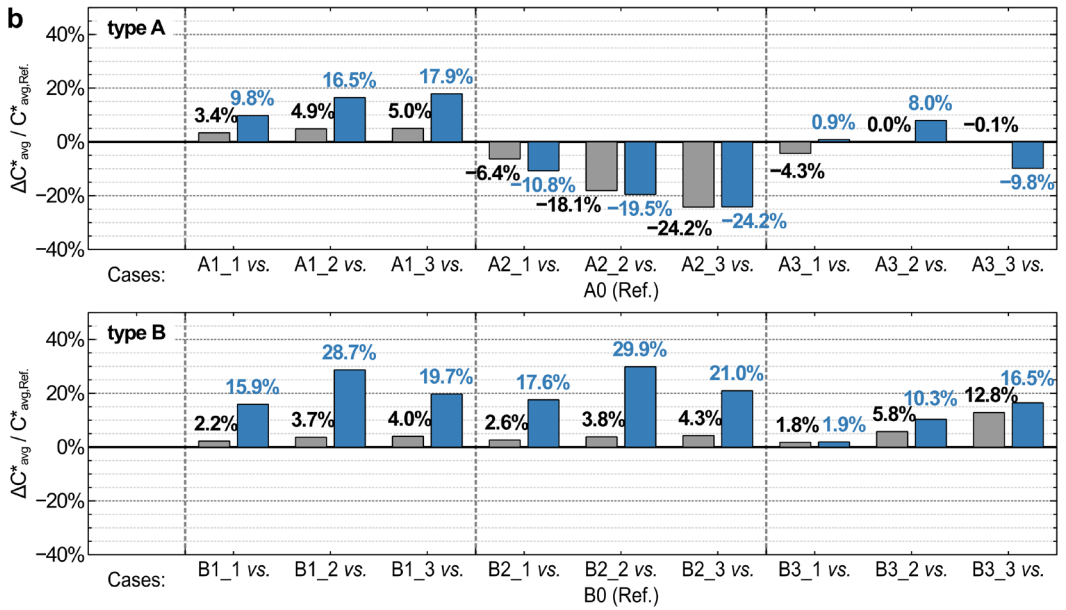

Changes in EFD and EFV generally have a relatively minor effect (e.g. < 5.8%) on the surface-averaged concentration when considering the entire region, while for local regions, the deviation ratio can reach up to 29.9%.

Conclusions & Future work

Changes in **ventilation configurations** have pronounced impact on the velocity distributions.

Changes in **EFD and EFV** primarily affect the local velocity distributions near the particle source.

Changes in **EFD** significantly influence both overall and local concentration distributions.

Changes in **EFV** have a less pronounced impact on overall concentration distribution while have a pronounced on local concentration distributions.

Future work: Inclusion of more detailed manikins and consideration of the impact of source locations

Thanks for you attention!

Dr. Peng Qin
Postdoc Researcher
Department of the Built Environment
Building Physics

T +31 (0)640714908
p.qin@tue.nl

PO Box 513, 5600 MB Eindhoven, the Netherlands
Visiting address Building 6, Vertigo 6.10
Navigation De Zaale, Eindhoven